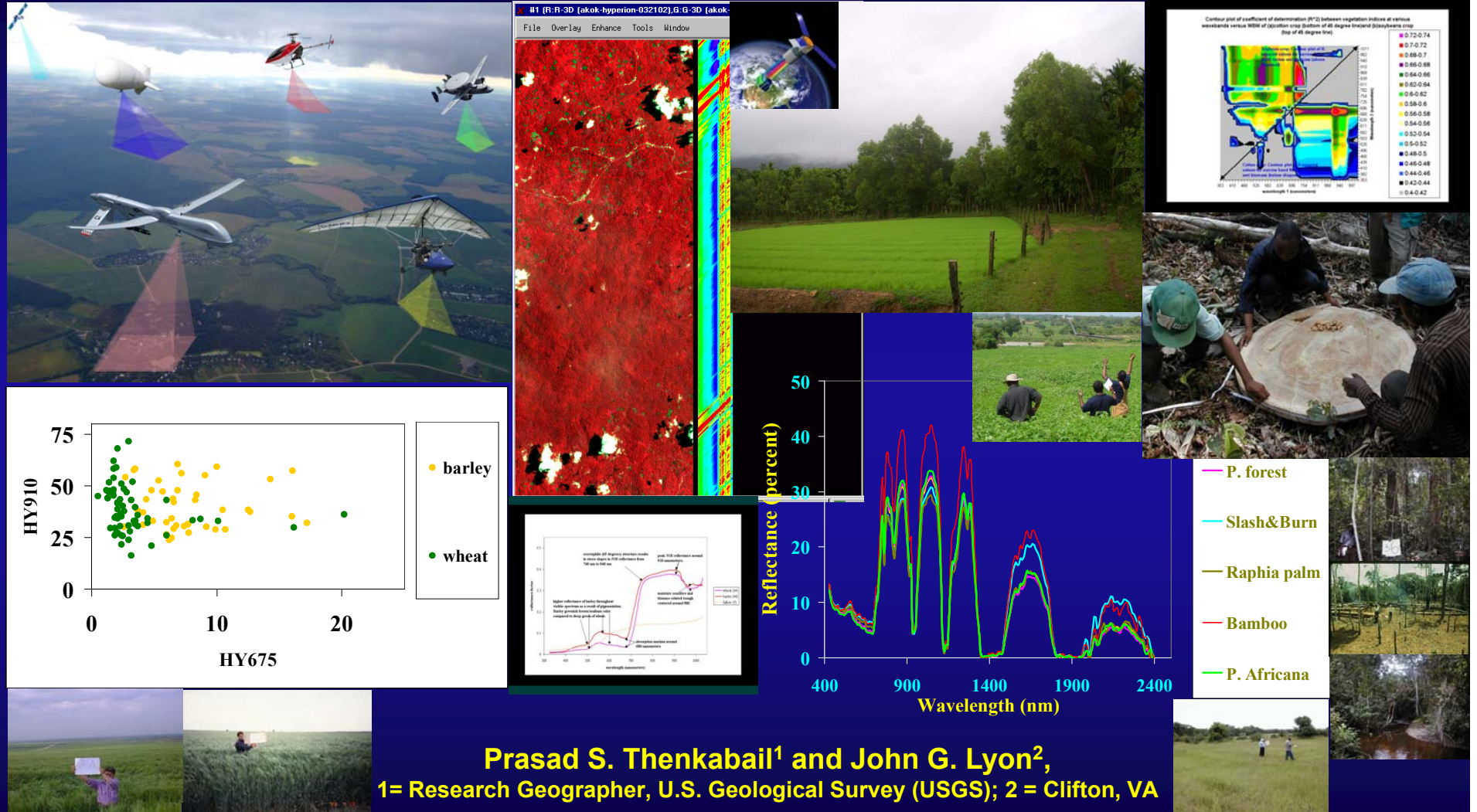
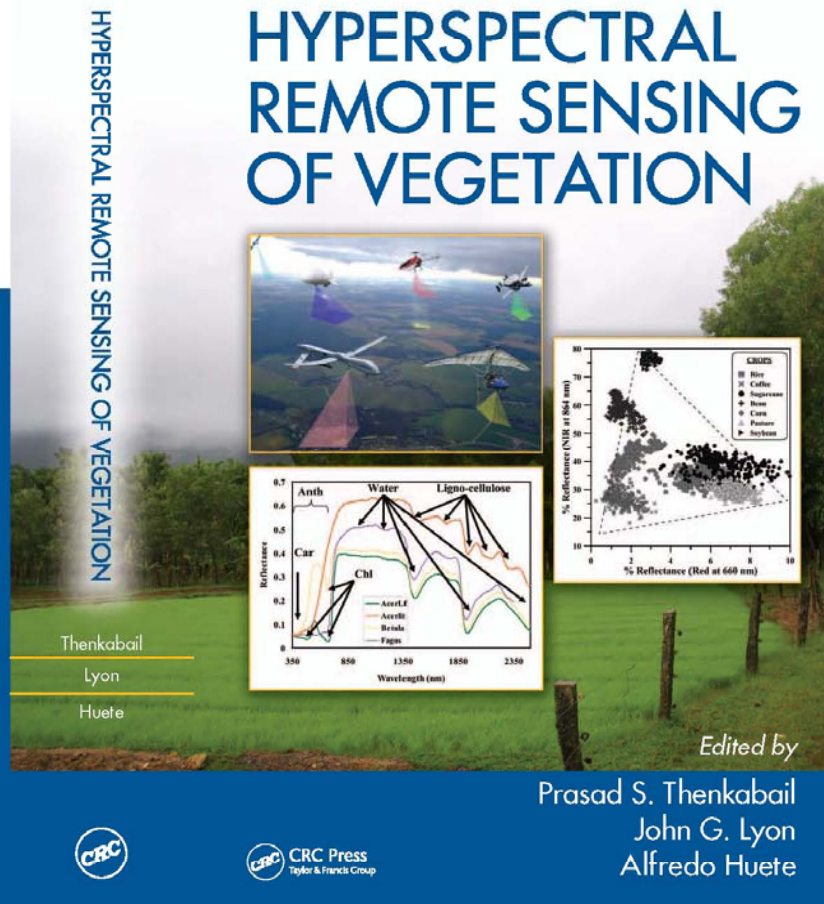
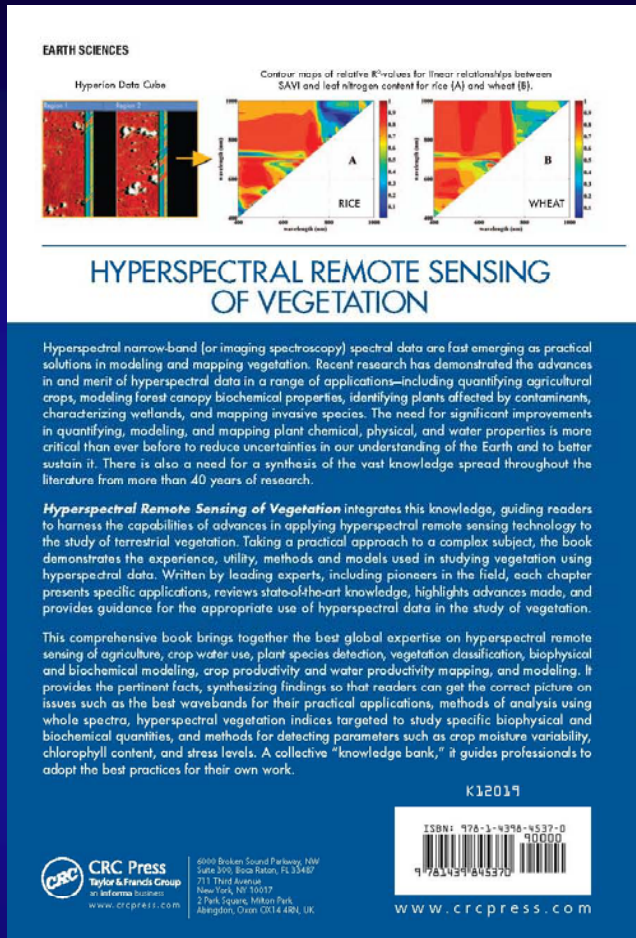


# Advanced Hyperspectral Remote sensing of the Terrestrial Environment

## Lecture # 2: Methods of Modeling and Mapping



# Hyperspectral Remote Sensing Vegetation References Pertaining to this Presentation



Thenkabail, P.S., Lyon, G.J., and Huete, A. 2011. Book entitled: “Advanced Hyperspectral Remote Sensing of Terrestrial Environment”. 28 Chapters. CRC Press- Taylor and Francis group, Boca Raton, London, New York. Pp. 781 (80+ pages in color).



U.S. Geological Survey  
U.S. Department of Interior



# Methods of Modeling Vegetation Biophysical and Biochemical Characteristics



# Hyperspectral Data (Imaging Spectroscopy data) Methods of Modeling Biophysical and Biochemical Characteristics

## 1. Band Selection

principal component analysis (PCA), band to band correlation, stepwise discriminant analysis (SDA)

## 2. Hyperspectral vegetation indices (HVI<sub>s</sub>)

two-band vegetation indices (TBVI<sub>s</sub>)

## 3. Linear and non-linear multivariate statistics and models

multi-band vegetation indices (MBVI<sub>s</sub>)- MAXR models, partial least square regressions (PLR), principal component regressions

## 4. Derivative indices

first order derivative vegetation indices

## 5. Classification accuracies

discriminant model

## 6. Radiative transfer physically based models

PROSPECT, LEAFMOD

## 7. Whole spectral analysis

spectral matching techniques

Note: see chapter 1, Thenkabail et al., chapter 13, Alchanatis and Cohen.



# Methods of Modeling Vegetation Characteristics using Hyperspectral Vegetation Indices (HVIs)



Hyperspectral Data (Imaging Spectroscopy data)

# Hyperspectral Vegetation Indices (HVs)

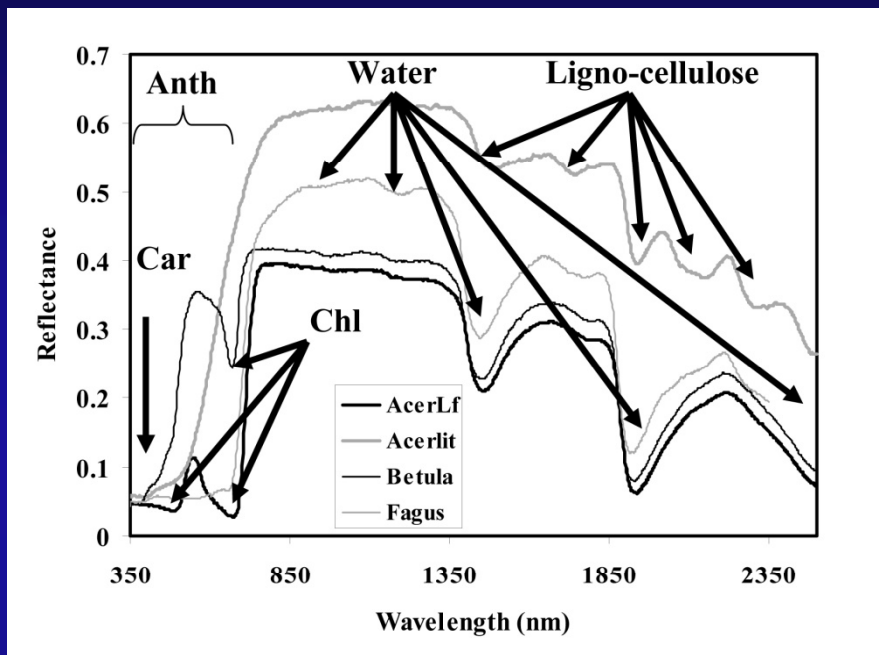
## Unique Features and Strengths of HVs

1. Eliminates redundant bands  
removes highly correlated bands
2. Physically meaningful HVs  
e.g., Photochemical reflective index (PRI) as proxy for light use efficiency (LUE)
3. Significant improvement over broadband indices  
e.g., reducing saturation of broadbands, providing greater sensitivity (e.g., an index involving NIR reflective maxima @ 900 nm and red absorption maxima @680 nm)
4. New indices not sampled by broadbands  
e.g., water-based indices (e.g., involving 970 nm or 1240 nm along with a nonabsorption band)
5. multi-linear indices  
indices involving more than 2 bands

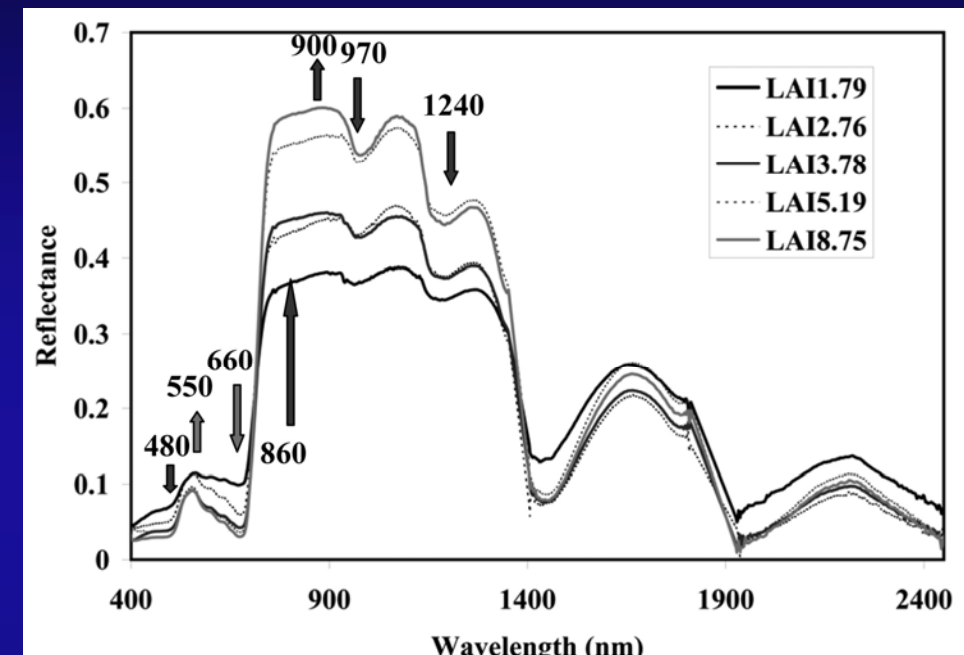
Note: see chapter 1, Thenkabail et al., chapter 14, Roberts et al.



## Hyperspectral Data (Imaging Spectroscopy data) e.g., Physically based Indices and New indices not Feasible in Broadbands



Reflectance spectra of leaves from a senesced birch (*Betula*), ornamental beech (*Fagus*), and healthy and fully senesced maple (*AcerLf*, *Acerlit*) illustrating carotenoid (Car), anthocyanin (Anth), chlorophyll (Chl), water, and ligno-cellulose absorptions.



Reflectance spectra of *Populus trichocarpa* hybrids over a range in LAI. Wavelengths labeled refer to absorption features (480, 660, 970, and 1240 nm) or NIR scattering regions (860 and 900 nm) typically used in combination to quantify structure. Arrows mark regions of decreasing reflectance due to absorption (down) or increasing reflectance due to scattering (up).

Note: see chapter 14, Roberts et al.



# Hyperspectral Data (Imaging Spectroscopy data)

## HVIs: Biophysical, Biochemical, Pigment, Water, Lignin and cellulose, and Physiology

## Major Hyperspectral Vegetation Indices, Including Relevant Formulas and Key Citations

Note: see chapter 14, Roberts et al.

Index	Equation	Reference
Structure (LAI, green biomass, fraction)		
*NDVI	$(R_{NIR}-R_{red})/(R_{NIR}+R_{red})$	Rouse et al.[15]
*SR	$R_{NIR}/R_{red}$	Jordan [3]
*EVI	$2.5*(R_{NIR}-R_{red})/(R_{NIR}+6*R_{red}-7.5*R_{blue}+1)$	Huete et al.[23]
*NDWI	$(R_{857}-R_{1241})/(R_{857}+R_{1241})$	Gao [29]
**WBI	$R_{900}/R_{970}$	Peñuelas et al.[28]
*ARVI	$(R_{NIR}-[R_{red}-\gamma*(R_{blue}-R_{red})])/(R_{NIR}+[R_{red}-\gamma*(R_{blue}-R_{red})])$	Kaufman & Tanré [22]
*SAVI	$[(R_{NIR}-R_{red})/(R_{NIR}+R_{red}+L)]*(1+L)$	Huete [21]
**IDL_DGVI	$\sum_{\lambda_{450-850\text{ nm}}}  R'(\lambda_i) - R'(\lambda_{626\text{ nm}})  \Delta \lambda_i$	Elvidge & Chen [1]
**IDZ_DGVI	$\sum_{\lambda_{450-850\text{ nm}}}  R'(\lambda_i)  \Delta \lambda_i$	Elvidge & Chen [1]
*VARI	$(R_{green}-R_{red})/(R_{green}+R_{red}-R_{blue})$	Gitelson et al.[13]
*VIgreen	$(R_{green}-R_{red})/(R_{green}+R_{red})$	Gitelson et al.[13]
Biochemical		
Pigments		
**SIP	$(R_{800}-R_{445})/(R_{800}-R_{680})$	Peñuelas et al. [31]
**PSSR	$(R_{800}/R_{675}); (R_{800}/R_{500})$	Blackburn [30]
**PSND	$[(R_{800}-R_{675})/(R_{800}+R_{675})]; [(R_{800}-R_{650})/(R_{800}+R_{650})]$	Blackburn [32]
**PSRI	$(R_{680}-R_{500})/R_{750}$	Merzlyak et al. [33]
Chlorophyll		
**CARI	$[(R_{700}-R_{670})-0.2*(R_{700}-R_{550})]$	Kim [34]
**MCARI	$[(R_{700}-R_{670})-0.2*(R_{700}-R_{550})]* (R_{700}/R_{670})$	Daughtry et al. [35]
**CI <sub>red edge</sub>	$R_{NIR}/R_{red\ edge}-1$	Gitelson et al. [36]
Anthocyanins		
**ARI	$(1/R_{green})-(1/R_{red\ edge})$	Gitelson et al.[40]
**mARI	$[(1/R_{green})-(1/R_{red\ edge})]*R_{NIR}$	Gitelson et al. [36]
**RGRI	$R_{red}/R_{green}$	Gamon & Surfus [7]
**ACI	$R_{green}/R_{NIR}$	Van den Berg & Perkins [41]
Carotenoids		
**CRI1	$(1/R_{510})-(1/R_{550})$	Gitelson et al.[42]
**CRI2	$(1/R_{510})-(1/R_{700})$	Gitelson et al. [42]
Water		
*NDII	$(R_{NIR}-R_{SWIR})/(R_{NIR}+R_{SWIR})$	Hunt & Rock [12]
*NDWI, **WBI	See Above	See Above
*MSI	$R_{SWIR}/R_{NIR}$	Rock et al. [43]
Lignin & Cellulose/Residues		
**CAI	$100*[0.5*(R_{2031}+R_{2211})-R_{2101}]$	Daughtry [47]
**NDLI	$[\log(1/R_{1754})-\log(1/R_{1680})]/[\log(1/R_{1754})+\log(1/R_{1680})]$	Serrano et al. [48]
Nitrogen		
**NDNI	$[\log(1/R_{1510})-\log(1/R_{1680})]/[\log(1/R_{1510})+\log(1/R_{1680})]$	Serrano et al. [48]
Physiology		
Light Use Efficiency		
**RGRI, **SIP	See Above	See Above
**PRI	$(R_{530}-R_{570})/(R_{530}+R_{570})$	Gamon et al. [9]
Stress		
*MSI	See Above	See Above
**REP	$l(\max\ first\ derivative: 680-750\ nm)$	Horler et al. [10]
**RVI	$[(R_{714}+R_{752})/2-R_{733}]$	Merton & Huntington [52]



# Methods of Modeling Vegetation Characteristics using Hyperspectral Indices



## Methods of Modeling Vegetation Characteristics using Hyperspectral Indices

Hyperspectral Two-band Vegetation Indices (TBVIs) = 12246 unique indices for 157 useful Hyperion bands of data

$$(R_j - R_i)$$

$$HTBVI_{ij} = \frac{(R_j - R_i)}{(R_j + R_i)}$$

### Hyperion:

A. acquired over 400-2500 nm in 220 narrow-bands each of 10-nm wide bands. Of these there are 196 bands that are calibrated. These are: (i) bands 8 (427.55 nm) to 57 (925.85 nm) in the visible and near-infrared; and (ii) bands 79 (932.72 nm) to band 224 (2395.53 nm) in the short wave infrared.

B. However, there was significant noise in the data over the 1206–1437 nm, 1790– 1992 nm, and 2365–2396 nm spectral ranges. When the Hyperion bands in this region were dropped, 157 useful bands remained.

### Spectroradiometer:

A. acquired over 400-2500 nm in 2100 narrow-bands each of 1-nm wide. However, 1-nm wide data were aggregated to 10-nm wide to coincide with Hyperion bands.

B. However, there was significant noise in the data over the 1350-1440 nm, 1790-1990 nm, and 2360-2500 nm spectral ranges. was seriously affected by atmospheric absorption and noise. The remaining good noise free data were in 400-1350 nm, and 1440-1790 nm, 1990-2360 nm.

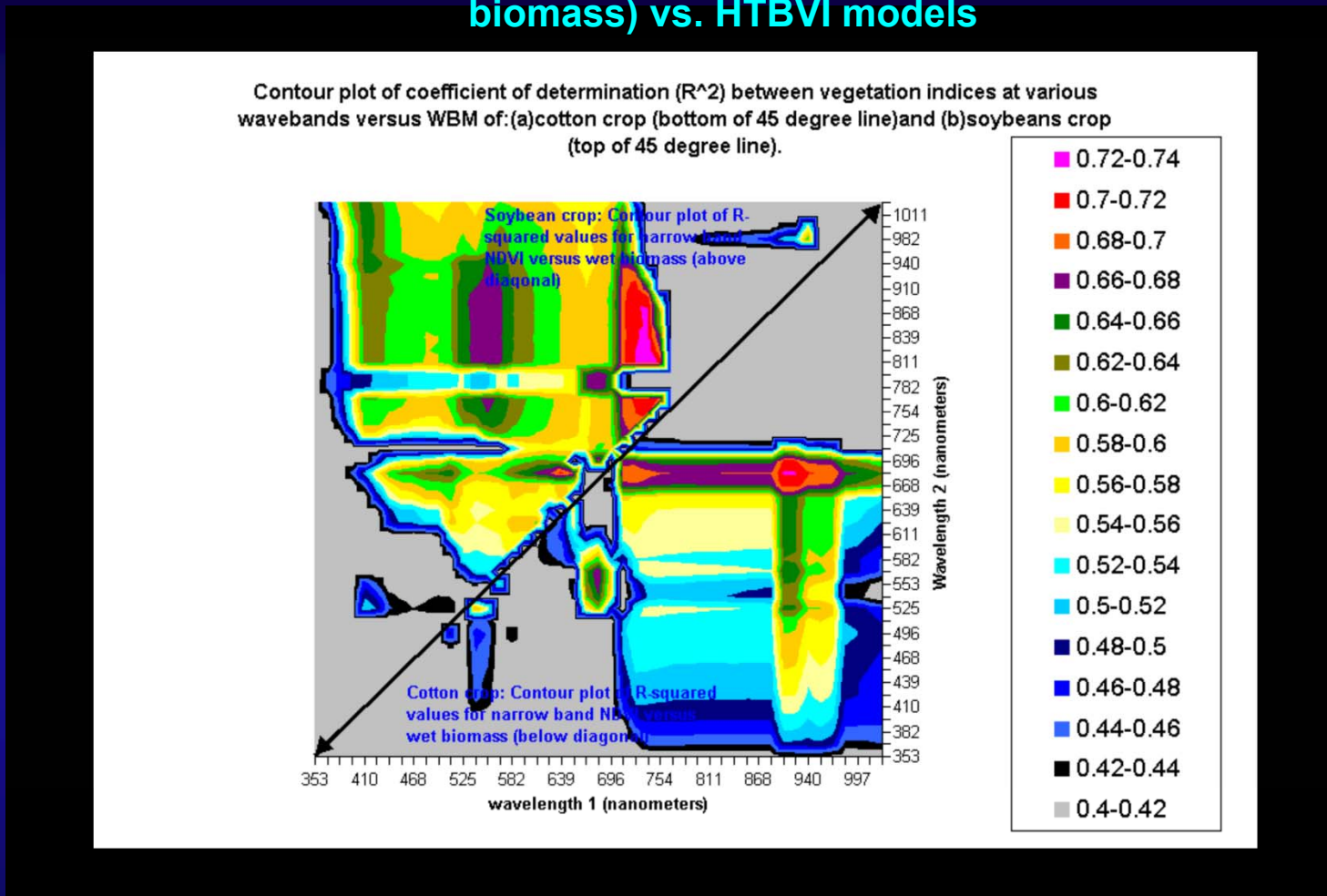
.....So, for both Hyperion and Spectroradiometer we had 157 useful bands, each of 10-nm wide, over the same spectral range.

where, i,j = 1, N, with N=number of narrow-bands= 157 (each band of 1 nm-wide spread over 400 nm to 2500 nm), R=reflectance of narrow-bands.

**Model algorithm:** two band NDVI algorithm in Statistical Analysis System (SAS). Computations are performed for all possible combinations of  $\lambda_1$  (wavelength 1 = 157 bands) and  $\lambda_2$  (wavelength 2 = 157 bands)- a total of 24,649 possible indices. It will suffice to calculate Narrow-waveband NDVI's on one side (either above or below) the diagonal of the 157 by 157 matrix as values on either side of the diagonal are the transpose of one another.

# Methods of Modeling Vegetation Characteristics using Hyperspectral Indices

## Lambda vs. Lambda R-square contour plot on non-linear biophysical quantity (e.g., biomass) vs. HTBVI models

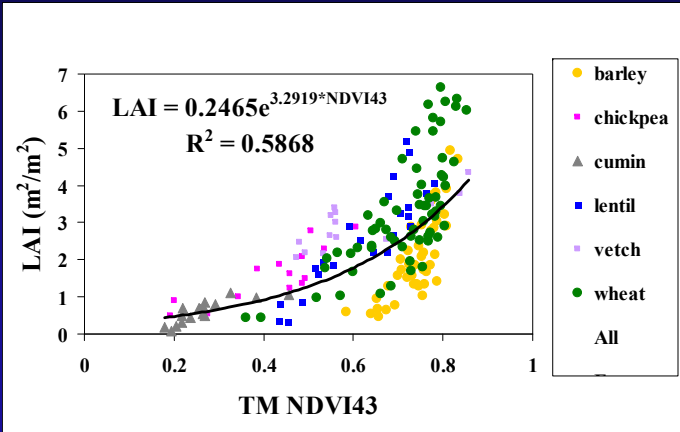


Illustrated for 2 crops here

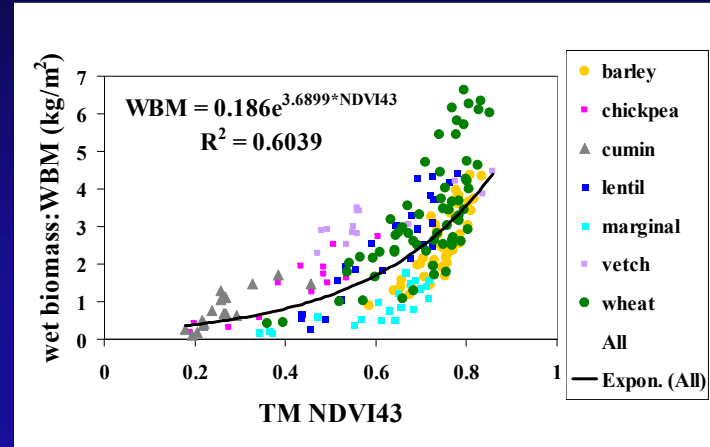


# Methods of Modeling Vegetation Characteristics using Hyperspectral Indices

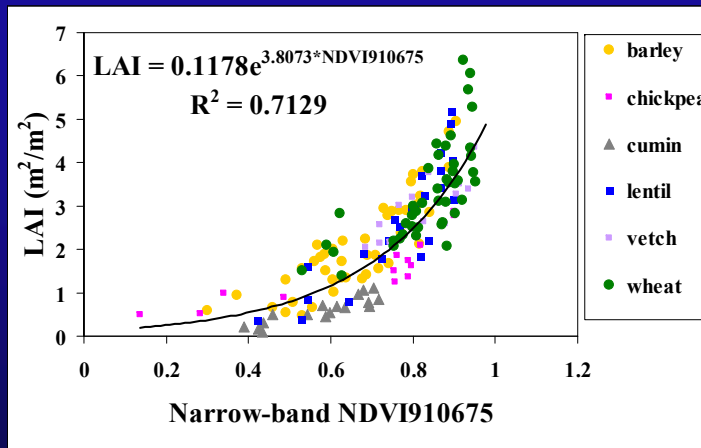
Non-linear biophysical quantities (e.g., biomass, LAI) vs.: (a) Broadband models (top two), & (b) Narrowband HTBVI models (bottom two)



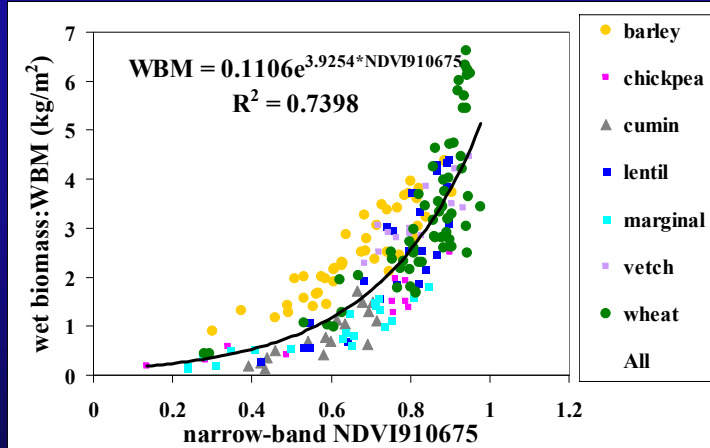
broad-band NDVI43 vs. LAI



broad-band NDVI43 vs. WBM



narrow-band NDVI43 vs. LAI



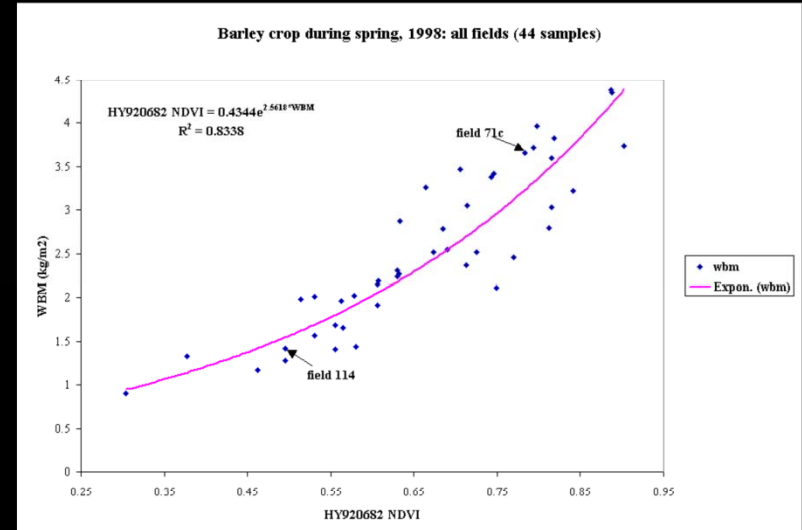
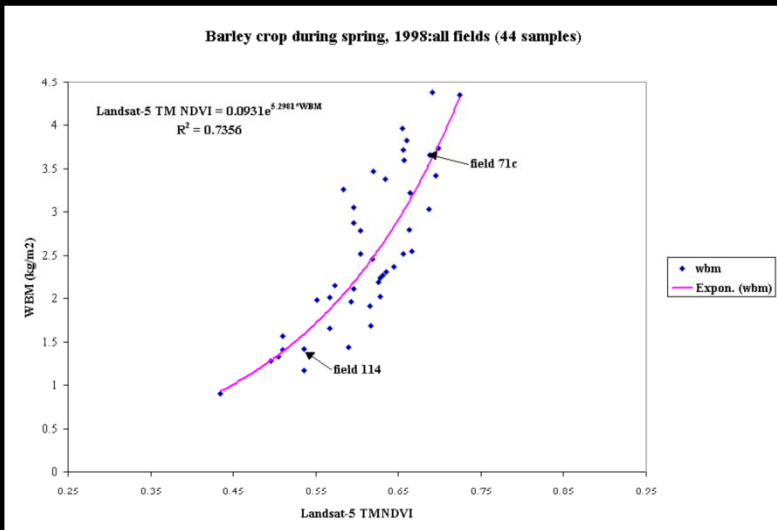
narrow-band NDVI43 vs. WBM

HTBVIs explain about 13 percent Greater Variability than Broad-band TM indices in modeling LAI and biomass



# Methods of Modeling Vegetation Characteristics using Hyperspectral Indices

## Non-linear biophysical quantities (e.g., Yield) vs.: (a)Broadband models (left), & (b)Narrowband HTBVI models (right)

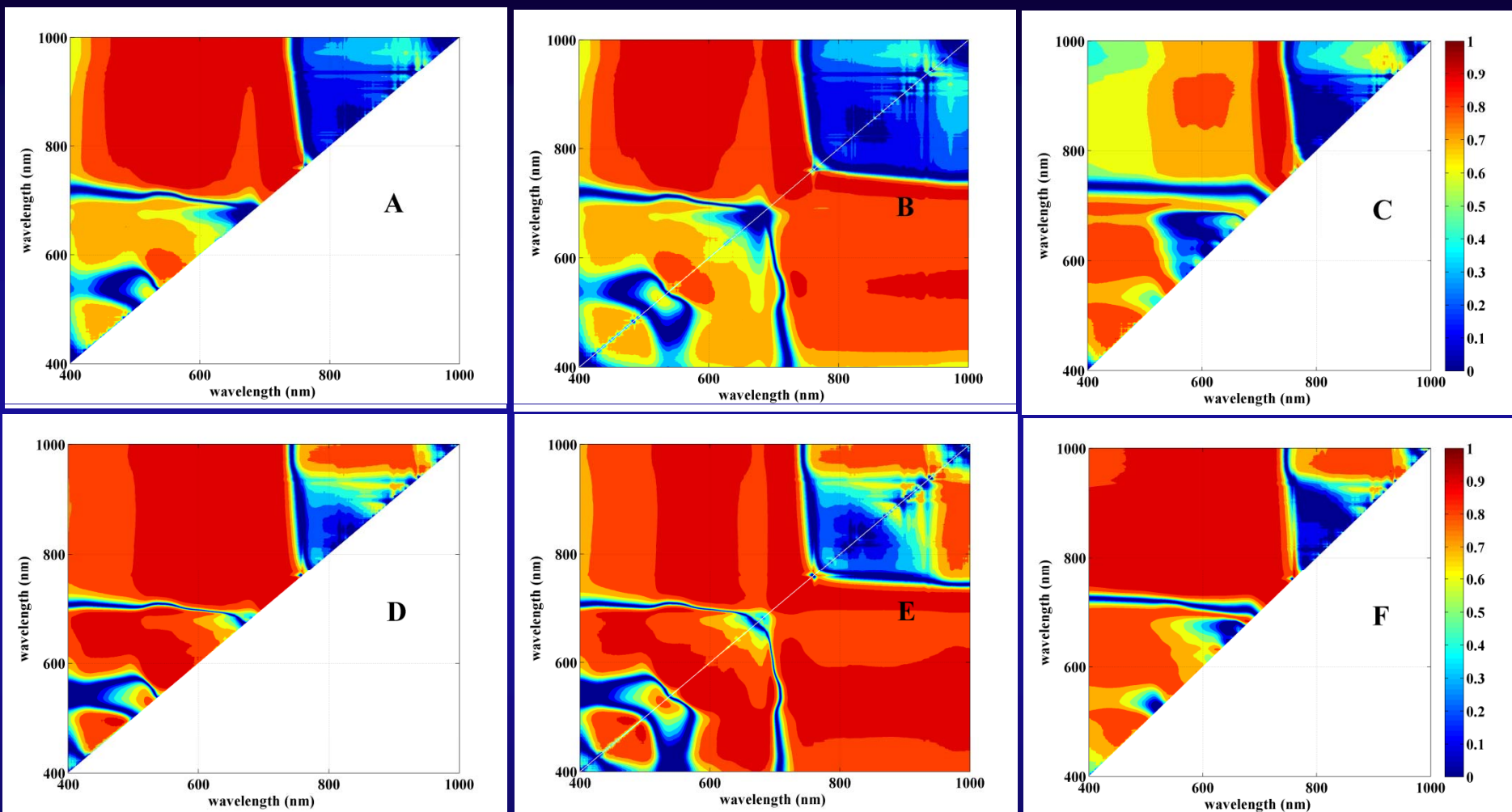


Narrow-band index explains about 10 % higher variability in Barley Crop Yield when compared with broad-band index



# Methods of Modeling Vegetation Characteristics using Hyperspectral Indices

Lambda vs. Lambda R-square contour plot on non-linear biochemical quantity (e.g., leaf Nitrogen) vs. HTBVI models



Contour maps of relative  $R^2$ -values for linear relationships of NDVI(A & D), RVI(B & E) and DVI(C & F) against canopy leaf nitrogen content during mid-late growing periods of rice (A, B, C) and wheat (D, E, F).

Note: see chapter 8

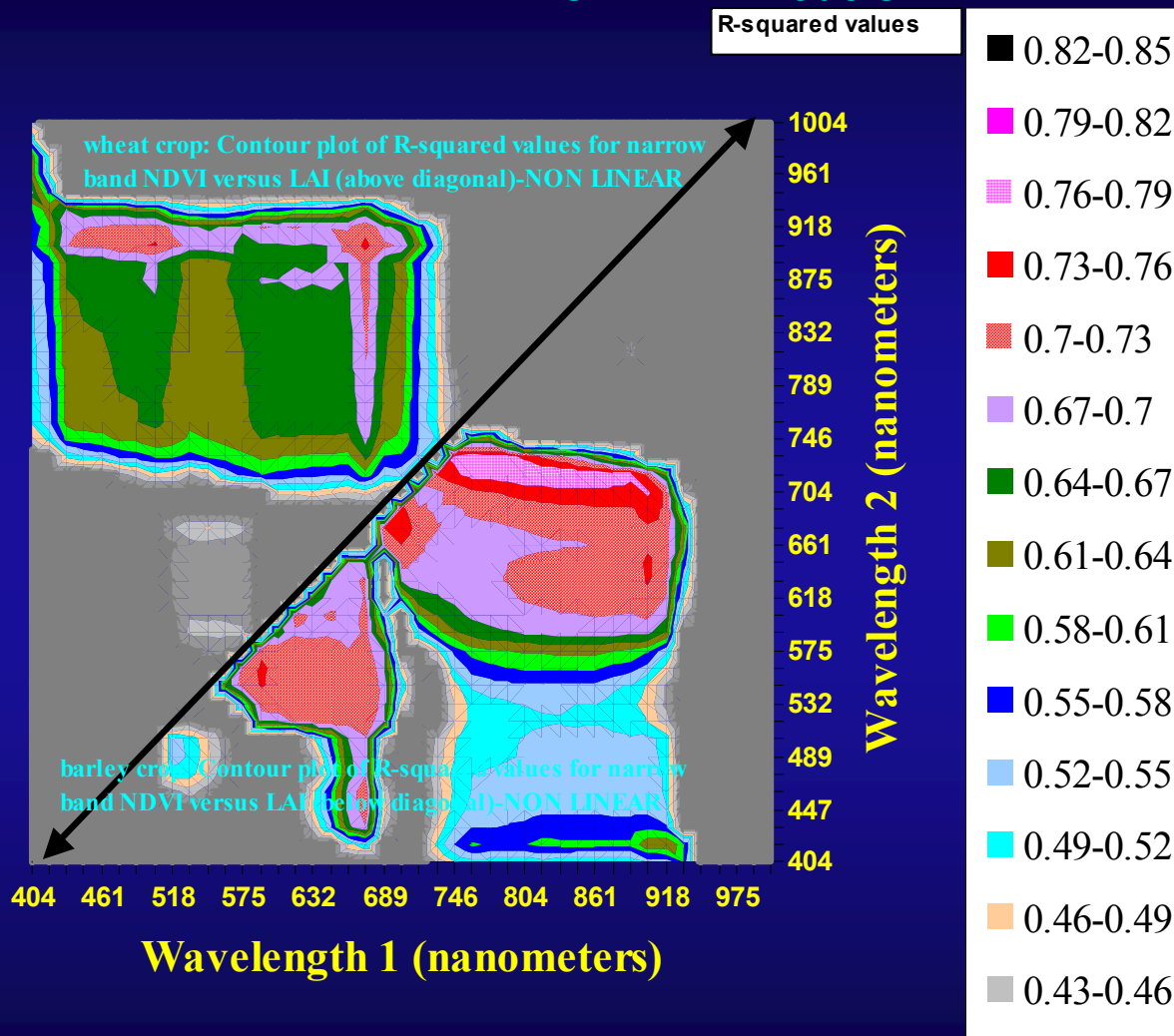


U.S. Geological Survey  
U.S. Department of Interior



# Methods of Modeling Vegetation Characteristics using Hyperspectral Indices

## Lambda vs. Lambda R-square contour plot on non-linear biophysical quantity (e.g., LAI) vs. HTBVI models

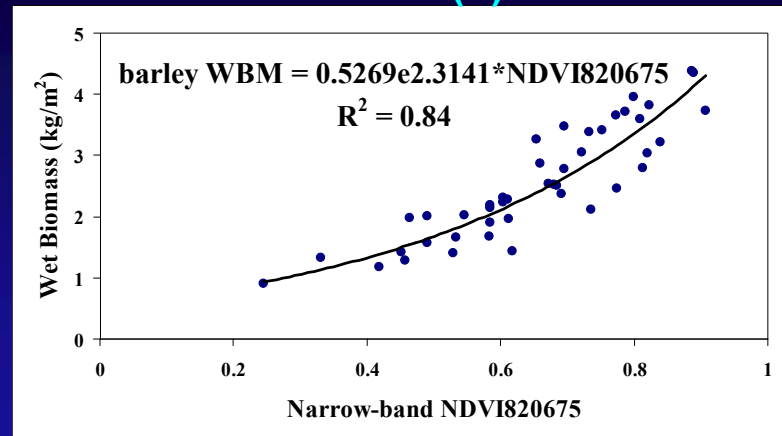


Look at the band combinations of HTBVIs that provide high R-squared values.....these are the band combinations you need for modeling crop biophysical variables.

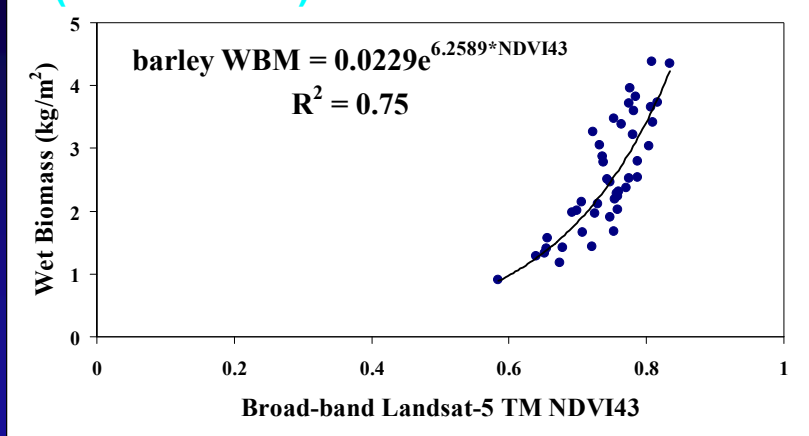


# Methods of Modeling Vegetation Characteristics using Hyperspectral Indices

## Non-linear biophysical quantities (e.g., biomass) vs.: (a) Broadband models (top two), & (b) Narrowband HTBVI models (bottom two)

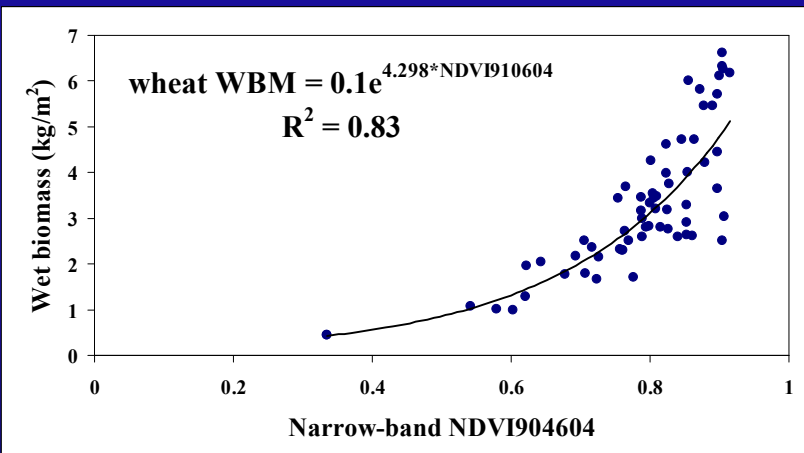


narrow-band NDVI820675 vs. WBM

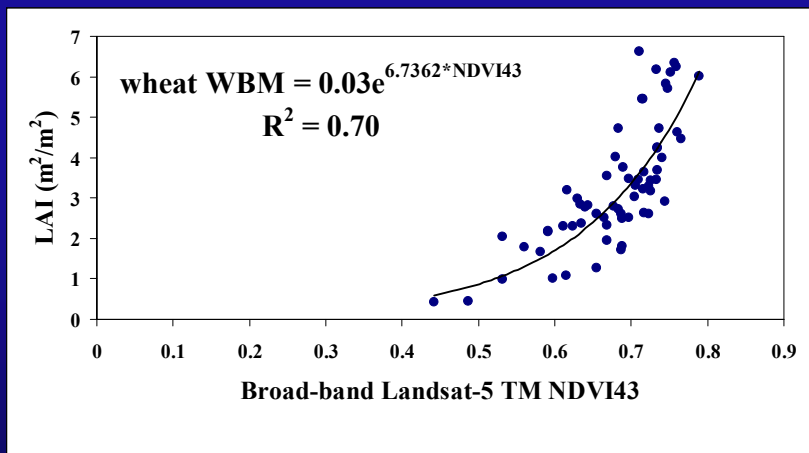


broad-band NDVI43 vs. WBM

HTBVIs  
explain  
about 13  
percent  
Greater  
Variability  
than  
Broad-  
band TM  
indices in  
modeling  
LAI and  
biomass



narrow-band NDVI910604 vs. WBM

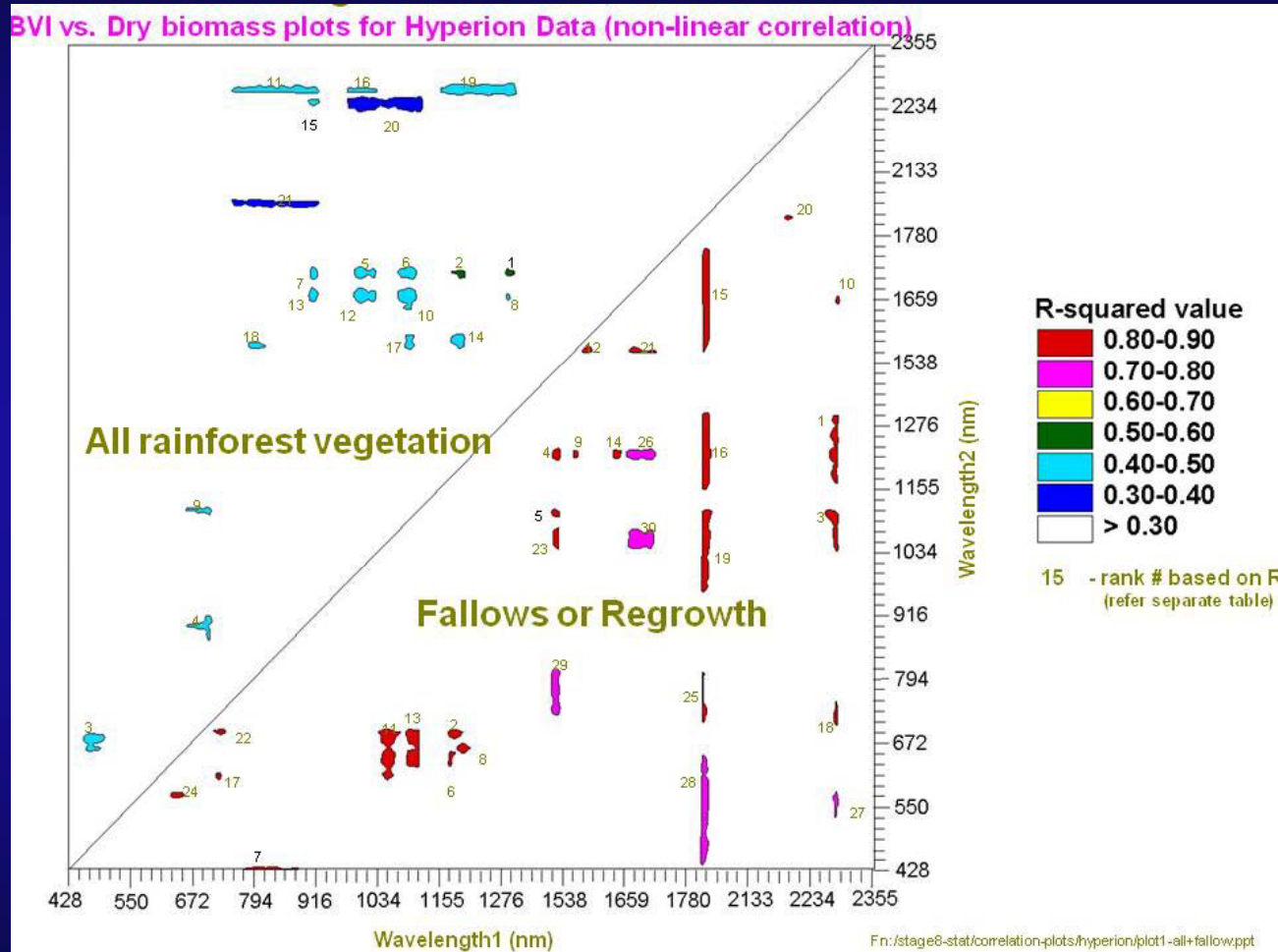


broad-band NDVI43 vs. WBM



# Methods of Modeling Vegetation Characteristics using Hyperspectral Indices

## Lambda vs. Lambda R-square contour plot on non-linear biophysical quantity (e.g., biomass) vs. HTBVI models



Waveband combinations with greatest  $R^2$  values  
Greater are ranked.....bandwidths can also be determined.



# Hyperspectral Data (Imaging Spectroscopy data)

## HVIs: Biophysical, Biochemical, Pigment, Water, Lignin and cellulose, and Physiology

Spectral index	Characteristics & functions	Definition	Reference
<b>Multiple bioparameters:</b>			
<b>LI</b> , Lepidium Index	To be sensitive to the uniformly bright reflectance displayed by <i>Lepidium</i> in the visible range.	$R_{630}/R_{586}$	[20]
<b>NDVI</b> , Normalized Difference Vegetation Index	Respond to change in the amount of green biomass and more efficiently in vegetation with low to moderate density.	$(R_{NIR}-R_R)/(R_{NIR}+R_R)$	[74]
<b>PSND</b> , Pigment-Specific Normalized Difference	Estimate LAI and carotenoids (Cars) at leaf or canopy level	$(R_{800}-R_{470})/(R_{800}+R_{470})$	[74]
<b>SR</b> , Simple Ratio	Same as <b>NDVI</b>	$R_{NIR}/R_R$	[76,77]
<b>Pigments:</b>			
<b>Chl<sub>green</sub></b> , Chlorophyll Index Using Green Reflectance	Estimate chlorophylls (Chls) content in anthocyanin-free leaves if NIR is set	$(R_{760-800}/R_{540-560})-1$	[78]
<b>Chl<sub>red-edge</sub></b> , Chlorophyll Index Using Red Edge Reflectance	Estimate Chls content in anthocyanin-free leaves if NIR is set	$(R_{760-800}/R_{690-720})-1$	[78]
<b>LCI</b> , Leaf Chlorophyll Index	Estimate Chl content in higher plants, sensitive to variation in reflectance caused by Chl absorption	$(R_{850}-R_{710})/(R_{850}+R_{680})$	[79]
<b>mND<sub>680</sub></b> , Modified Normalized Difference	Quantify Chl content and sensitive to low content at leaf level.	$(R_{800}-R_{680})/(R_{800}+R_{680}-2R_{445})$	[80]
<b>mND<sub>705</sub></b> , Modified Normalized Difference	Quantify Chl content and sensitive to low content at leaf level. <b>mND<sub>705</sub></b> performance better than <b>mND<sub>680</sub></b>	$(R_{750}-R_{705})/(R_{750}+R_{705}-2R_{445})$	[80,81]
<b>mSR<sub>705</sub></b> , Modified Simple Ratio	Quantify Chl content and sensitive to low content at leaf level.	$(R_{750}-R_{445})/(R_{705}-R_{445})$	[80]

Note: see chapter 19, Pu et al.



# Hyperspectral Data (Imaging Spectroscopy data)

## HVIs: Biophysical, Biochemical, Pigment, Water, Lignin and cellulose, and Physiology

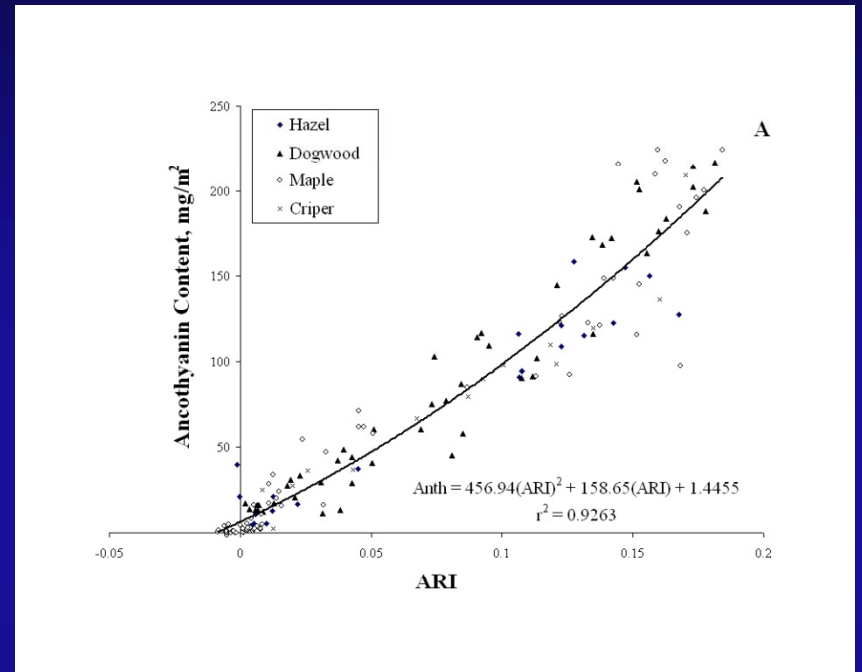
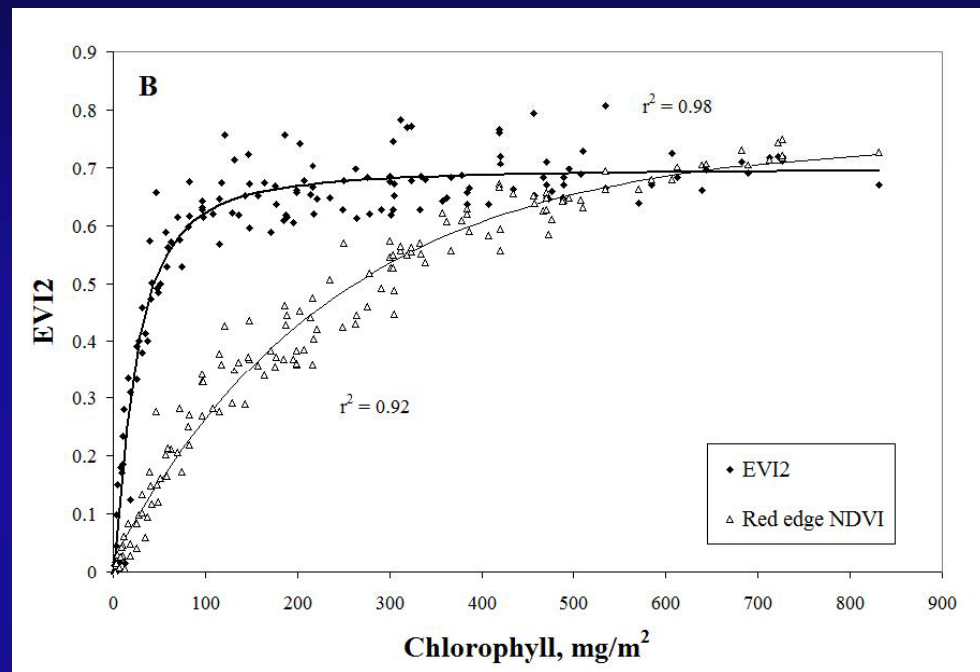
<b>mSR<sub>705</sub></b> , Modified Simple Ratio	Quantify Chl content and sensitive to low content at leaf level.	$(R_{750}-R_{445})/(R_{705}-R_{445})$	[80]
<b>NPCI</b> , Normalized Pigment Chlorophyll ratio Index	Assess Cars/Chl ratio at leaf level	$(R_{680}-R_{430})/(R_{680}+R_{430})$	[82]
<b>PBI</b> , Plant Biochemical Index	Retrieve leaf total Chl and nitrogen concentrations from satellite hyperspectral data	$R_{810}/R_{560}$	[83]
<b>PRI</b> , Photochemical / Physiological Reflectance Index	Estimate Car pigment contents in foliage	$(R_{531}-R_{570})/(R_{531}+R_{570})$	[84]
<b>PI2</b> , Pigment index 2	Estimate pigment content in foliage	$R_{695}/R_{760}$	[85]
<b>RGR</b> , Red:Green Ratio	Estimate anthocyanin content with a green and a red band	$R_{683}/R_{510}$	[80,86]
<b>SGR</b> , Summed Green Reflectance	Quantify Chl content	Sum of reflectances from 500 to 599 nm	[81]
<b>Foliage chemistry:</b>			
<b>CAI</b> , Cellulose Absorption Index	Cellulose & lignin absorption features, discriminates plant litter from soils	$0.5(R_{2020}+R_{2220})-R_{2100}$	[87]
<b>NDLI</b> , Normalized Difference Lignin Index	Quantify variation of canopy lignin concentration in native shrub vegetation	$[\log(1/R_{1754})-\log(1/R_{1680})] / [\log(1/R_{1754})+\log(1/R_{1680})]$	[88]
<b>NDWI</b> , ND Water Index	Improving the accuracy in retrieving the vegetation water content at both leaf and canopy levels	$(R_{860}-R_{1240})/(R_{860}+R_{1240})$	[89,90]
<b>RVI<sub>hyp</sub></b> , Hyperspectral Ratio VI	Quantify LAI and water content at canopy level.	$R_{1088}/R_{1148}$	[91]
<b>WI</b> , Water Index	Quantify relative water content at leaf level	$R_{900}/R_{970}$	[92]

Note: see chapter 19, Pu et al.



# Methods of Modeling Vegetation Characteristics using Hyperspectral Indices

## Non-linear Pigments\biochemical quantities (e.g., Chlorophyll, Anthrocyanin, Carotenoids, Nitrogen) vs. Narrowband HTBVI models (bottom two)



Note: see chapter 6, 15

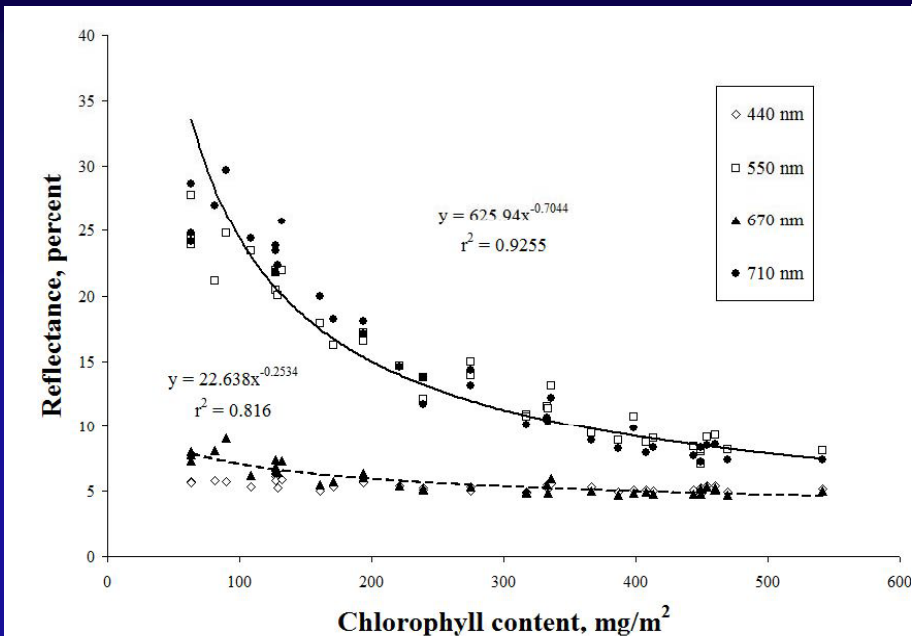


U.S. Geological Survey  
U.S. Department of Interior



# Methods of Modeling Vegetation Characteristics using Hyperspectral Indices

## Non-linear Pigments\biochemical quantities (e.g., Chlorophyll, Anthrocyanin, Carotenoids, Nitrogen) vs. Narrowband HTBVI models (bottom two)



Property (BB-PAC)	Example crops	Agro-technical management parameter
<i>Biophysical</i>		
Biomass [ $\text{kg m}^{-2}$ ]	wheat, rice, corn	fertilization
Leaf Area Index/ Crop cover [No units / %]	wheat, soybean, corn, cotton	fertilization
Crop height [m]	cotton, wheat	irrigation, application of growth regulators
Canopy volume [ $\text{m}^3$ ]	orchards, wheat	irrigation, fertilization
Yield [ $\text{kg m}^{-2}$ ]	wheat, corn, cotton	-
Stomata conductance [ $\text{mmol sec}^{-1}$ ]	vineyards	irrigation
Leaf/Stem water potential [MPa]	cotton, orchards, vineyards	irrigation
Flowering intensity [Relative units]	orchards	growth regulators, mechanical thinning
<i>Biochemical</i>		
Nitrogen content [%N]	corn, wheat, potatoes	fertilization
Chlorophyll content [ $\mu\text{g cm}^{-2}$ ]	corn, wheat, cotton	fertilization
Salinity [ $\text{mg l}^{-1}$ ]	cotton	water quality management, not used in practice
Leaf water content [%]	wheat, potato	irrigation
Leaf macro-elements like phosphorus (P) and potassium (K) [ $\text{mg Kg}^{-1}$ ]	olives	fertilization, not used in practice

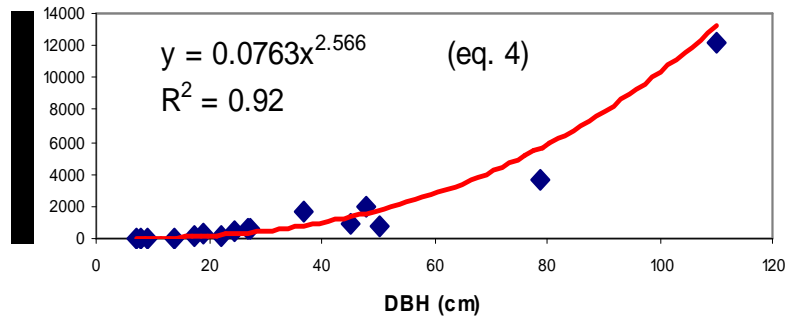
Note: see chapter 6, 15, 25



# Developing Allometric Equations in African Rainforests



Dry weight vs. dbh



## Methods of Modeling Vegetation Characteristics using Hyperspectral Indices

### Hyperspectral Multi-band Vegetation Indices (HMBVIs)

$$HMBVI_i = \sum_{j=1}^N a_{ij} R_j$$

where, OMBVI = crop variable i, R = reflectance in bands j (j= 1 to N with N=157; N is number of narrow wavebands); a = the coefficient for reflectance in band j for i th variable.

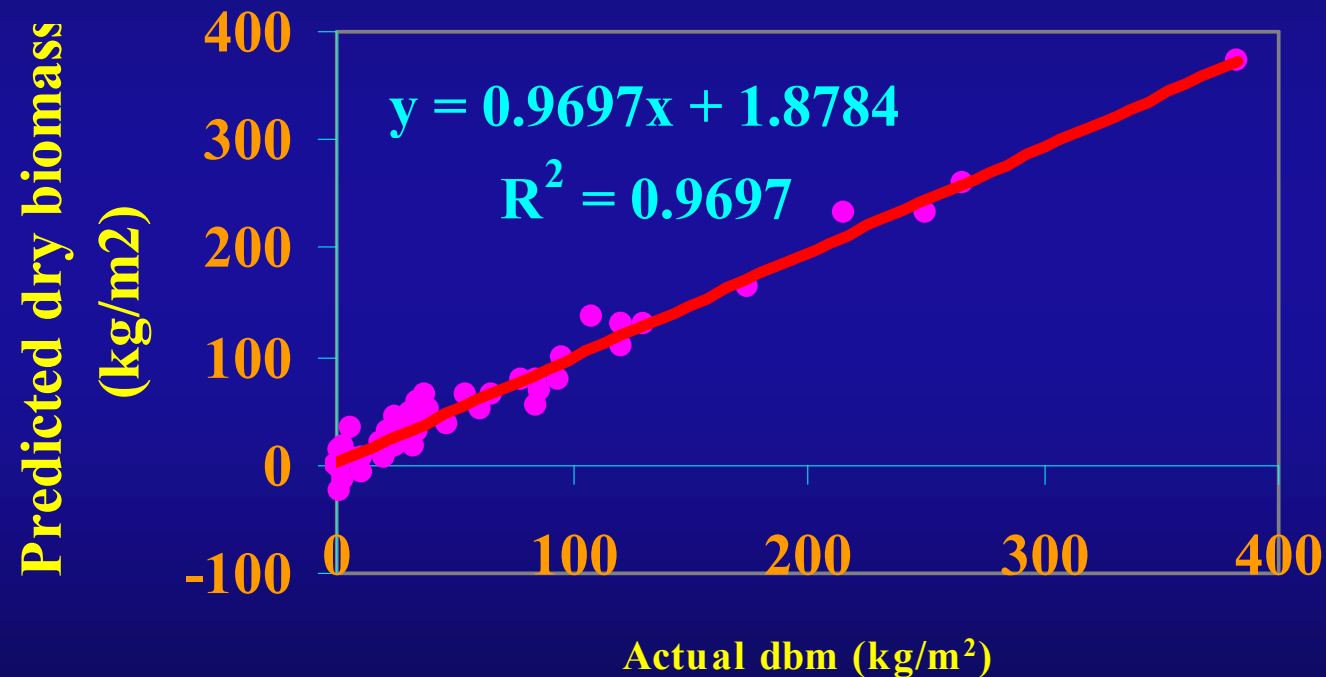
Model algorithm: MAXR procedure of SAS (SAS, 1997) is used in this study. The MAXR method begins by finding the variable ( $R_j$ ) producing the highest coefficient of determination ( $R^2$ ) value. Then another variable, the one that yields the greatest increase in  $R^2$  value, is added.....and so on.....so we will get the best 1-variable model, best 2-variable model, and so on to best n-variable model.....when there is no significant increase in  $R^2$ -value when an additional variable is added, the model can stop.



## Methods of Modeling Vegetation Characteristics using Hyperspectral Indices

Predicted biomass derived using MBVI involving 21 narrowbands vs. Actual biomass

21 bands predicting biomass compared to actual biomass of all rainforest vegetation

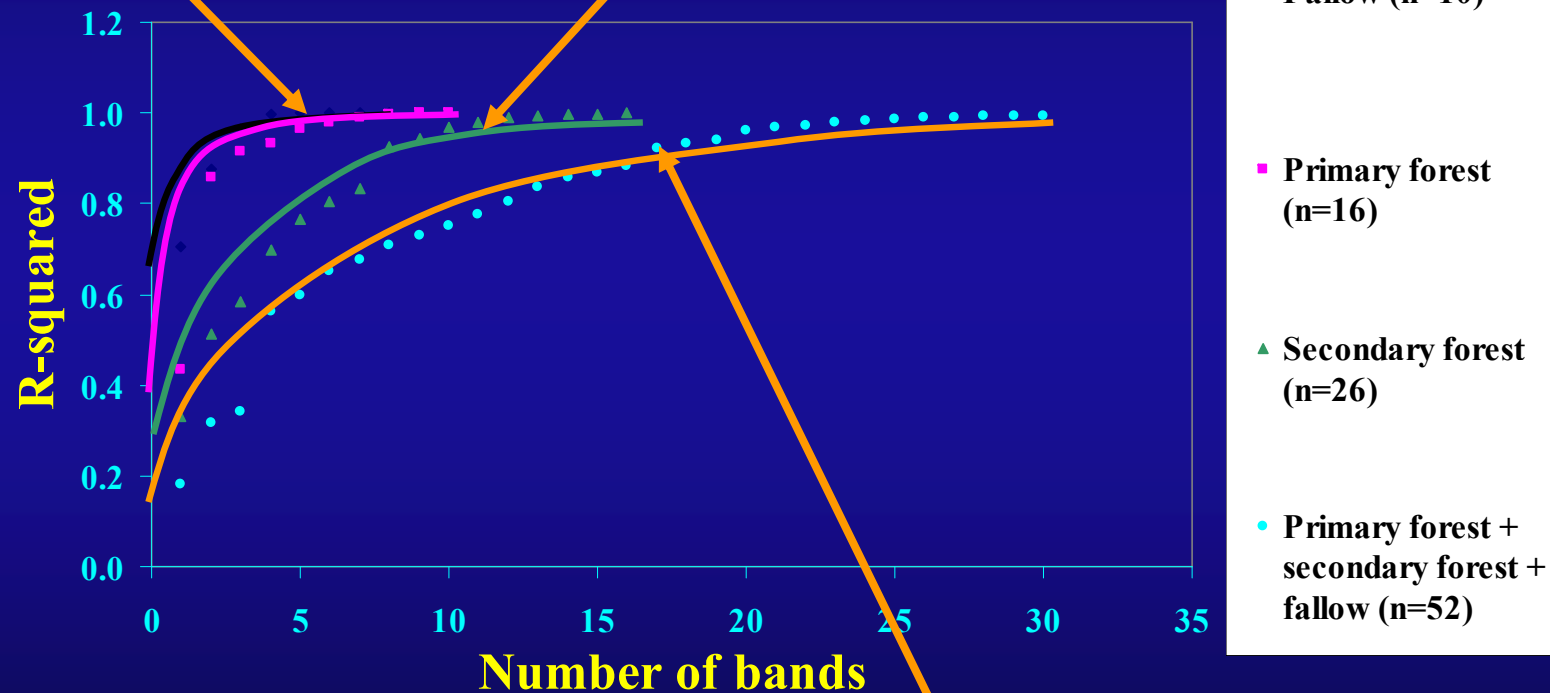


# Methods of Modeling Vegetation Characteristics using Hyperspectral Indices

Predicted biomass derived using MBVI's involving various narrowbands in African Rainforests

Note: Increase in  $R^2$  values beyond 6 bands is negligible

Note: Increase in  $R^2$  values beyond 11 bands is negligible



Note: Increase in  $R^2$  values beyond 17 bands is negligible



# Methods of Modeling Vegetation Characteristics using Hyperspectral Indices

## Hyperspectral Derivative Greenness Vegetation Indices (DGVIs)

### First Order Hyperspectral Derivative Greenness Vegetation Index (HDGVI) (Elvidge and Chen, 1995):

These indices are integrated across the (a) chlorophyll red edge: 626-795 nm, (b) Red-edge more appropriately 690-740 nm.....and other wavelengths.

$$\text{DGVI}_1 = \frac{\lambda_n (\rho'(\lambda_i) - \rho'(\lambda_j))}{\lambda_1 \Delta \lambda_i}$$

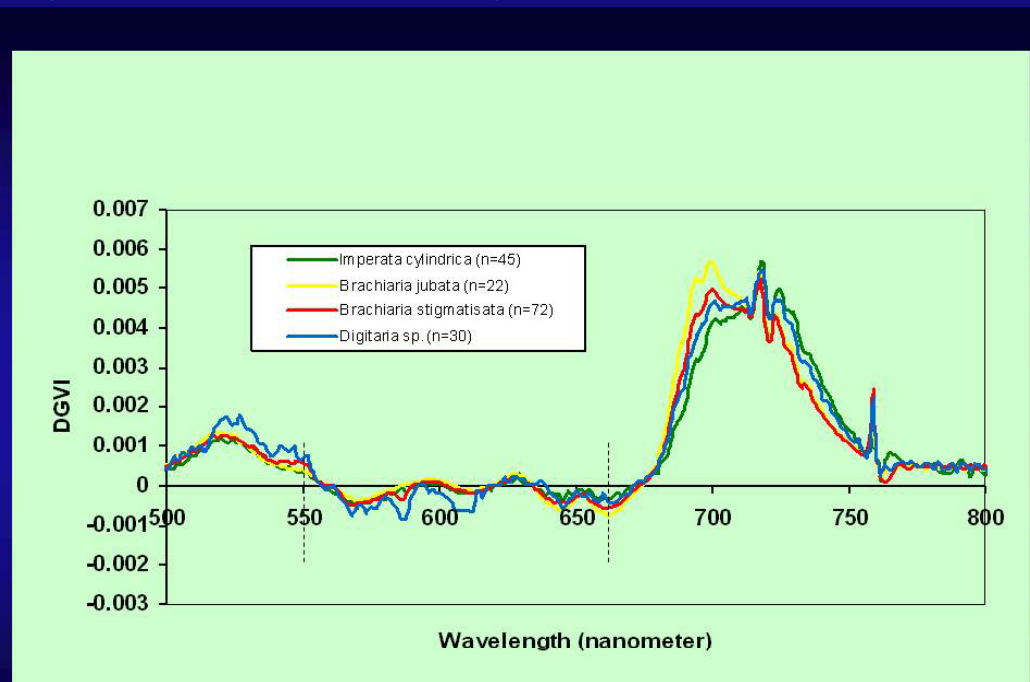
Where, i and j are band numbers,

$\lambda$  = center of wavelength,

$\lambda_1 = 0.626 \mu\text{m}$ ,

$\lambda_n = 0.795 \mu\text{m}$ ,

$\rho'$  = first derivative reflectance.

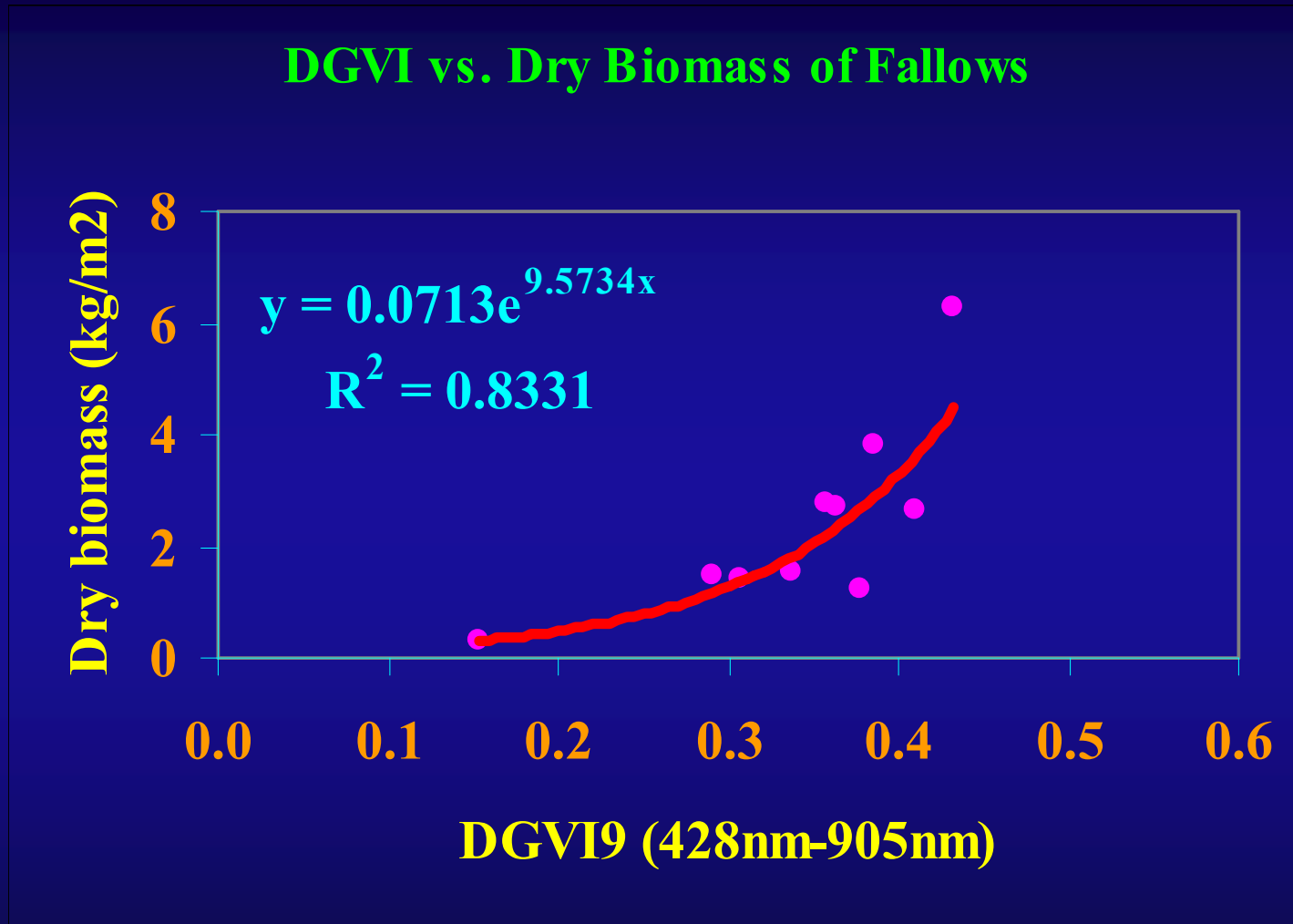


Note: HDGVIs are near-continuous narrow-band spectra integrated over certain wavelengths



## Methods of Modeling Vegetation Characteristics using Hyperspectral Indices

### Hyperspectral Derivative Greenness Vegetation Indices (DGVI<sub>s</sub>) vs. Forest Biomass



# Rainforest Vegetation Studies: biomass, tree height, land cover, species in African Rainforests



Fallows biomass

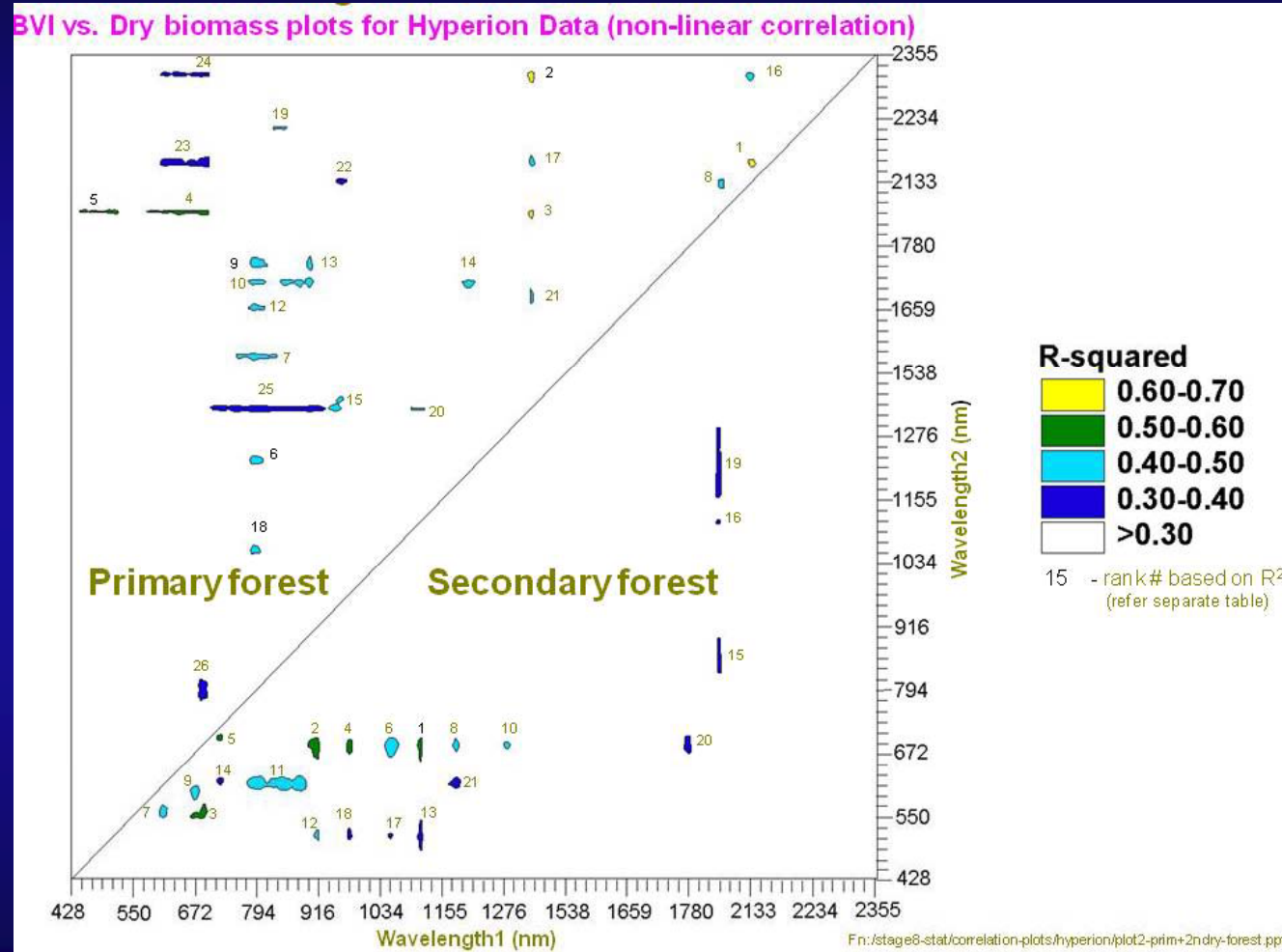


Tree height



# Methods of Modeling Vegetation Characteristics using Hyperspectral Indices

## Lambda vs. Lambda R-square contour plot on non-linear biophysical quantity (e.g., biomass) vs. HTBVI models



Waveband combinations with greatest R<sup>2</sup> values  
Greater are ranked.....bandwidths can also be determined.

HTBVI vs. Dry Biomass for Primary and Secondary Forests Across the Hyperion Spectral Regions of 400-2500 nm



# Methods of Modeling Vegetation Characteristics using Hyperspectral Indices

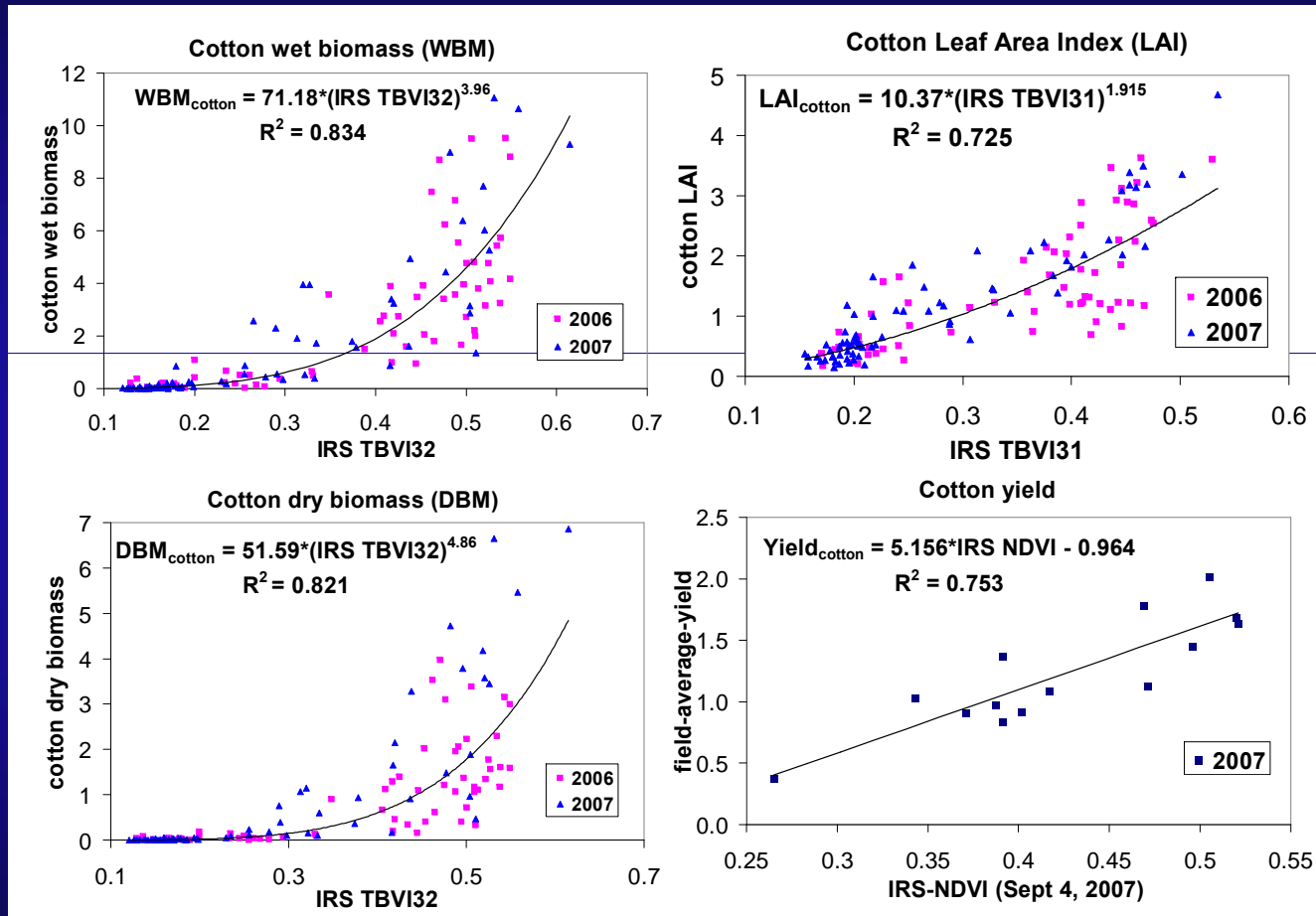
## Selecting Best Indices and Wavebands from Lambda by Lambda R-square Plots

Crop	Parameter	Sensor	Best bands				Best indices		
			sample size	Best model	band	R-square	band combination		R-square
							Best model	combination	
Cotton	Wet Biomass	IRS	140	Exp	2	0.697	Power	2, 3	<b>0.834</b>
		QB	41	Multi-linear	1, 4	<b>0.813</b>	Multi-linear	1,4; 3,4	0.506
	Dry Biomass	IRS	136	Power	2	0.620	Power	2, 3	<b>0.821</b>
		QB	41	Exp	2	0.521	Exp	1, 2	<b>0.661</b>
	LAI	IRS	135	Multi-linear	3, 4	0.634	Power	1, 3	<b>0.725</b>
		QB	41	Multi-linear	2, 4	0.511	Quadratic	2, 4	<b>0.574</b>
	Yield	IRS <sup>A</sup>	14				Linear	2, 3	<b>0.753</b>
		QB <sup>B</sup>	7				Linear	3, 4	<b>0.610</b>
Wheat	Wet Biomass	IRS	9	Quadratic	2	0.425	Quadratic	1, 3	<b>0.678</b>
	Dry Biomass	IRS	14	Quadratic	1	0.205	Quadratic	3, 4	<b>0.309</b>
	LAI	IRS	18	Quadratic	4	<b>0.8</b>	Multi-linear	1,3; 2,3	0.465
	Yield	IRS	12				Linear	2, 3	<b>0.67</b>
Maize <sup>D</sup>	Wet Biomass	IRS	19	Power	2	0.815	Power	2, 3	<b>0.871</b>
	Dry Biomass	IRS	17	Exp	2	<b>0.928</b>	Power	2, 3	0.903
	LAI	IRS	19	Multi-linear	1, 3	0.777	Multi-linear	1,2; 2,3	<b>0.839</b>
Rice <sup>E</sup>	Wet Biomass	QB	10	Multi-linear	1, 2	0.535	Multi-linear	1,2; 2,4	<b>0.600</b>
	Dry Biomass	QB	10	Multi-linear	1, 2	0.395	Multi-linear	1,3; 2,3	<b>0.414</b>
	LAI	QB	10	Multi-linear	2, 4	<b>0.879</b>	Quadratic	2, 3	0.234
Alfalfa	Wet Biomass	IRS	21	Power	2	0.838	Quadratic	1, 2	<b>0.853</b>
		QB	8	Multi-linear	2, 4	0.772	Multi-linear	1,2; 2,3; 3,4	<b>0.887</b>
	Dry Biomass	IRS	21	Power	2	<b>0.817</b>	Exp	1, 2	0.812
		QB	8	Multi-linear	2, 4	0.732	Multi-linear	1,2; 2,3; 3,4	<b>0.867</b>
	LAI	IRS	21	Power	3	0.499	Exp	3, 4	<b>0.639</b>
		QB	8	Multi-linear	1, 3, 4	<b>0.927</b>	Multi-linear	1,3; 3,4	0.858



# Methods of Modeling Vegetation Characteristics using Hyperspectral Indices

Plots of some of the best R-square Values between narrowband indices vs. biophysical quantities



# Methods of Modeling Vegetation Characteristics using Hyperspectral Indices

## Some Common Narrowband Indices

Narrow-band vegetation indices calculated from Hyperion data.

Vegetation Index	Formula <sup>a</sup>	Reference
<b>ARVI</b>	$(\rho_{864} - (2*\rho_{671} - \rho_{467})) / (\rho_{864} + (2*\rho_{671} - \rho_{467}))$	Kaufman and Tanré [37]
<b>EVI</b>	$2.5 * ((\rho_{864} - \rho_{671}) / (\rho_{864} + 6 * \rho_{671} - 7.5 * \rho_{467} + 1))$	Huete et al. [38]
<b>NDVI</b>	$(\rho_{864} - \rho_{671}) / (\rho_{864} + \rho_{671})$	Rouse et al. [39]
<b>SR</b>	$\rho_{864}/\rho_{671}$	Rouse et al. [39]
<b>SGI</b>	$(\rho_{508} + \rho_{518} + \rho_{528} + \rho_{538} + \rho_{549} + \rho_{559} + \rho_{569} + \rho_{579} + \rho_{590} + \rho_{600}) / 10$	Lobell and Asner [4]
<b>NDII</b>	$(\rho_{823} - \rho_{1649}) / (\rho_{823} + \rho_{1649})$	Hunt Jr. and Rock [40]
<b>NDWI</b>	$(\rho_{854} - \rho_{1245}) / (\rho_{854} + \rho_{1245})$	Gao [41]
<b>WBI</b>	$\rho_{905}/\rho_{973}$	Penuelas et al. [42]
<b>LWVI-2</b>	$(\rho_{1094} - \rho_{1205}) / (\rho_{1094} + \rho_{1205})$	Galvão et al. [13]
<b>DWSI</b>	$\rho_{803}/\rho_{1598}$	Apan et al. [43]
<b>MSI</b>	$\rho_{1598}/\rho_{823}$	Hunt Jr. and Rock [40]
<b>PSRI</b>	$(\rho_{681} - \rho_{498}) / \rho_{752}$	Merzlyak et al. [44]
<b>CRI</b>	$(1/\rho_{508}) - (1/\rho_{701})$	Gitelson et al. [45]
<b>ARI</b>	$(1/\rho_{549}) - (1/\rho_{701})$	Gitelson et al. [46]
<b>PRI</b>	$(\rho_{529} - \rho_{569}) / (\rho_{529} + \rho_{569})$	Gamon et al. [47]
<b>SICI</b>	$(\rho_{803} - \rho_{467}) / (\rho_{803} + \rho_{681})$	Penuelas et al. [48]
<b>RENDVI</b>	$(\rho_{752} - \rho_{701}) / (\rho_{752} + \rho_{701})$	Gitelson et al. [49]
<b>REP</b>	$(\rho_{n+1} - \rho_n) / 10$ in the 690-750 nm interval	Curran et al. [50]
<b>VOG-1</b>	$\rho_{742}/\rho_{722}$	Vogelmann et al. [51]
<b>VARI</b>	$(\rho_{559} - \rho_{640}) / (\rho_{559} + \rho_{640} - \rho_{467})$	Gitelson et al. [52]
<b>VIg</b>	$(\rho_{559} - \rho_{640}) / (\rho_{559} + \rho_{640})$	Gitelson et al. [52]

<sup>a</sup>  $\rho$  is the reflectance of the closest Hyperion bands ( $n$ , centre in nanometers) to the original wavelength formulations.

Note: see chapter 17

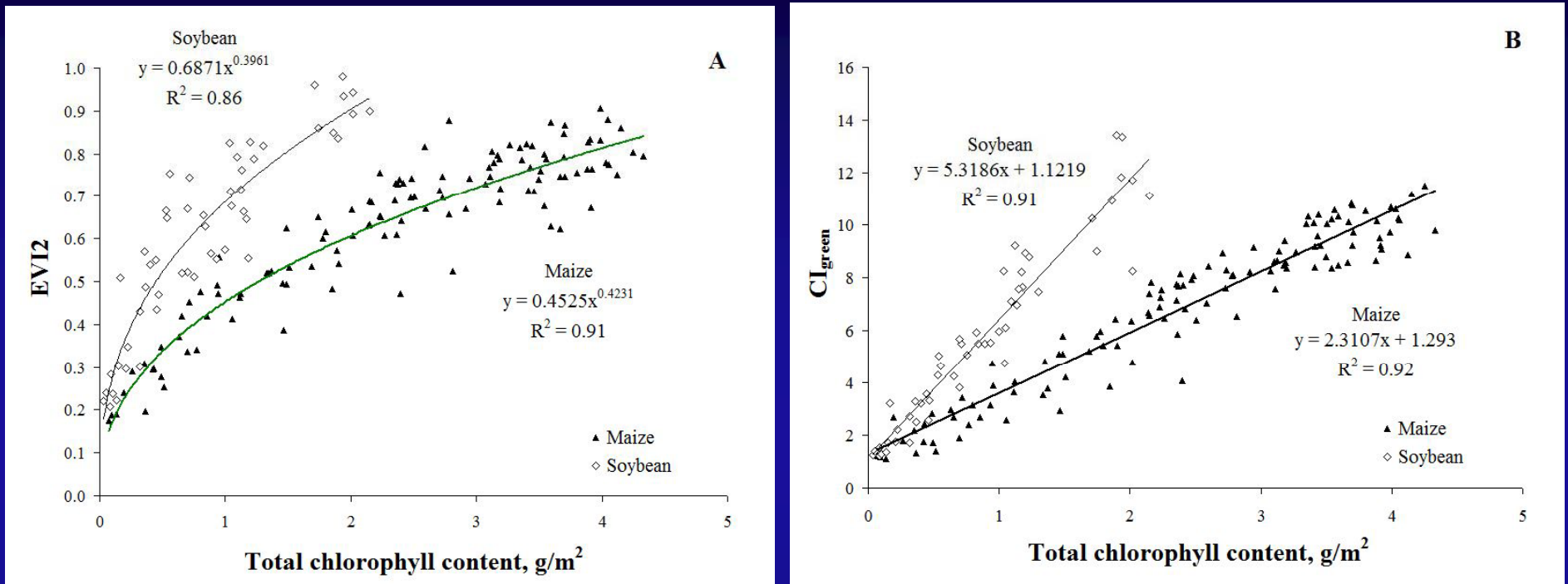


U.S. Geological Survey  
U.S. Department of Interior



# Methods of Modeling Vegetation Characteristics using Hyperspectral Indices

Non-linear Pigments\biochemical quantities (e.g., Chlorophyll, Anthrocyanin, Carotenoids, Nitrogen) vs. Narrowband HTBVI models (bottom two)



Products of Red edge NDVI and CI<sub>red edge</sub> and incident PAR, plotted versus mid day gross primary production in maize (three sites; three years) and soybeans (two sites; two years). Indices were calculated with red edge band

720-740 nm and MODIS NIR band ■

Note: see chapter 15

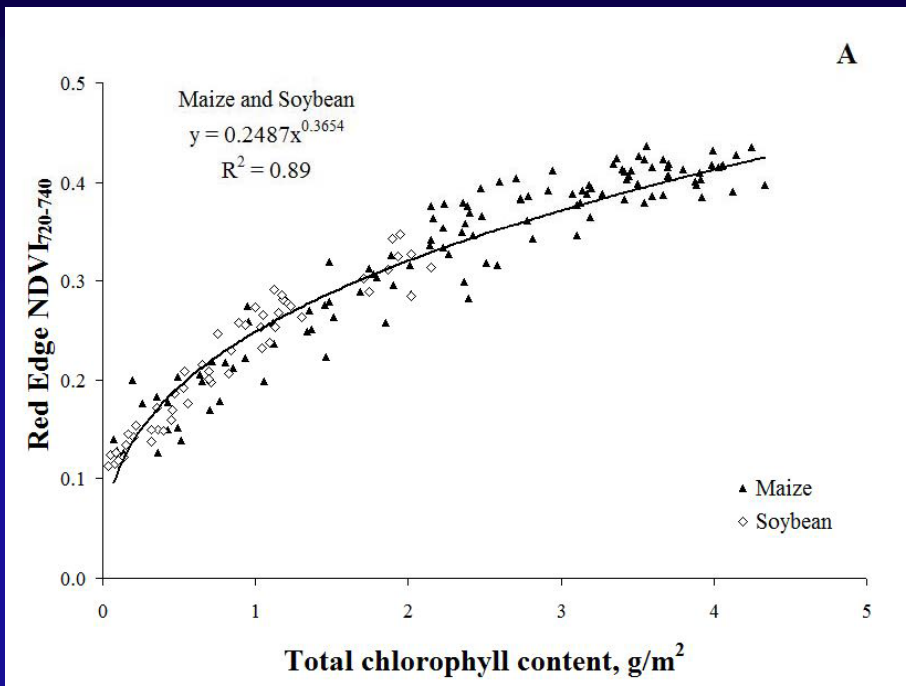


U.S. Geological Survey  
U.S. Department of Interior

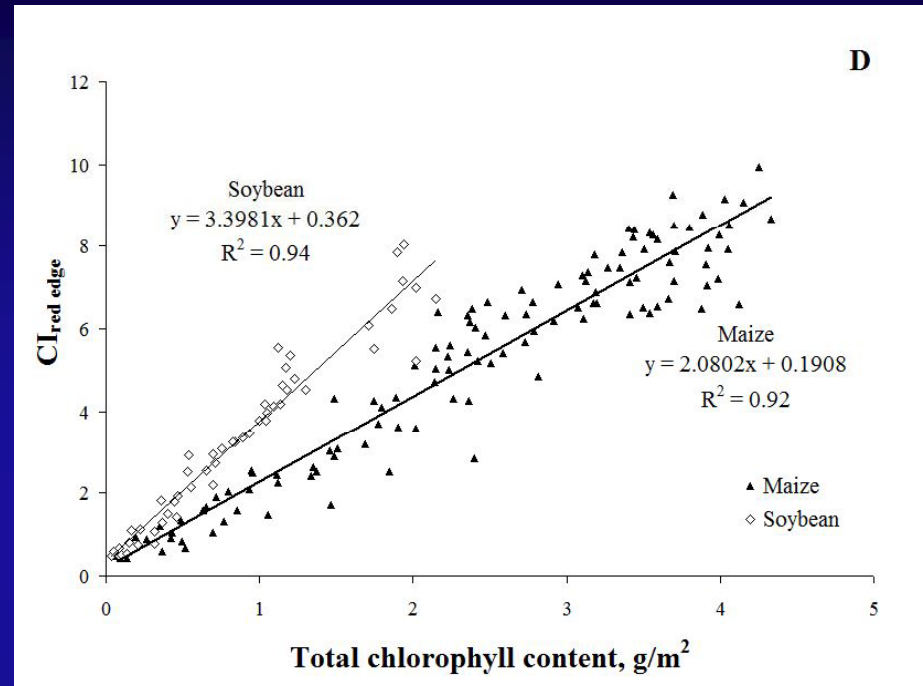


# Methods of Modeling Vegetation Characteristics using Hyperspectral Indices

Non-linear Pigments\biochemical quantities (e.g., Chlorophyll, Anthrocyanin, Carotenoids, Nitrogen) vs. Narrowband HTBVI models (bottom two)



Red Edge NDVI<sub>720-740</sub> and red edge chlorophyll index Cl<sub>720-740</sub> with red edge spectral band 720 to 740 nm



EVI2 and Cl<sub>green</sub>, in spectral bands of MODIS,

Note: see chapter 15



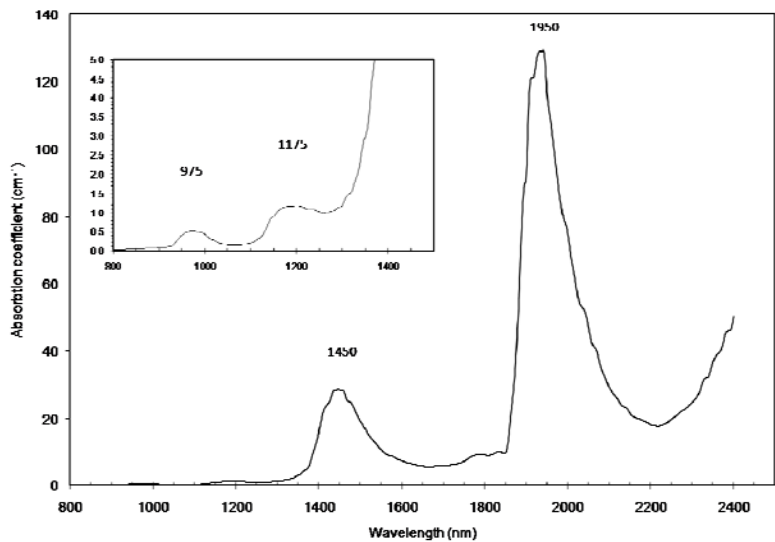
U.S. Geological Survey  
U.S. Department of Interior



# Methods of Modeling Vegetation Characteristics using Hyperspectral Indices

## Some Common Narrowband Indices in infrared (750-1300 nm) and SWIR (1300-2500 nm)

Water absorption coefficients are extremely low in the visible part of the electromagnetic spectrum whereas in the near and short wave infrared four major absorption peaks are present (Figure 10.1). These peaks are located at approximately 975 nm, 1175 nm, 1450 nm, and 1950 nm and increase in magnitude with wavelength.



Note: see chapter 10



U.S. Geological Survey  
U.S. Department of Interior



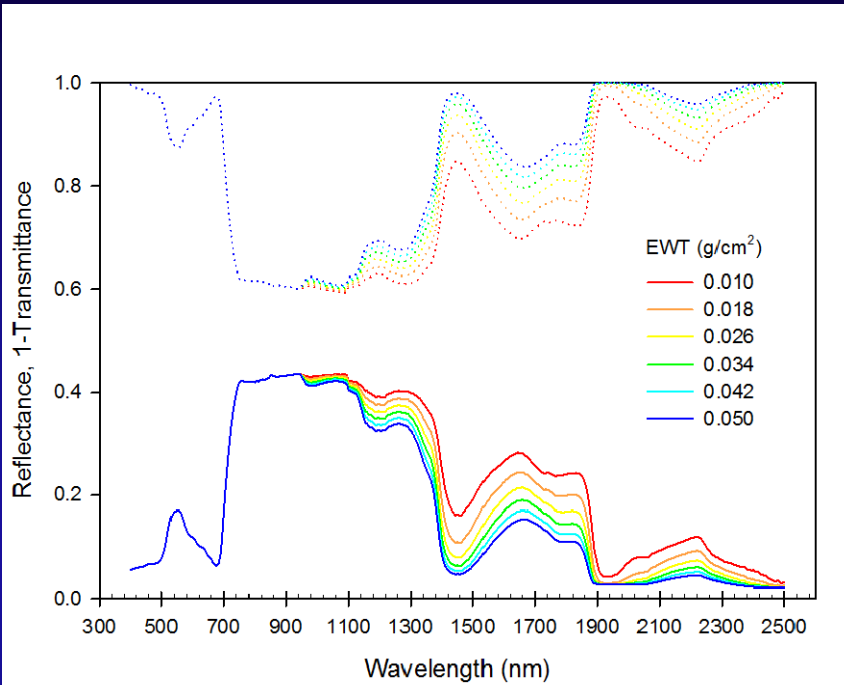
TABLE 10.1.

Summary of reflectance-based indices developed for estimating vegetation water content at different scales (Leaf L, Ground G, Airborne A, Spaceborne S).

Index	Full name	Formulation	Reference	Estimated variable	Level	Device and bandwidth
<b>NIR (750-1300 nm)</b>						
WI	Water Index	$\rho_{900}/\rho_{750}$	[6]	RWC	G	Spectron, 15 nm
NDWI						
	Normalised Difference Water index	$(\rho_{900} - \rho_{1300})/(\rho_{900} + \rho_{1300})$	[41]	EWT <sub>c</sub>	A	MODIS, 20-35 nm
WI/NDVI	Ratio WI Normalised Difference Vegetation Index	$\frac{(\rho_{900}/\rho_{750})}{(\rho_{900} - \rho_{1300})/(\rho_{900} + \rho_{1300})}$	[42]	FMC	G	Spectron, 15 nm
RDI	Relative Depth Index @1175	$(\rho_{max} - \rho_{min})/\rho_{max}$	[16]	EWT <sub>c</sub>	G	GER IRIS MK IV, 2, 4 nm
SRWI	Simple Ratio Water Index	$\rho_{900}/\rho_{1240}$	[43]	EWT <sub>L</sub>	S	MODIS, 20-35 nm
R975	Ratio @975	$2\rho_{900-950}/(\bar{\rho}_{950-940} + \bar{\rho}_{1050-1100})$	[44]	FMC	L	ASD FieldSpec Pro Fr, 1.4, 2 nm
<b>SWIR (1300-2500 nm)</b>						
NDII	Normalised Difference Infrared Index	$(\rho_{1200} - \rho_{1650})/(\rho_{1200} + \rho_{1650})$	[45]	EWT <sub>c</sub>	S	TM, 140, 195 nm
RS/R7	Ratio of TM band 5 to band 7	$\rho_{1650}/\rho_{2210}$	[46]	EWT <sub>L</sub>	A	ATM 195, 340 nm
LWCI	Leaf Water Content Index	$\frac{-\log(1 - (\rho_{1200} - \rho_{1650}))}{-\log(1 - (\rho_{1200,FT} - \rho_{1650,FT}))}$	[47]	RWC	L	MK I TM, 140, 195 nm
MSI	Moisture Stress Index	$\rho_{1600}/\rho_{1200}$	[48, 21]	RWC, EWT <sub>L</sub>	L	GER VIRIS, 3, 12 nm
DRI	Datt Reflectance Index	$(\rho_{2150} - \rho_{2210})/(\rho_{2150} + \rho_{2210})$	[33]	EWT <sub>L</sub>	L	GER IRIS MK IV, 2, 4 nm
GVMI	Global Vegetation Moisture Index	$\frac{(\rho_{1200,MT} + 0.1) - (\rho_{1600} + 0.02)}{(\rho_{1200,MT} + 0.1) + (\rho_{1600} + 0.02)}$	[28]	EWT <sub>c</sub>	S	SPOT VGT 20, 170 nm
RDI1450	Relative Depth Index @1450	$(\rho_{max} - \rho_{min})/\rho_{max}$	[49]	EWT <sub>L</sub>	G	ASD FieldSpec Pro Fr, 1.4, 2 nm
NDWI2130	Normalised Difference Water index @2130	$(\rho_{900} - \rho_{2130})/(\rho_{900} + \rho_{2130})$	[50]	EWT <sub>c</sub>	S	MODIS, 24, 50 nm
NMDI	Normalized Multi-band Drought Index	$\frac{\rho_{2130} - (\rho_{1640} - \rho_{2130})}{\rho_{2130} + (\rho_{1640} - \rho_{2130})}$	[51]	EWT <sub>L</sub>	S	MODIS, 24, 50 nm
MSI/SR	Ratio MSI/Simple Ratio	$\frac{\rho_{1600}}{\rho_{900}} / \frac{\rho_{900}}{\rho_{1250}}$	[52]	EWT <sub>L</sub>	A	MIVIS, 2, 9 nm

# Methods of Modeling Vegetation Characteristics using Hyperspectral Indices

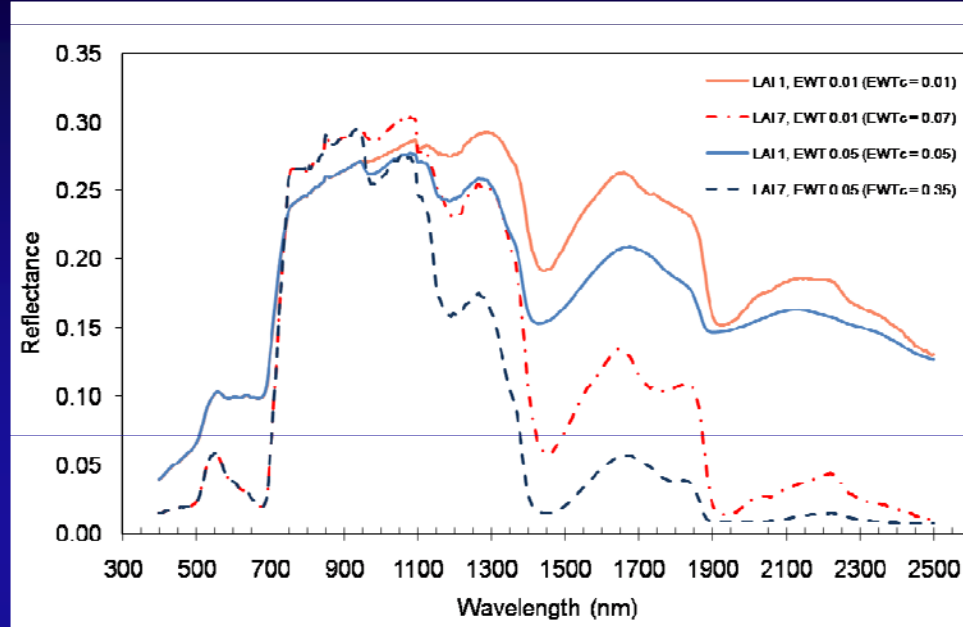
## Some Common Narrowband Indices in infrared (750-1300 nm) and SWIR (1300-2500 nm)



shows leaf reflectance and transmittance simulation results for a leaf characterized by six levels of Equivalent Water Thickness of a leaf ( $EWT_L$ )

$$EWT_L = \frac{FW - DW}{A}$$

FW = fresh weight of leaf  
 DW = dry weight of leaf  
 A = area of leaf, one side



shows the spectral reflectance simulated by PROSAILH for a canopy with different values of LAI and  $EWT_L$ .

Note: see chapter 10



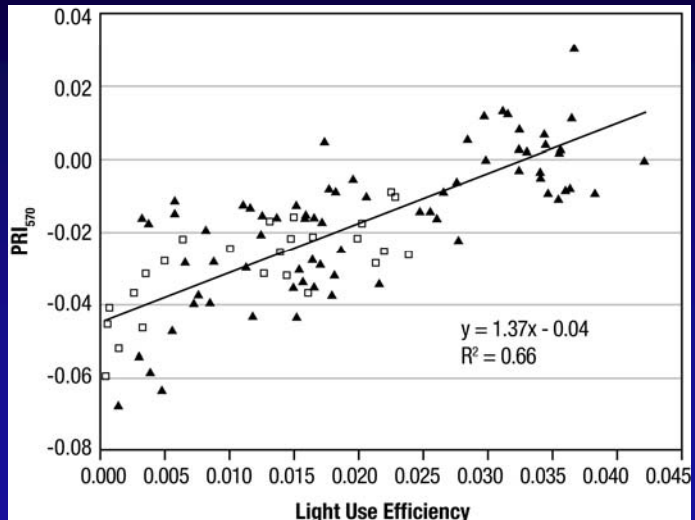
U.S. Geological Survey  
 U.S. Department of Interior

Note: Water absorption coefficients are extremely low in the visible part of the electromagnetic spectrum whereas in the near and short wave infrared four major absorption peaks are present (Figure 10.1). These peaks are located at approximately 975 nm, 1175 nm, 1450 nm, and 1950 nm and increase in magnitude with wavelength.



# Methods of Modeling Vegetation Characteristics using Hyperspectral Indices

Other Narrowband Indices addressing Specific Issues (e.g., Pigments, Photochemical reflectance index)



Relationship between LUE and  $\text{PRI}_{570}$  for cornfield in Beltsville, MD, USA collected at multiple times during selected clear days during the 2007 (□) and 2008 (▲) growing seasons.

$\text{PRI}_{570}$  values from averages of nadir spectral reflectance collected along a 100 m transect in field. LUE (with units of  $\text{mol C mol}^{-1} \text{APAR}$ ) are hourly values calculated using GEP and incident PAR from flux tower and green fPAR estimated from NDVI from reflectance data. Flux data from W.P. Kustas (USDA/Beltsville Agricultural Research Service).

Note: see chapter 12



U.S. Geological Survey  
U.S. Department of Interior

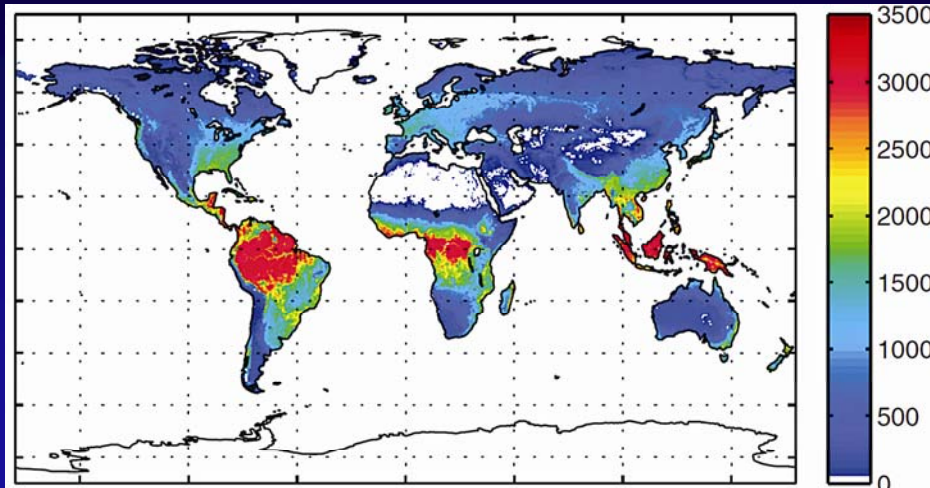
Summary of 21 spectral indices extracted from hyperspectral data, appearing in detecting and mapping invasive plant species

Spectral index	Characteristics & functions	Definition	Reference
<b>Multiple bioparameters:</b>			
LI, Lepidium Index	To be sensitive to the uniformly bright reflectance displayed by <i>Lepidium</i> in the visible range.	$R_{630}/R_{586}$	[20]
NDVI, Normalized Difference Vegetation Index	Respond to change in the amount of green biomass and more efficiently in vegetation with low to moderate density.	$(R_{NIR}-R_R)/(R_{NIR}+R_R)$	[74]
PSND, Pigment-Specific Normalized Difference	Estimate LAI and carotenoids (Cars) at leaf or canopy level	$(R_{800}-R_{470})/(R_{800}+R_{470})$	[74]
SR, Simple Ratio	Same as NDVI	$R_{NIR}/R_R$	[76,77]
<b>Pigments:</b>			
$\text{Chl}_{green}$ , Chlorophyll Index Using Green Reflectance	Estimate chlorophylls (Chls) content in anthocyanin-free leaves if NIR is set	$(R_{760-800}/R_{540-560})-1$	[78]
$\text{Chl}_{red-edge}$ , Chlorophyll Index Using Red Edge Reflectance	Estimate Chls content in anthocyanin-free leaves if NIR is set	$(R_{760-800}/R_{690-720})-1$	[78]
LCI, Leaf Chlorophyll Index	Estimate Chl content in higher plants, sensitive to variation in reflectance caused by Chl absorption	$(R_{850}-R_{710})/(R_{850}+R_{680})$	[79]
$mND_{680}$ , Modified Normalized Difference	Quantify Chl content and sensitive to low content at leaf level.	$(R_{800}-R_{680})/(R_{800}+R_{680}-2R_{445})$	[80]
$mND_{705}$ , Modified Normalized Difference	Quantify Chl content and sensitive to low content at leaf level. $mND_{705}$ performance better than $mND_{680}$	$(R_{750}-R_{705})/(R_{750}+R_{705}-2R_{445})$	[80,81]
$mSR_{705}$ , Modified Simple Ratio	Quantify Chl content and sensitive to low content at leaf level.	$(R_{750}-R_{445})/(R_{705}-R_{445})$	[80]
NPCL, Normalized Pigment Chlorophyll ratio Index	Assess Cars/Chl ratio at leaf level	$(R_{680}-R_{430})/(R_{680}+R_{430})$	[82]
PBI, Plant Biochemical Index	Retrieve leaf total Chl and nitrogen concentrations from satellite hyperspectral data	$R_{810}/R_{560}$	[83]
PRI, Photochemical / Physiological Reflectance Index	Estimate Car pigment contents in foliage	$(R_{531}-R_{570})/(R_{531}+R_{570})$	[84]
PI2, Pigment index 2	Estimate pigment content in foliage	$R_{695}/R_{760}$	[85]
RGR, Red:Green Ratio	Estimate anthocyanin content with a green and a red band	$R_{683}/R_{510}$	[80,86]
SGR, Summed Green Reflectance	Quantify Chl content	Sum of reflectances from 500 to 599 nm	[81]
<b>Foliar chemistry:</b>			
CAI, Cellulose Absorption Index	Cellulose & lignin absorption features, discriminates plant litter from soils	$0.5(R_{2020}+R_{2220})-R_{2100}$	[87]
NDLI, Normalized Difference Lignin Index	Quantify variation of canopy lignin concentration in native shrub vegetation	$[\log(1/R_{1754})-\log(1/R_{1680})] / [\log(1/R_{1754})+\log(1/R_{1680})]$	[88]
NDWI, ND Water Index	Improving the accuracy in retrieving the vegetation water content at both leaf and canopy levels	$(R_{860}-R_{1240})/(R_{860}+R_{1240})$	[89,90]
RVI <sub>hyp</sub> , Hyperspectral Ratio VI	Quantify LAI and water content at canopy level.	$R_{1088}/R_{1148}$	[91]
WI, Water Index	Quantify relative water content at leaf level	$R_{900}/R_{970}$	[92]

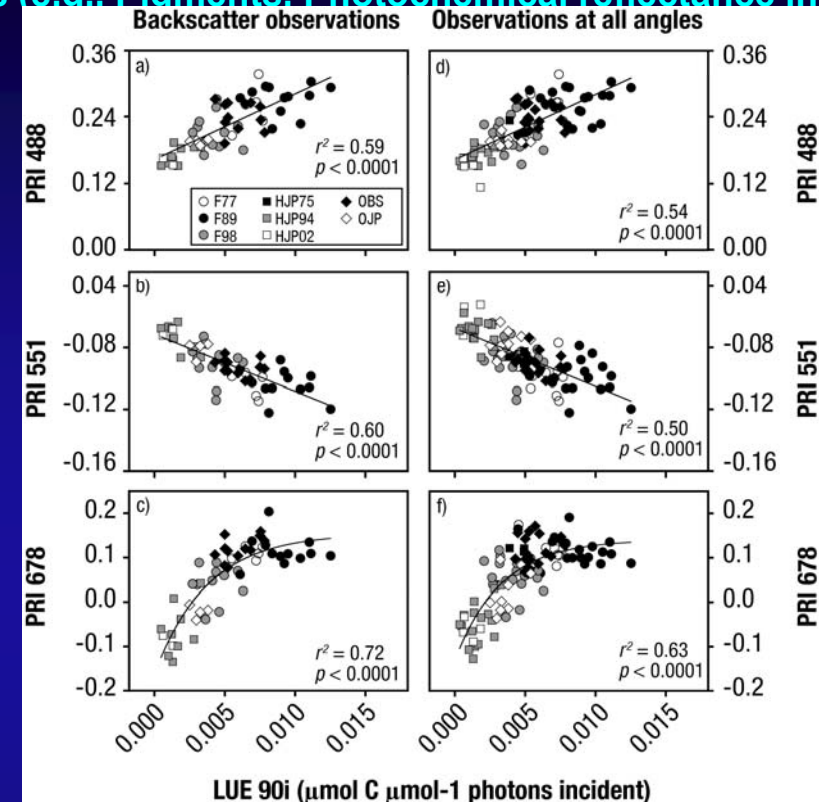


# Methods of Modeling Vegetation Characteristics using Hyperspectral Indices

Other Narrowband Indices addressing Specific Issues (e.g., Pigments, Photochemical reflectance index)



Spatial variations of the global median annual GPP ( $\text{gC}/\text{m}^2/\text{a}$ ) from various spatially explicit approaches. Source: Beer et al. 2010 [7].



Note: PRI is used to quantify light use efficiency (LUE) and LUE to measure gross primary productivity (GPP)

This figure describes the relationship between the Photochemical Reflectance Index (PRI) and photosynthetic light use efficiency ( $\text{LUE}_{\text{foliage}}$ ,  $\mu\text{mol C } \mu\text{mol}^{-1} \text{ APAR}$ ) for foliage exposed to a range of illumination conditions in a Douglas-fir forest in Canada. The lowest PRI and  $\text{LUE}_{\text{foliage}}$  values are associated with sunlit foliage throughout the 2006 growing season. The highest PRI and  $\text{LUE}_{\text{foliage}}$  values measured were associated with shaded foliage, but high values are also expected for foliage residing in the deeply shaded canopy sectors that could not be measured. Source: Middleton et al. 2009 [35].

Note: see chapter 12

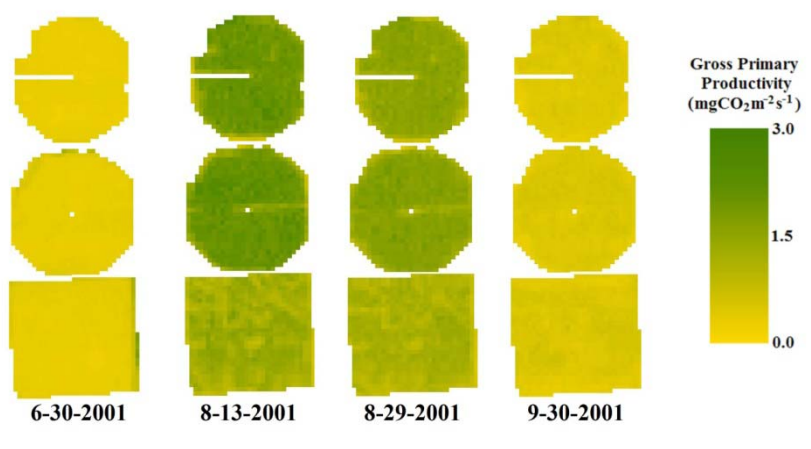
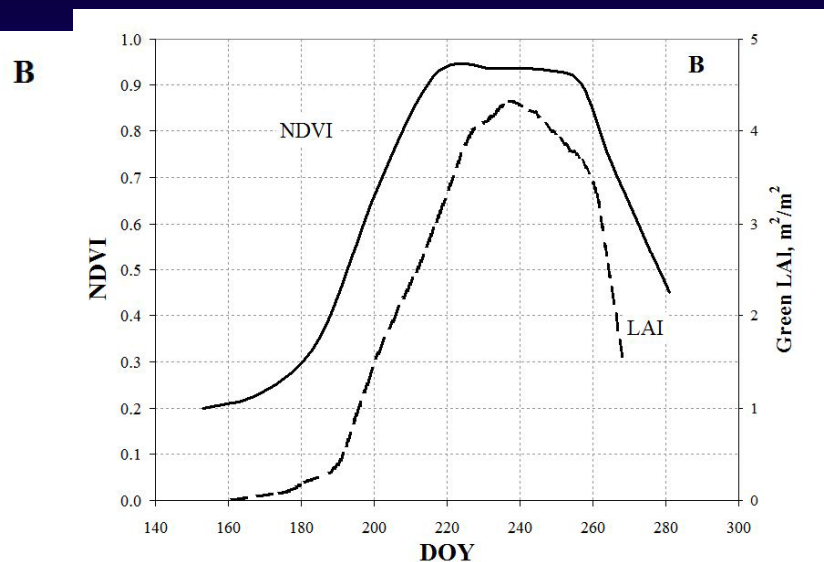
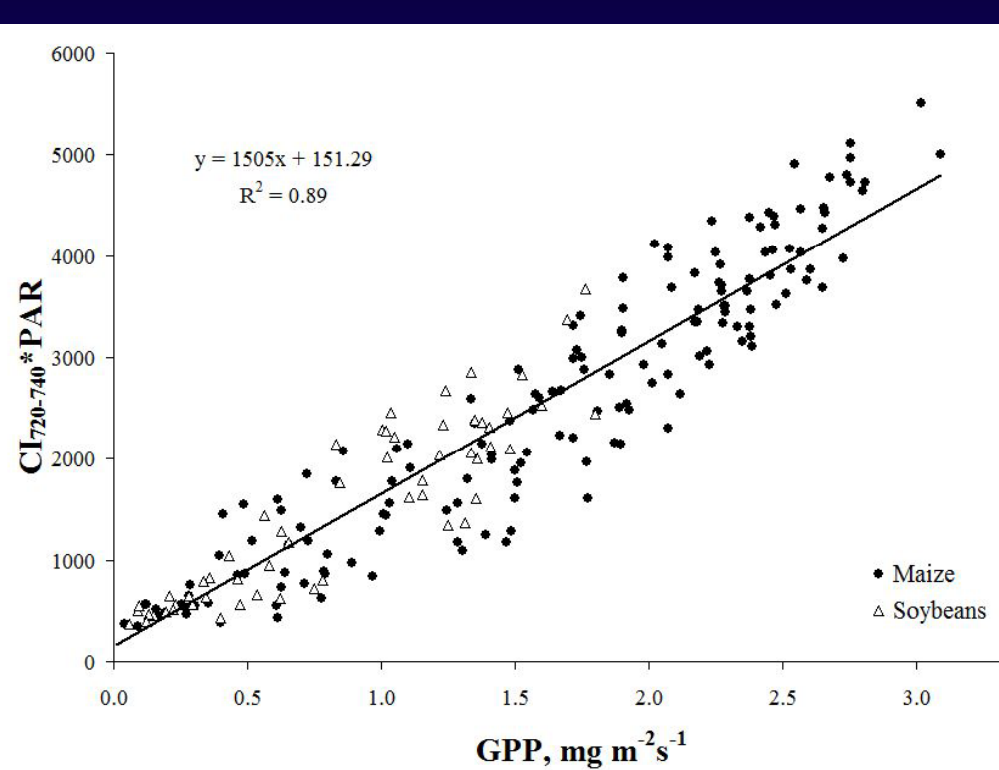


U.S. Geological Survey  
U.S. Department of Interior



# Methods of Modeling Vegetation Characteristics using Hyperspectral Indices

## Other Narrowband Indices addressing Specific Issues (e.g., GPP)



Mid day gross primary production (GPP) in maize (first and second rows) and soybean (bottom row) retrieved from atmospherically corrected ETM+ Landsat imagery taken over Nebraska in 2001 and 2002.

Note: see chapter 15



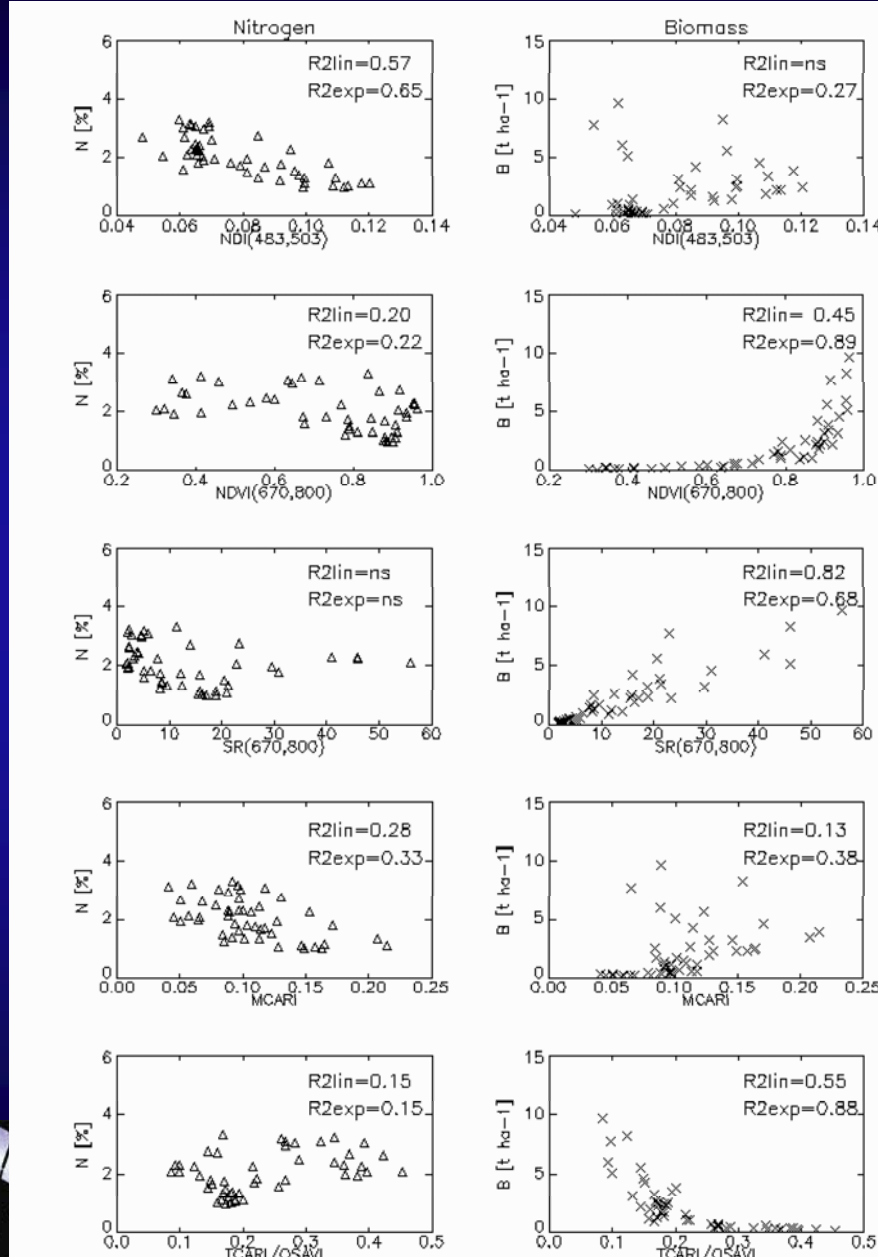
U.S. Geological Survey  
U.S. Department of Interior



# Methods of Modeling Vegetation Characteristics using Hyperspectral Indices

## Various types of narrowband indices vs. Biochemical (e.g., nitrogen) and biophysical (e.g., Biomass)

Scatter plots of VI-N [%] and VI-Biomass [t ha<sup>-1</sup>] for a subset of HVIs described above. Field spectra data were acquired with FieldSpec FR PRO spectroradiometer for experimental paddy fields in Italy [20]. The coefficient of determination ( $R^2$ ) for linear and exponential regressive models is given in the panels.



Note: see chapter 11

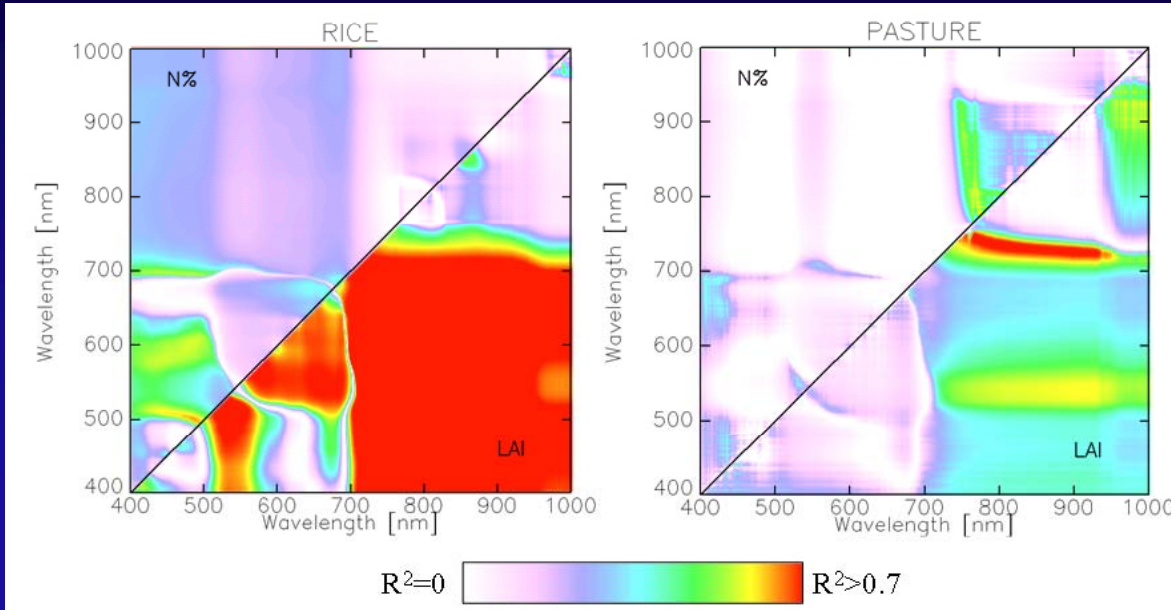


U.S. Geological Survey  
U.S. Department of Interior



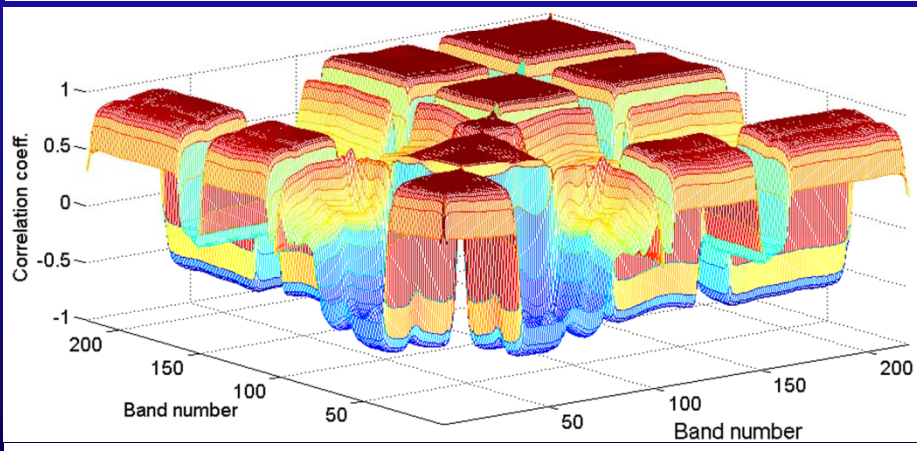
# Methods of Modeling Vegetation Characteristics using Hyperspectral Indices

## Lambda vs. Lambda R-square contour plot on non-linear biochemical quantity (e.g., leaf Nitrogen) and biophysical (e.g., LAI) vs. HTBVI models



Linear correlation ( $R^2$ ) between N concentration/LAI and ND for rice (left, [20]) and SR for pasture (right, [21]) for field canopy spectra acquired with a FieldSpec FR PRO spectroradiometer.

Note: see chapter 11



Correlation between the bands of hyperspectral image shown in Fig.4.1. Only the alternate bands are used to compute the correlation.

Note: see chapter 4



# Methods of Modeling Vegetation Biochemical Characteristics using Hyperspectral Vegetation Indices (HVIs)



# Hyperspectral Remote Sensing of Vegetation

## Study of Biochemical Properties (e.g., Pigments)

### 1. Pigments

**Chlorophylls: chl-a, chl-b, total chl ( $\mu\text{g}/\text{cm}^2$ )**

chlorophyll content can directly determine photosynthetic potential and primary production, plant stress, and senescence;

**Carotenoids**

represented by two ( $\alpha$ - and  $\beta$ -) carotenes and xanthophylls (lutein, zeaxanthin, violaxanthin, antheraxanthin, and neoxanthin), which exhibit strong light absorption in the blue region of the spectrum; and

**Anthocyanins**

The anthocyanins are pigments frequently occurring in higher plants and responsible for their red coloration.

### 2. Nitrogen ( $\text{kg}/\text{ha}$ )

### 3. Water ( $\text{g}/\text{cm}^2$ )

### 4. Plant structural materials

**Lignin ( $\text{g}/\text{cm}^2$ )**

**Cellulose ( $\text{g}/\text{cm}^2$ )**

Note: see chapter 6; Gitelson et al.



# Hyperspectral Remote Sensing of Vegetation

## Study of Biochemical Properties (e.g., Pigments)

### 1. Pigments

#### Chlorophylls: chl-a, chl-b, total chl ( $\mu\text{g}/\text{cm}^2$ )

Chlorophyll-a and chlorophyll-b absorb the greatest proportion of radiation and provide energy for the reactions of photosynthesis. Chlorophylls absorb radiation mainly in the blue (~450 nm) and red (~680 nm) wavelengths, whereas carotenoids have an absorption feature in the blue overlapping with chlorophyll. The red absorption peak is solely due to the presence of chlorophylls but low concentrations might saturate the 660–680 nm region, thus making it poorly sensitive to high chlorophyll contents. Longer (~700 nm, red edge) shorter (~550 nm, green) wavelengths are therefore preferred because reflectance is more sensitive to moderate-to-high chlorophyll content. An increase in the amount of chlorophyll in the canopy, either due to increases in the chlorophyll concentration or to Leaf Area Index (LAI), results in the broadening of the red absorption feature, and, consequently, in the shift of the red-edge position (REP) toward longer wavelengths; and

#### Carotenoids

carotenoids protect the reaction centers from excess light and help intercept PAR as auxiliary pigments of chlorophyll-a. carotenoids have an absorption feature in the blue overlapping with chlorophyll.

Note: see chapter 11; Stroppiana et al.



U.S. Geological Survey  
U.S. Department of Interior



## Hyperspectral Remote Sensing of Vegetation Inter-relationships of Crop Parameters (e.g., Nitrogen vs. Chlorophyll) and the Related difficulty in Studying any one Crop Parameter in Isolation

The relationship between nitrogen supply and chlorophyll formation has long been observed.

Since part of leaf nitrogen is contained in chlorophyll molecules, the amount of available nitrogen largely determines the amount of chlorophyll formed in plants, provided that other requirements for chlorophyll formation, such as light, iron supply, and magnesium, are present in sufficient quantities.

However, the nitrogen/chlorophyll relation can be influenced by environmental conditions (nutrients and water stress), leaf position in the canopy, genotype, temperature, and leaf growth stage. Since nitrogen stress induces a physiological change (pigment concentration), which in turn produces changes in leaf spectra, reflectance can be used to assess nitrogen status.

Note: see chapter 11; Stroppiana et al.



## **Hyperspectral Remote Sensing of Vegetation Inter-relationships of Crop Parameters (e.g., Nitrogen vs. Chlorophyll) and the Related difficulty in Studying any one Crop Parameter in Isolation**

Relation between leaf nitrogen and canopy spectra is indirectly due to its association with chlorophyll since canopy spectra are determined by optical leaf properties besides density and geometry of the canopy (LAI and Leaf Angle Distribution [LDA]) and background reflectivity.

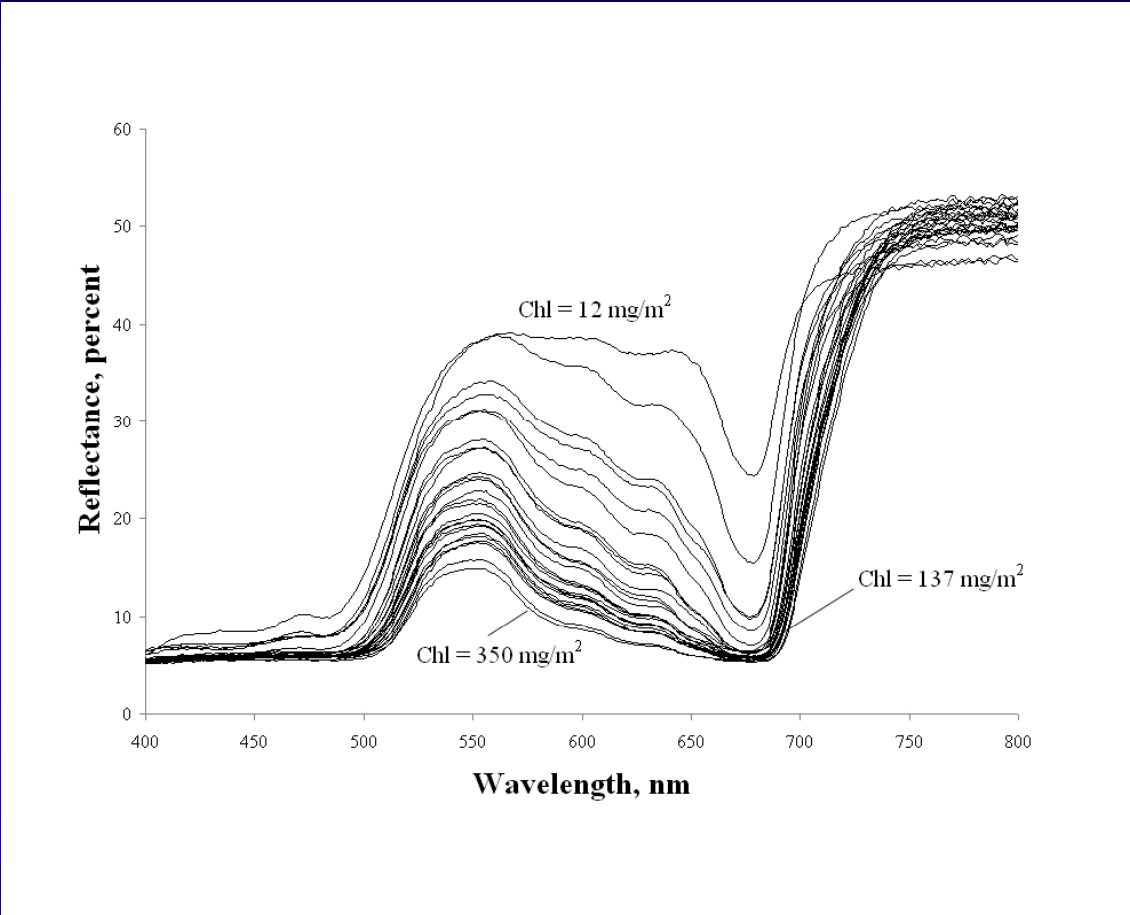
**Canopy spectra can change dramatically during the season as a consequence of changes in the architecture and arrangement of plant components and changes in the proportion of soil and vegetation. Reflectance from a canopy is considerably less than that from an individual leaf, although in the NIR wavelengths attenuation is less pronounced. In fact, the radiation transmitted through the upper leaves is reflected by the lower strata and transmitted up to enhance the reflectivity of the upper leaves.**

**In conclusion, the use of leaf and canopy spectra for nitrogen assessment generally relies on the close relation between nitrogen and chlorophylls in the cell metabolism although the experimental relationship established at the canopy scale remains purely empirical. Kokaly et al. in fact state that the two variables are only moderately correlated within and across ecosystems.**

**Note: see chapter 11; Stroppiana et al.**



# Hyperspectral Remote Sensing of Vegetation Study of Pigments: chlorophyll



e.g., Reflectance spectra of beech leaves...red-edge (700-740 nm) one of the best.

Note: see chapter 6; Gitelson et al.

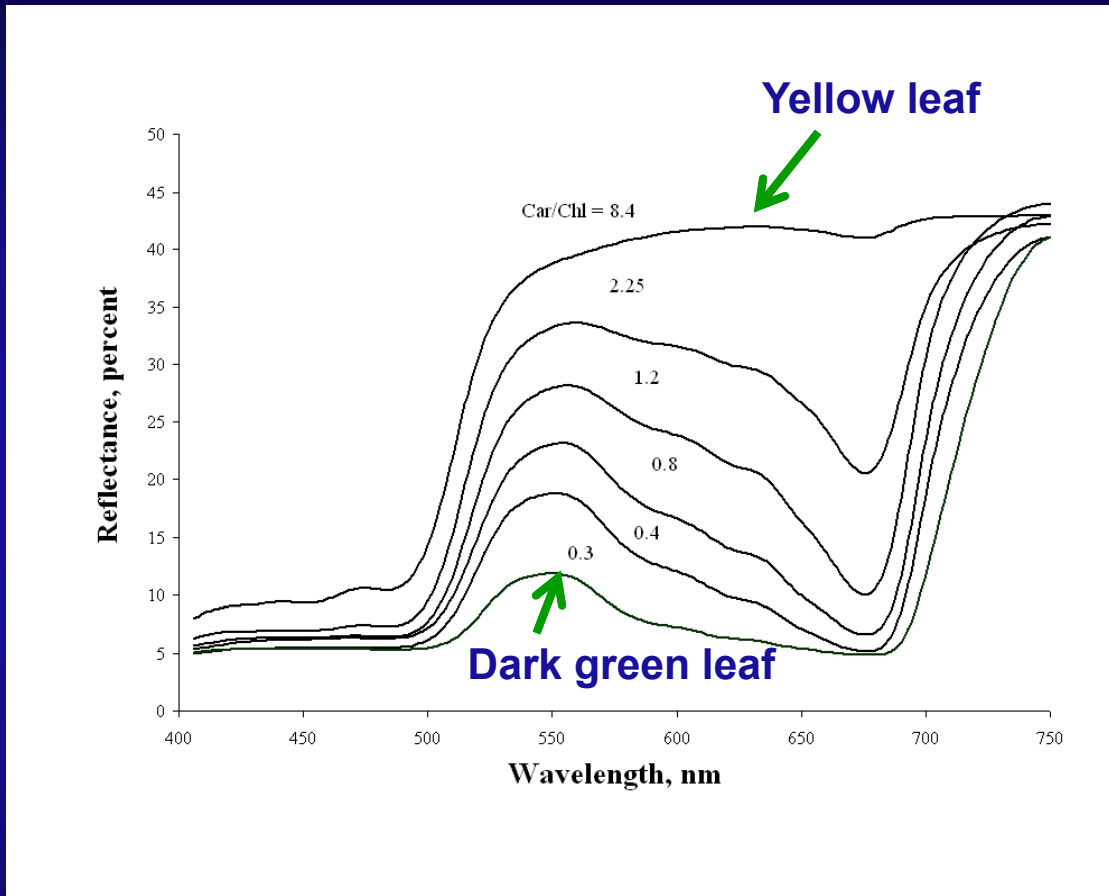


U.S. Geological Survey  
U.S. Department of Interior



# Hyperspectral Remote Sensing of Vegetation

## Study of Pigments: carotenoids/chlorophyll



e.g., Reflectance spectra of chestnut leaves...difference reflectance of (680-500 nm)/750 nm  
quantitative measurement of plant senescence

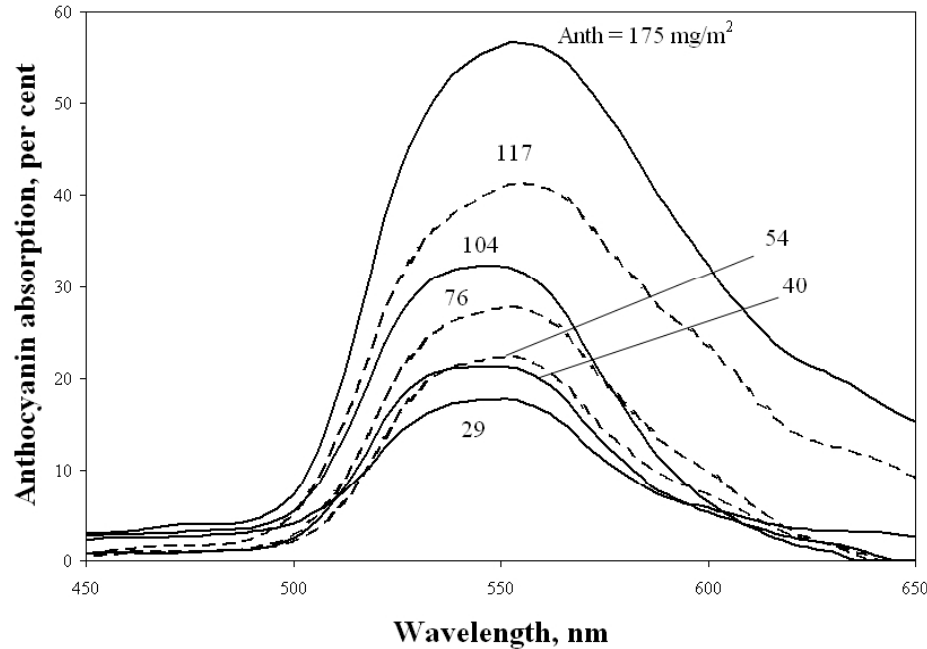
Note: see chapter 6; Gitelson et al.



U.S. Geological Survey  
U.S. Department of Interior



# Hyperspectral Remote Sensing of Vegetation Study of Pigments: Anthocyanin



e.g., Reflectance spectra of cotoneaster and dogwood... Spectra of anthocyanin absorption of cotoneaster (solid line) and dogwood (dashed line) leaves.

Note: see chapter 6; Gitelson et al.



U.S. Geological Survey  
U.S. Department of Interior



# Hyperspectral Remote Sensing of Vegetation Modeling Biophysical Properties for Forests

Derivative Chlorophyll Index (DCI) is a ration of 2 red-edge bands centered @: 705 nm and 722 nm

Logarithmic bivariate models to predict field metrics from the mean derivative chlorophyll index.

Field Metric versus DCI (n=24)	r <sup>2</sup>	r <sup>2</sup> <sub>adj</sub>	RMSE	Plot Mean
Mean Dominant Height (m) <sup>f</sup>	0.59 (0.64)	0.57 (0.62)	2.16 m	20.4 m
Quadratic DBH (cm)	0.55	0.53	3.51 cm	19.3 cm
Total Above Ground Biomass (v) <sup>f</sup>	0.63, (0.67)	0.61, (0.65)	1740	4426.5
Total Above Ground Carbon (v) <sup>f</sup>	0.63, (0.67)	0.61, (0.65)	870.5	2208.3
Crown Closure	0.75	0.74	0.48	0.98
Stem Density (#/ha)	No significant relationship.			

Note: see chapter 20; Thomas et al.



U.S. Geological Survey  
U.S. Department of Interior



# Hyperspectral Remote Sensing of Vegetation Study of Pigments

**Accurate retrieval of three foliar pigments (chlorophylls, carotenoids, and anthocyanins), one needs reflectances in only four, relatively wide spectral bands:**

**blue-green (around 510 nm),  
green (540–560 nm),  
red edge (700–720 nm), and  
NIR (beyond 760 nm).**

Note: see chapter 6; Gitelson et al.



# Methods of Modeling Vegetation Biophysical Characteristics using Hyperspectral Vegetation Indices (HVIs)



# Hyperspectral Remote Sensing of Vegetation Study of Biophysical Characteristics

1. Biomass: wet and dry; ( $\text{kg}/\text{m}^2$ );
2. Leaf area index (LAI), Green LAI; ( $\text{m}^2/\text{m}^2$ )
3. Plant height; (mm)
4. Vegetation fraction; (%)
5. Fraction of PAR absorbed by photosynthetically active vegetation (fAPAR); ( $\text{MJ}/\text{m}^2$ )
6. Total crop chlorophyll content; ( $\text{g}/\text{m}^2$ ) and
7. Gross primary production. ( $\text{g C}/\text{m}^2/\text{yr}$ )

Note: see chapter 1, Thenkabail et al.; chapter 6, Gitelson et al.

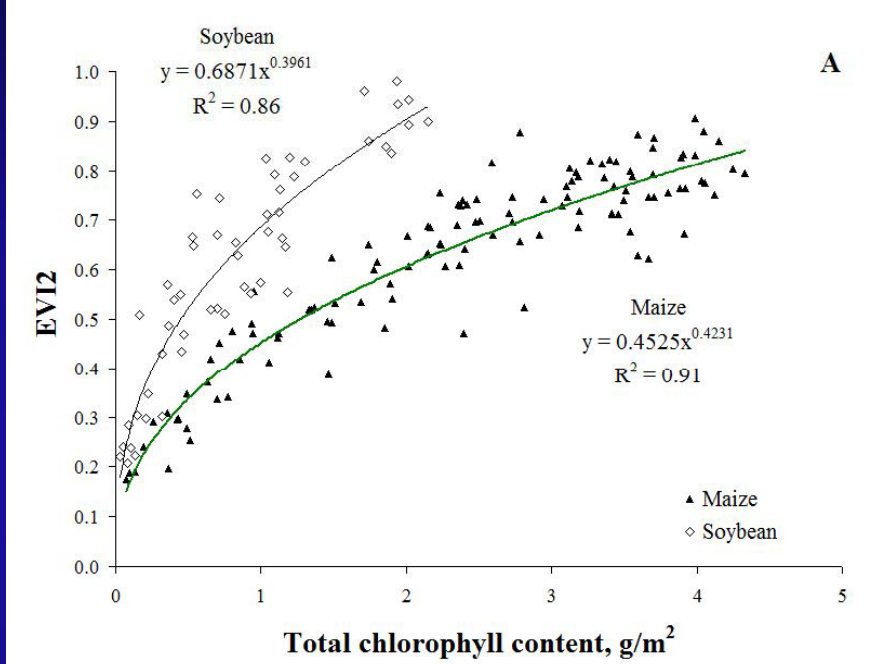
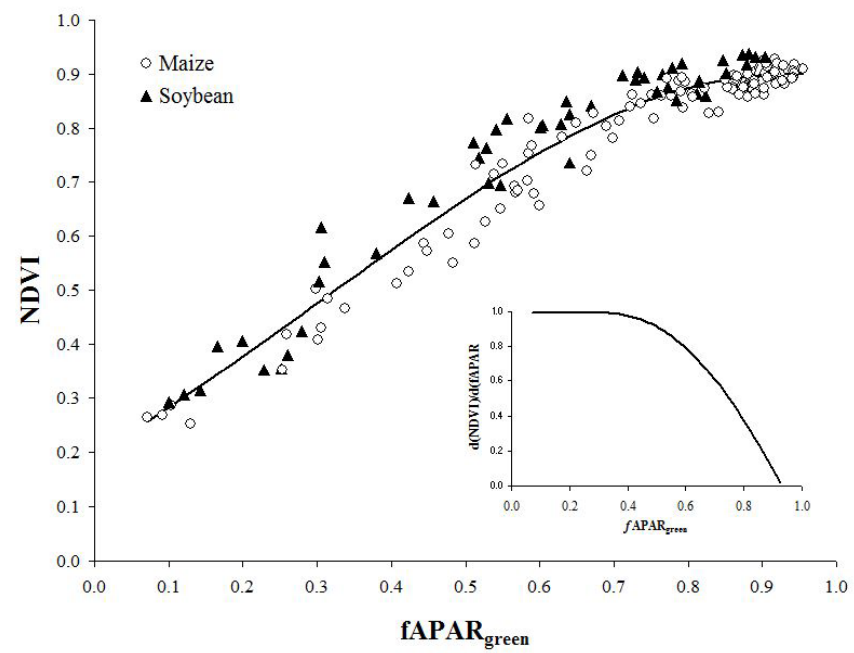


U.S. Geological Survey  
U.S. Department of Interior



# Hyperspectral Remote Sensing of Vegetation

## fAPAR vs. NDVI; total Chlorophyll vs. EVI2 for Corn and Soybeans



Note: see chapter 15, Gitelson et al.



U.S. Geological Survey  
U.S. Department of Interior



# Hyperspectral Remote Sensing of Vegetation Total Chlorophyll Vs. HVIs for Corn and Soybeans

(A) Maize

VI	VI vs.Chl	R <sup>2</sup>
EVI	y = 0.4525x <sup>0.423</sup>	0.88
Red edge NDVI	y = 0.195Ln(x) + 0.538	0.92
WDRVI, a = 0.1	y = 0.39+1.39/(1+exp(x-1.1)/0.87)	0.92
CI <sub>green</sub>	y = 2.311x + 1.293	0.92
CI <sub>red edge</sub>	y = 2.080x + 0.191	0.92
MTCI	y = 3.189x + 2.449	0.93

(B) Soybean

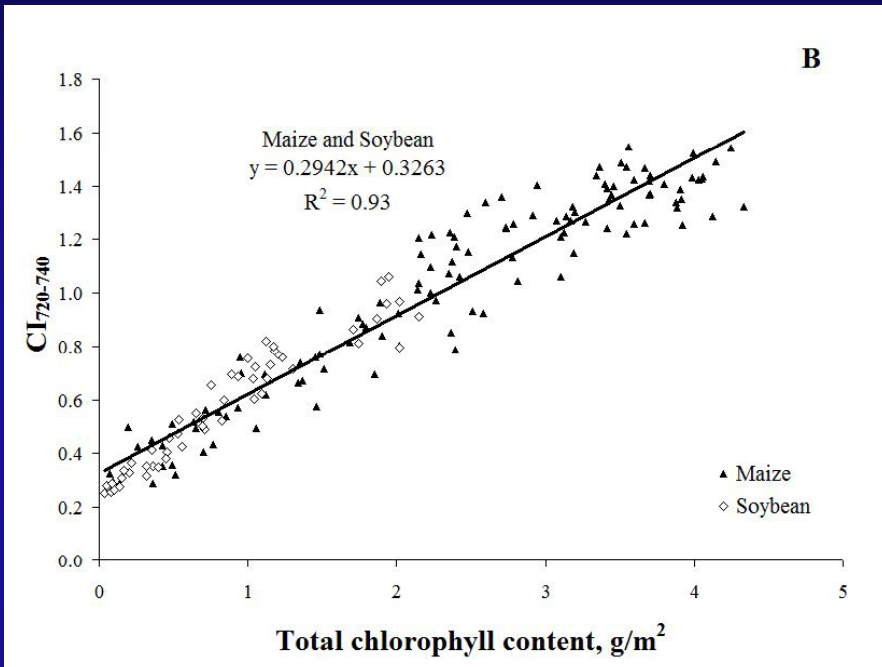
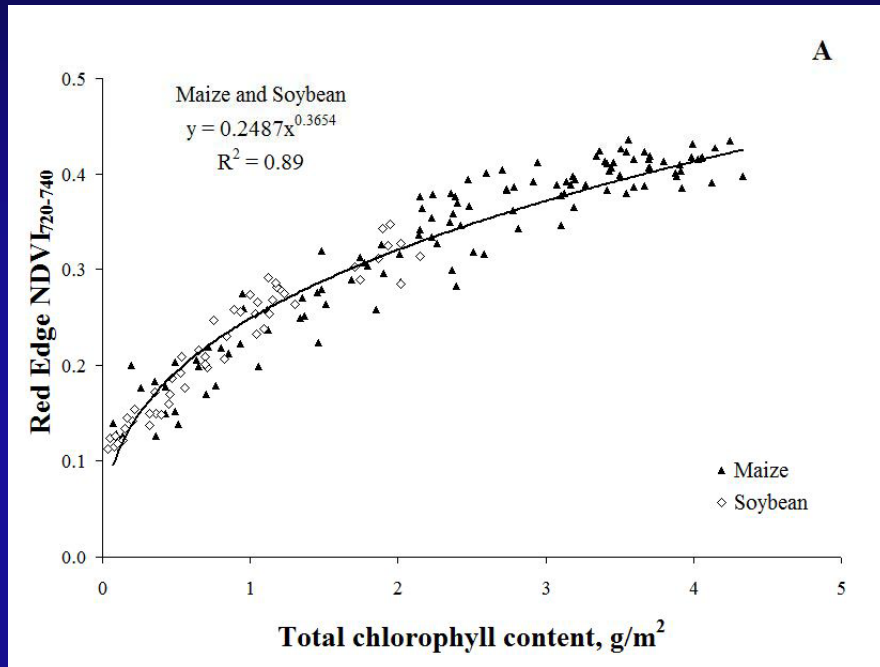
VI	VI vs. Chl	R <sup>2</sup>
WDRVI, a = 0.1	y = -0.2778x <sup>2</sup> + 1.1518x - 0.7432	0.95
EVI2	y = 0.6871x <sup>0.396</sup>	0.88
Red edge NDVI	y = 0.163Ln(x) + 0.576	0.92
CI <sub>green</sub>	y = 5.319x + 1.122	0.91
MTCI	y = 3.917x + 2.254	0.89
CI <sub>red edge</sub>	y = 3.398x + 0.362	0.94

Note: see chapter 15, Gitelson et al.



# Hyperspectral Remote Sensing of Vegetation

## Total Chlorophyll vs. red-edge and CL (chlorophyll) red-edge indices for Corn and Soybeans



Sensors which provide data in red-edge (e.g., MERIS, Hyperion, Rapideye) allow red-edge indices

Note: see chapter 15, Gitelson et al.



U.S. Geological Survey  
U.S. Department of Interior



# Hyperspectral Remote Sensing of Vegetation

## Gross Primary Productivity Vs. HVIs for Corn and Soybeans

(A) Maize

VI	VI×PAR vs. GPP	R <sup>2</sup>
Green NDVI	y = 278.04x + 581.93	0.69
NDVI	y = -76.261x <sup>2</sup> + 600.3x + 368.38	0.79
EVI2	y = 378.37x + 226.92	0.80
WDRVI, a = 0.1	y = 594.68x - 1036.4	0.80
Red edge NDVI	y = -41.49x <sup>2</sup> + 498.06x + 230.31	0.85
CI <sub>green</sub>	y = 1205.9x <sup>2</sup> + 1760.5x + 2064.3	0.90
MTCI	y = 1135x <sup>2</sup> + 1514.1x + 2620.4	0.90
CI <sub>red edge</sub>	y = 1217.9x <sup>2</sup> + 1176x + 650.59	0.92

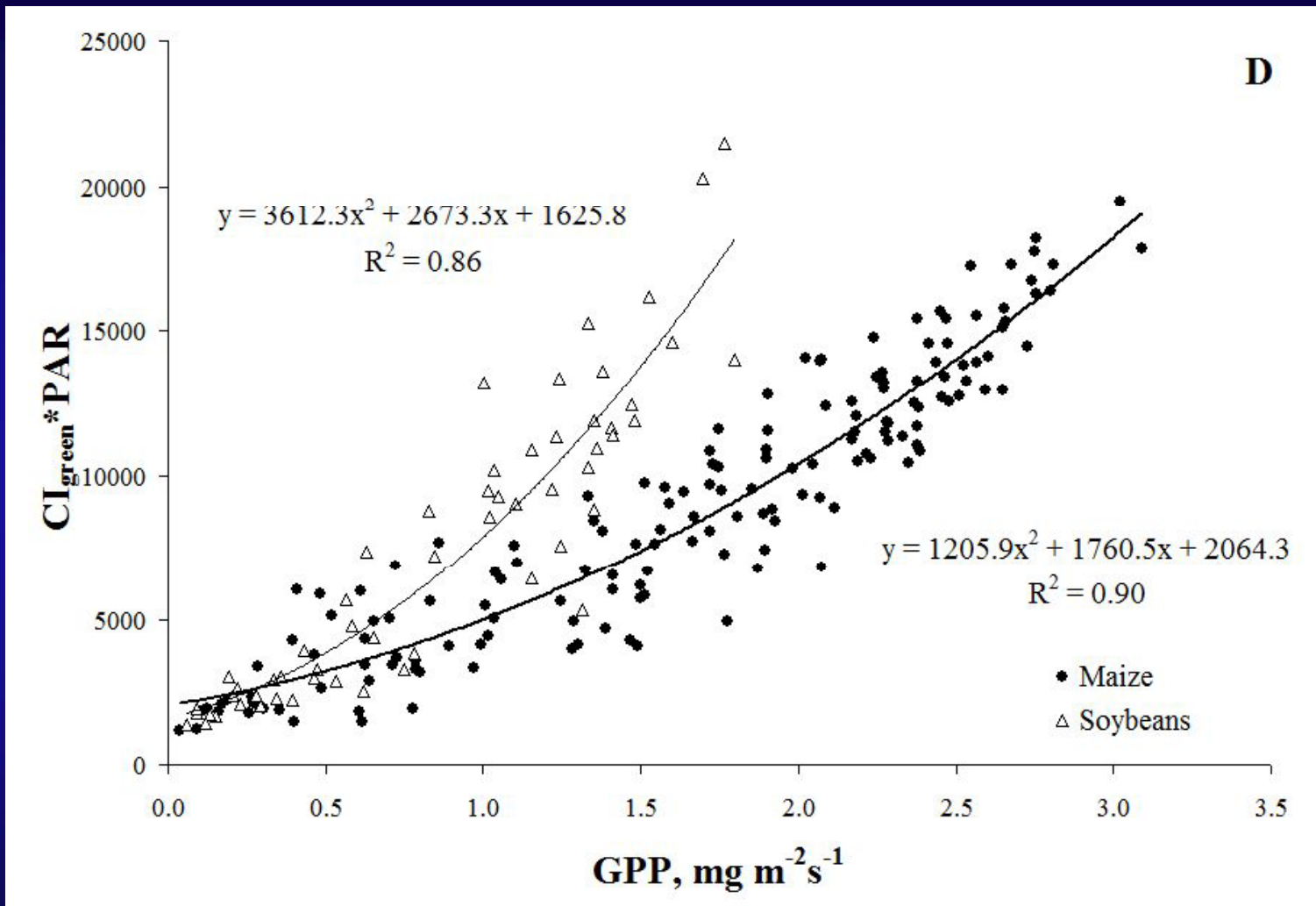
(B) Soybean

VI	VI×PAR vs. GPP	R <sup>2</sup>
Green NDVI	y = 442.9x + 545.49	0.62
MTCI	y = 1678.7x <sup>2</sup> + 3671.9x + 2874.2	0.76
NDVI	y = -376.44x <sup>2</sup> + 1237.6x + 292.43	0.78
Red edge NDVI	y = 514.8x + 213.78	0.78
WDRVI, a = 0.1	y = 1109.5x - 1142.9	0.81
EVI2	y = 624.49x + 256.1	0.82
CI <sub>green</sub>	y = 3612.3x <sup>2</sup> + 2673.3x + 1625.8	0.86
CI <sub>red edge</sub>	y = 1948.5x <sup>2</sup> + 2363.6x + 346.87	0.88

Note: see chapter 15, Gitelson et al.



# Hyperspectral Remote Sensing of Vegetation Study of Biophysical Characteristics



Note: see chapter 15, Gitelson et al.



# Hyperspectral Data (Imaging Spectroscopy data)

## Study of the Affects of Heavy Metals on Vegetation using Hyperspectral Data

hydrogen 1 <b>H</b> 1.0079	beryllium 4 <b>Be</b> 9.0122	boron 5 <b>B</b> 10.811	carbon 6 <b>C</b> 12.011	nitrogen 7 <b>N</b> 14.007	oxygen 8 <b>O</b> 15.999	fluorine 9 <b>F</b> 18.998	neon 10 <b>Ne</b> 20.180
lithium 3 <b>Li</b> 6.941	magnesium 12 <b>Mg</b> 24.305	aluminum 13 <b>Al</b> 26.982	silicon 14 <b>Si</b> 28.086	phosphorus 15 <b>P</b> 30.974	sulfur 16 <b>S</b> 32.065	chlorine 17 <b>Cl</b> 35.453	argon 18 <b>Ar</b> 39.948
sodium 11 <b>Na</b> 22.990	calcium 20 <b>Ca</b> 40.078	copper 29 <b>Cu</b> 63.546	zinc 30 <b>Zn</b> 65.39	gallium 31 <b>Ga</b> 69.723	germanium 32 <b>Ge</b> 72.61	arsenic 33 <b>As</b> 74.022	selenium 34 <b>Se</b> 78.96
potassium 19 <b>K</b> 39.098	scandium 21 <b>Sc</b> 44.956	titanium 22 <b>Ti</b> 47.867	vanadium 23 <b>V</b> 50.942	chromium 24 <b>Cr</b> 51.996	manganese 25 <b>Mn</b> 54.938	iron 26 <b>Fe</b> 55.845	cobalt 27 <b>Co</b> 58.933
rubidium 37 <b>Rb</b> 85.468	strontium 38 <b>Sr</b> 87.62	yttrium 39 <b>Y</b> 88.906	zirconium 40 <b>Zr</b> 91.224	niobium 41 <b>Nb</b> 92.906	molybdenum 42 <b>Mo</b> 95.94	technetium 43 <b>Tc</b> [98]	ruthenium 44 <b>Ru</b> 101.07
caesium 55 <b>Cs</b> 132.91	barium 56 <b>Ba</b> 137.33	lutetium 71 <b>Lu</b> 174.97	hafnium 72 <b>Hf</b> 178.49	tantalum 73 <b>Ta</b> 180.95	tungsten 74 <b>W</b> 183.84	rhenum 75 <b>Re</b> 186.21	osmium 76 <b>Os</b> 190.23
francium 87 <b>Fr</b> [223]	radium 88 <b>Ra</b> [226]	lawrencium 103 <b>Lr</b> [262]	rutherfordium 104 <b>Rf</b> [261]	dubnium 105 <b>Db</b> [262]	seaborgium 106 <b>Sg</b> [266]	bohrium 107 <b>Bh</b> [269]	hassium 108 <b>Hs</b> [268]
						rhodium 45 <b>Rh</b> 102.91	palladium 46 <b>Pd</b> 106.42
						silver 47 <b>Ag</b> 107.87	cadmium 48 <b>Cd</b> 112.41
						tin 49 <b>In</b> 114.82	indium 50 <b>Sn</b> 119.71
						antimony 51 <b>Sb</b> 124.76	antimony 52 <b>Te</b> 127.60
						thallium 81 <b>Tl</b> 204.29	thallium 82 <b>Pb</b> 207.2
						mercury 80 <b>Hg</b> 206.59	mercury 83 <b>Bi</b> 209.09
						lead 84 <b>Po</b> 209	lead 85 <b>At</b> [210]
						ununquadium 114 <b>Uuq</b> [289]	ununquadium 115 <b>Uuu</b> [277]
							ununquadium 116 <b>Uub</b> [277]

The Periodic Table showing the elements generally considered heavy metals.  
Lanthanides and actinides are not shown.

Note: see chapter 23, Slonecker et al.



U.S. Geological Survey  
U.S. Department of Interior



# Hyperspectral Data (Imaging Spectroscopy data)

## Study of the Affects of Heavy Metals on Vegetation using Hyperspectral Data

Metal	Characteristics	Reference(s)
Arsenic	Red/brown necrotic spots on old leaves, yellow/brown roots, reduced growth	[36, 37]
Aluminum	Stunted growth, inhibition of root elongation, purple Coloration, curling and yellowing of leaf tips	[72, 73]
Cadmium	Brown edges to leaves, chlorosis, necrosis, curled leaves, stunted roots	[74, 75]
Copper	Chlorosis, yellow and purple coloration, decreased root growth and leaf biomass	[76-78]
Lead	Dark green leaves, stunted growth, chlorosis and blackening of root system	[79]
Mercury	Severe stunting of seedlings and roots, chlorosis, reduced biomass	[80]
Nickel	Chlorosis, necrosis, stunting, reduced root and leaf growth	[81]
Selenium	Interveneed chlorosis, black spots, bleaching and yellowing of young leaves, pink spots on roots	[17]
Zinc	Chlorosis, stunting, reduced root elongation	[82]

### Examples of Visual Symptoms of Metals Stress in Plants

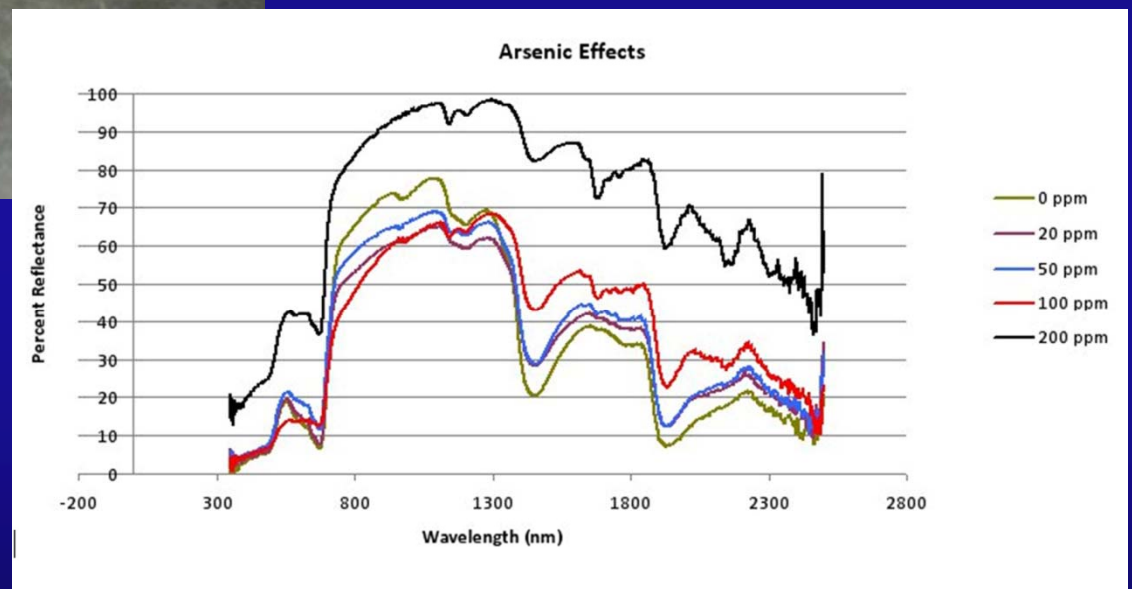
Note: see chapter 23, Slonecker et al.

Spectral Feature	Metal(s)	Vegetation Type	Sensor	Reference(s)
DVI, REP	ni, cd, cu, pb, zn	floodplain, ryegrass	ASD	[32]
EGFN	zn	conifers	CASI	[55]
NDVI	cr, pb, zn, v	Gray Birch	ASD	[39]
RGI			Ikonos	
NDVI	ni, cd, cu, pb, zn	rice	Landsat TM	[83]
PRI	general HM	floodplain	ASD	[56]
PRI	as	ferns	ASD	[36, 37]
REP	pb	rice	ASD	[41]
REP	cu zn	peas, maize sunflower	PE 554	[61]
REP	general HM	floodplain bluegrass, ryegrass	ASD	[34, 35]
RVI NDVI, REP	hg	mustard spinach	ASD	[59]
NPCI, PRI, REP	general HM	Stinging Nettles Reed canarygrass Meadow foxtail	ASD	[56]
R <sub>850</sub> ,	cd, cu, pb, zn, as	peas	PE 554	[18]
R <sub>1650</sub> ,	cd, cu, pb, zn, as	peas	PE 554	[18]
CR <sub>1730</sub>	general HM	floodplain	ASD	[56]
R <sub>2200</sub>	cd, cu, pb, zn, as	peas	PE 554	[18]

### Spectral Features and Vegetation Indices related to Metal Stress

# Hyperspectral Data (Imaging Spectroscopy data)

## Study of the Affects of Heavy Metals on Vegetation using Hyperspectral Data



Note: see chapter 23, Slonecker et al.

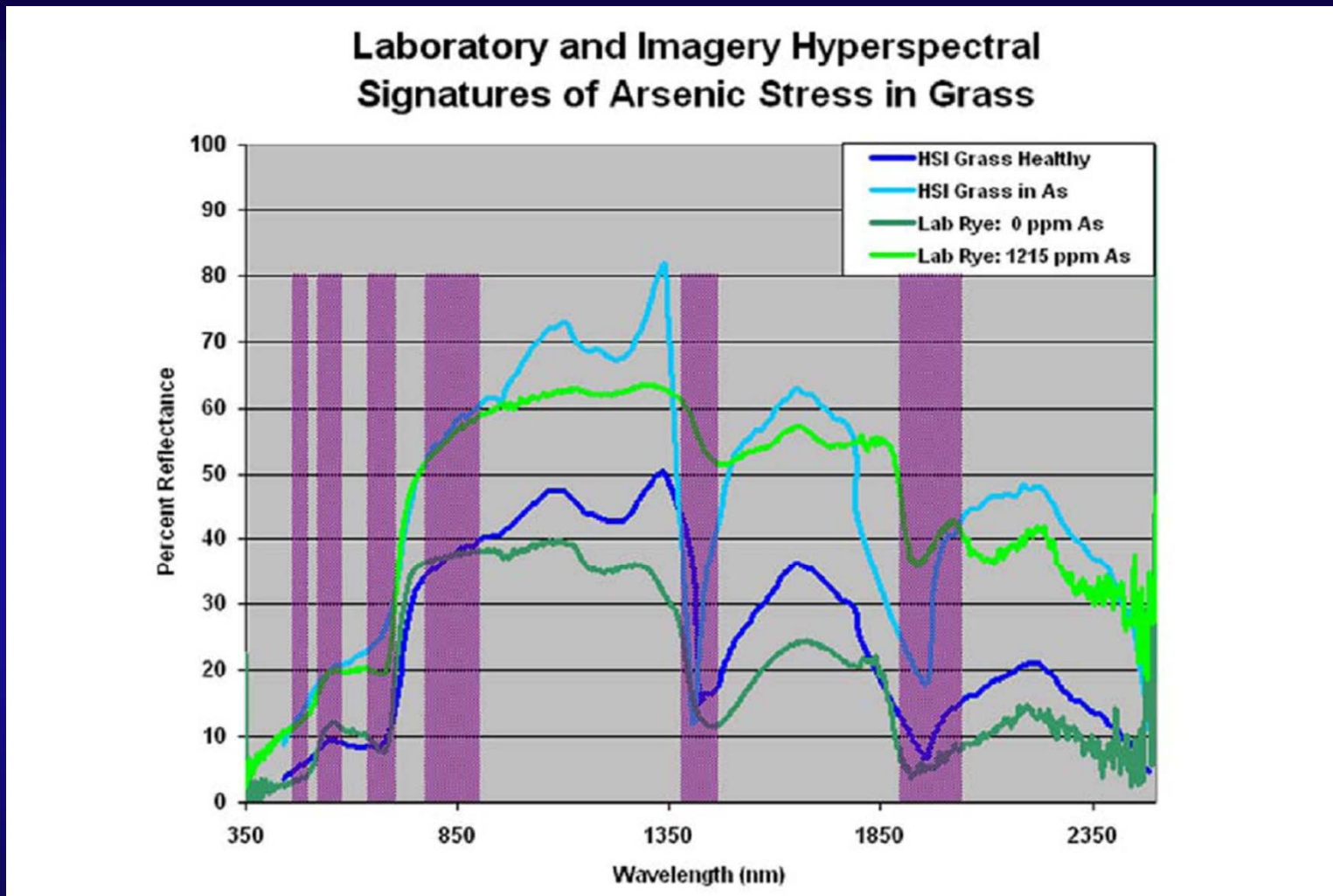


U.S. Geological Survey  
U.S. Department of Interior



# Hyperspectral Data (Imaging Spectroscopy data)

## Study of the Affects of Heavy Metals on Vegetation using Hyperspectral Data



Note: see chapter 23, Slonecker et al.



**Hyperspectral Data (Imaging Spectroscopy data)**  
**Precision Farming Studies**

- (1) Soil management zoning,**
- (2) weed control,**
- (3) N stress detection,**
- (4) crop yield estimation,**
- (5) pest and disease control.**

Note: see chapter 25, Yao et al.



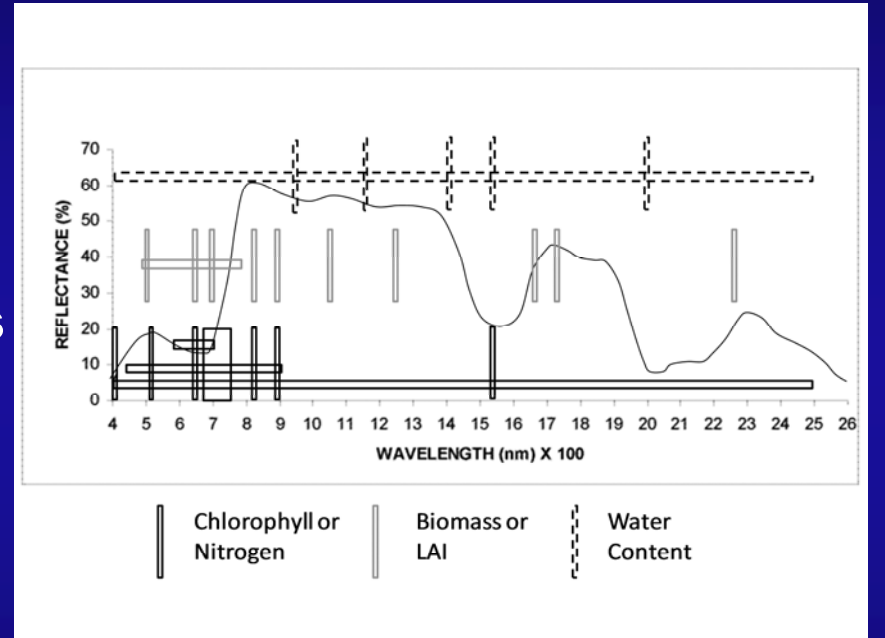
# Methods of Analysis of Whole Spectra



# Hyperspectral Remote Sensing of Vegetation Analysis of Whole Spectra

Figure shows single bands and band ranges that were used in the numerous reviewed studies (from literature) for estimating LAI and biomass, water content, and nitrogen and chlorophyll. Selected bands were neither identical for the same crop property in different studies nor to different crop properties in the same study.

This overview strongly demonstrates the necessity of HS systems that provide contiguous spectra for the estimation of key biophysical and biochemical properties of crops.



Note: see chapter 13, Alchanatis and Cohen



# Hyperspectral Remote Sensing of Vegetation Analysis of Whole Spectra

## 1. Partial least squares regression (PLSR)

PLS chemometric method enable the analysis of the whole spectra avoiding the colinearity or over-fitting complexities. Recent studies have confirmed the potential of PLS analysis to interpret HS remote sensing data for the estimation of crop properties.

2. wavelet analysis,

3. Continuum removal,

4. Spectral angle mapper (SAM),

5. Area under the spectra (integral),

6. Spectral Matching Technique

Note: see chapter 13, Alchanatis and Cohen



U.S. Geological Survey  
U.S. Department of Interior



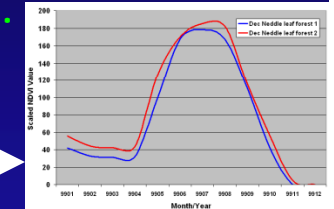
# Development of Automated Algorithm for Global Cropland Mapping

## Quantitative Spectral Matching Techniques (SMTs)

QSMTs compare class spectra of one class with class spectra of every other class & determine, quantitatively, similarities and dissimilarities between classes through automated process; facilitates rapid identification of classes.

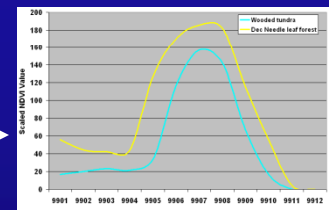
### 1. Spectral Correlation Similarity (SCS)

- shape measure →
- Values vary between 0 to 1 (theoretically between -1 and +1). Negative values have no meaning here. Ignore.
- Greater the SCS greater is the similarity between class spectra and target spectra



### 2. Spectral Similarity Value (SSV)

- Shape and magnitude measure →
- Values vary between 0 to 1.415
- Smaller the SSV value greater the similarity between class spectra and target spectra



Reference: Thenkabail, P.S., GangadharaRao, P., Biggs, T., Krishna, M., and Turrall, H., 2007. Spectral Matching Techniques to Determine Historical Land use/Land cover (LULC) and Irrigated Areas using Time-series AVHRR Pathfinder Datasets in the Krishna River Basin, India. Photogrammetric Engineering and Remote Sensing. 73(9): 1029-1040. (Second Place Recipients of the 2008 John I. Davidson ASPRS President's Award for Practical papers).

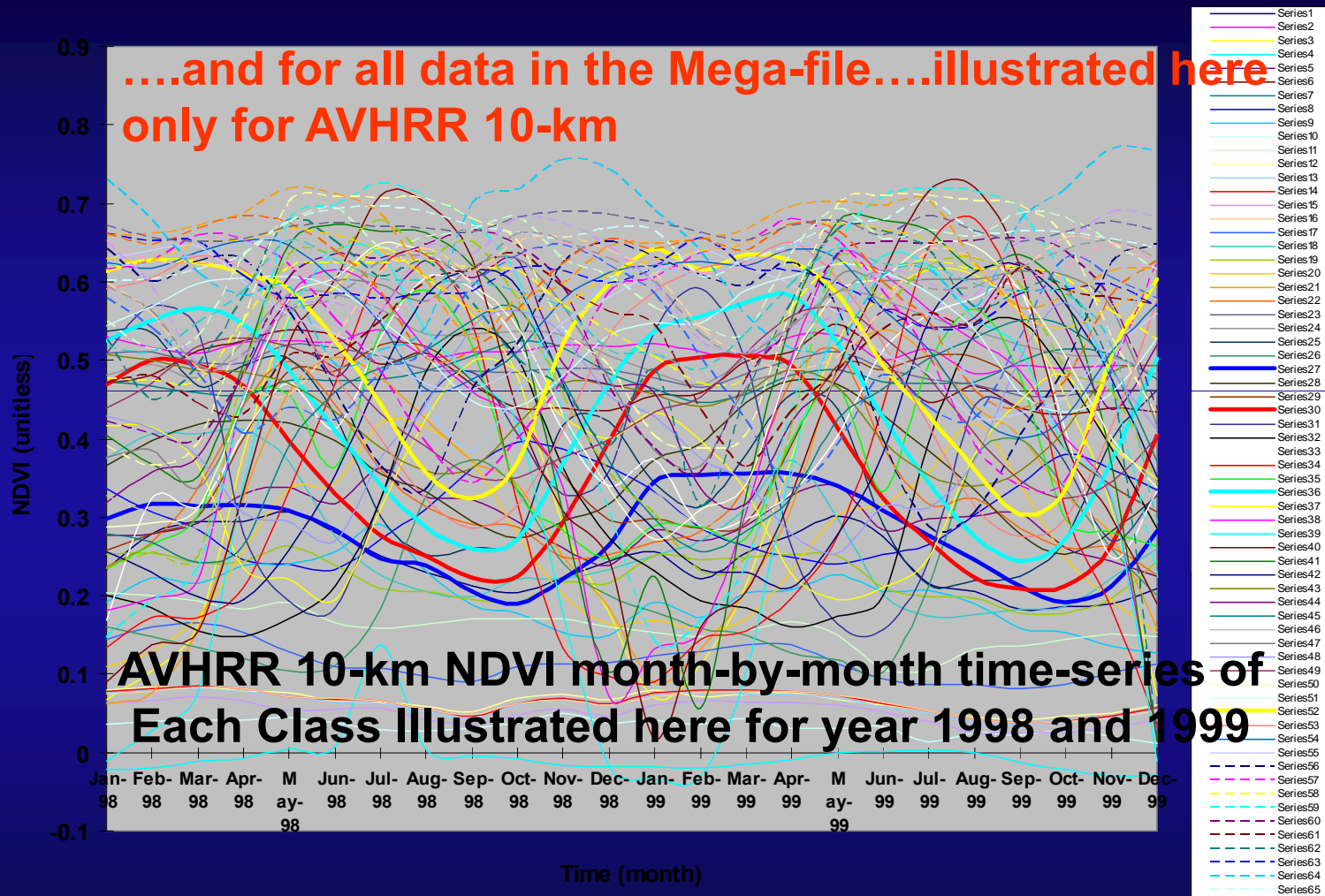


U.S. Geological Survey  
U.S. Department of Interior



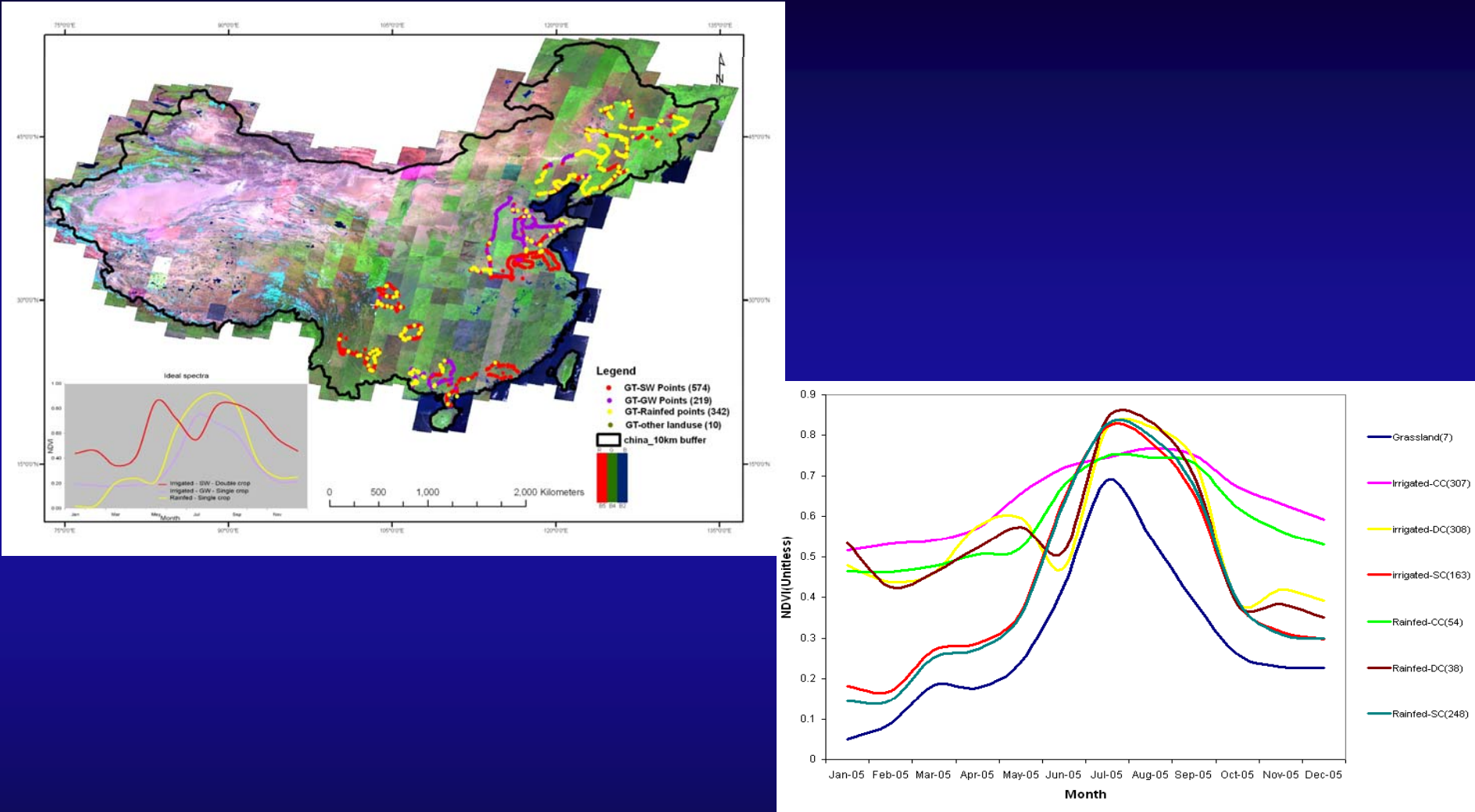
# Development of Automated Algorithm for Global Cropland Mapping

## Quantitative Spectral Matching Techniques (SMTs): Generating Class Spectra



# Development of Automated Algorithm for Global Cropland Mapping

## Quantitative Spectral Matching Techniques (SMTs): Generating Ideal or Target Spectra



Groundtruth points displayed on Landsat ETM+ imagery (example China)

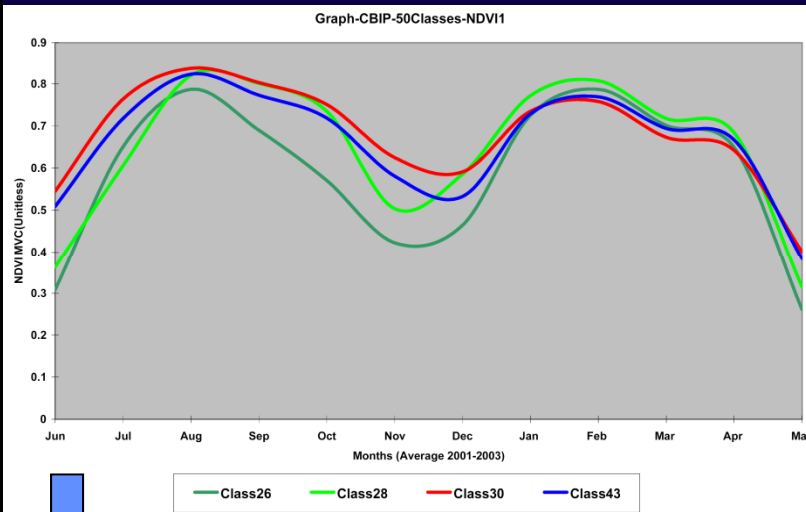
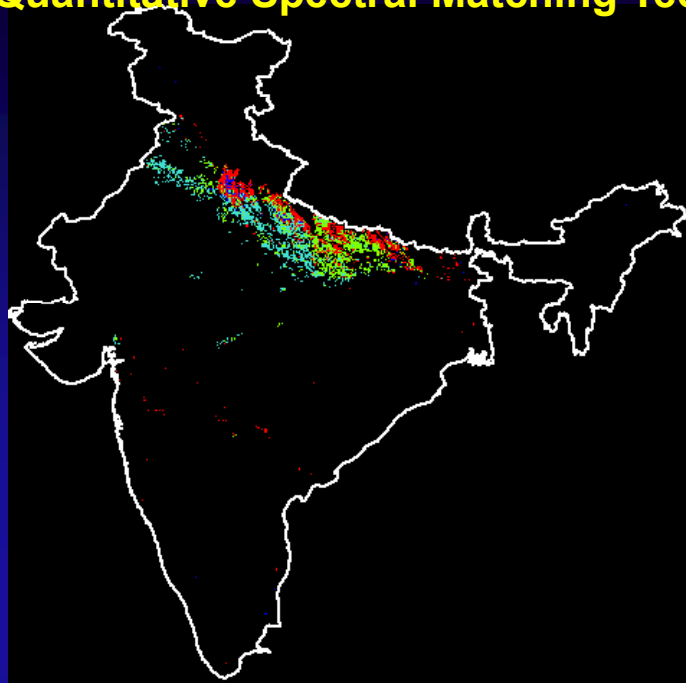


U.S. Geological Survey  
U.S. Department of Interior

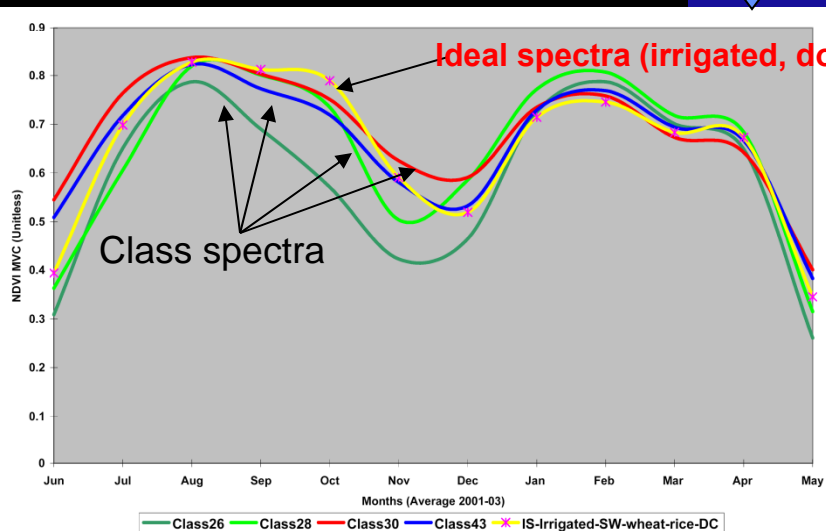


# Development of Automated Algorithm for Global Cropland Mapping

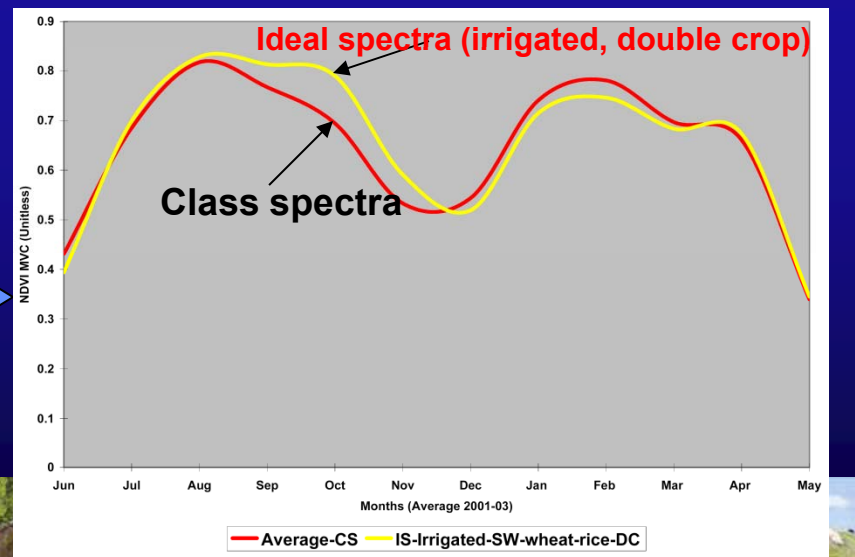
Quantitative Spectral Matching Techniques (SMTs): Matching Class Spectra with Ideal Spectra



Similar Class spectras



Matching Ideal Spectra with similar class spectras

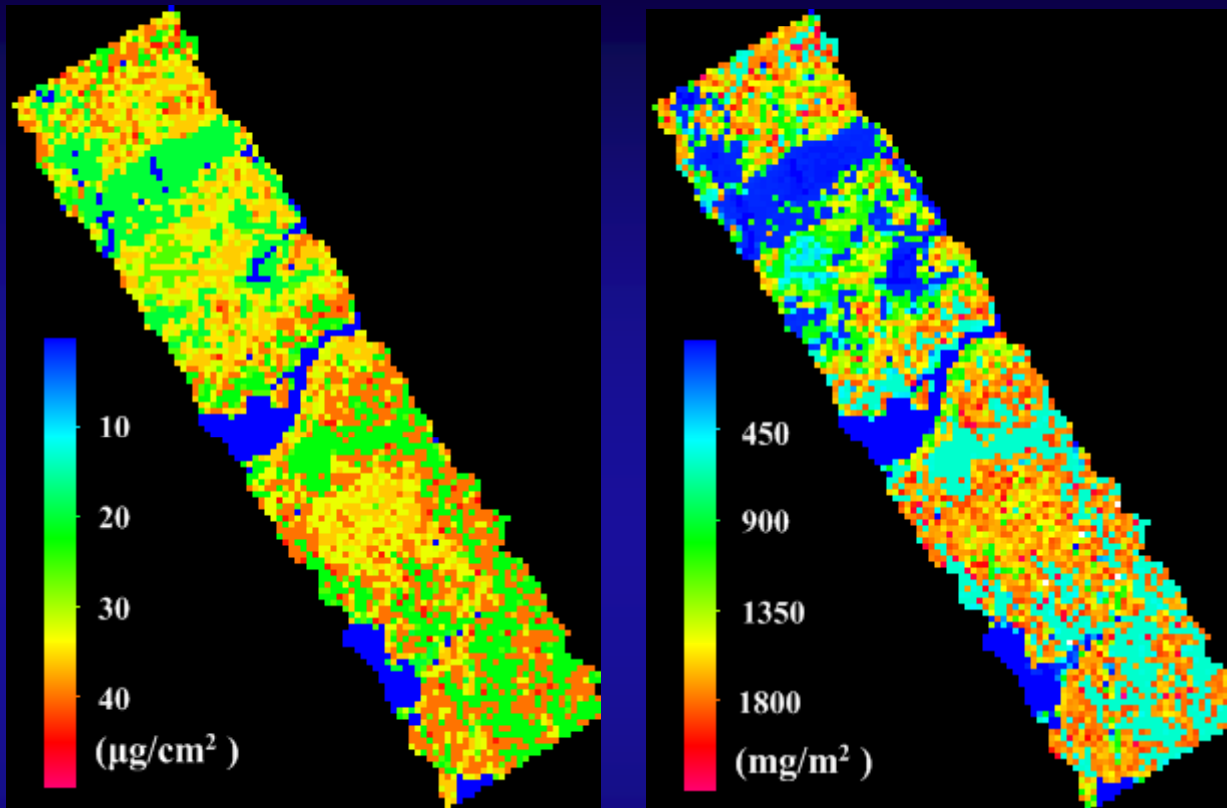


Ideal Spectra Matches with class spectras

# Maps of Vegetation Characteristics using the Best Hyperspectral Narrowband Models



## Maps of Showing Leaf and Canopy Chlorophyll produced using the Best spectro-biochemical models



The spatial variability of leaf chlorophyll<sub>a+b</sub> content, ranging from  $16.2 \mu\text{g}/\text{cm}^2$  to  $43.6 \mu\text{g}/\text{cm}^2$  (Figure 5, left), and canopy chlorophyll content, ranging from  $30 \text{ mg}/\text{m}^2$  to  $2170 \text{ mg}/\text{m}^2$  (Figure 5, right), for vegetated pixels were clearly seen from the map.

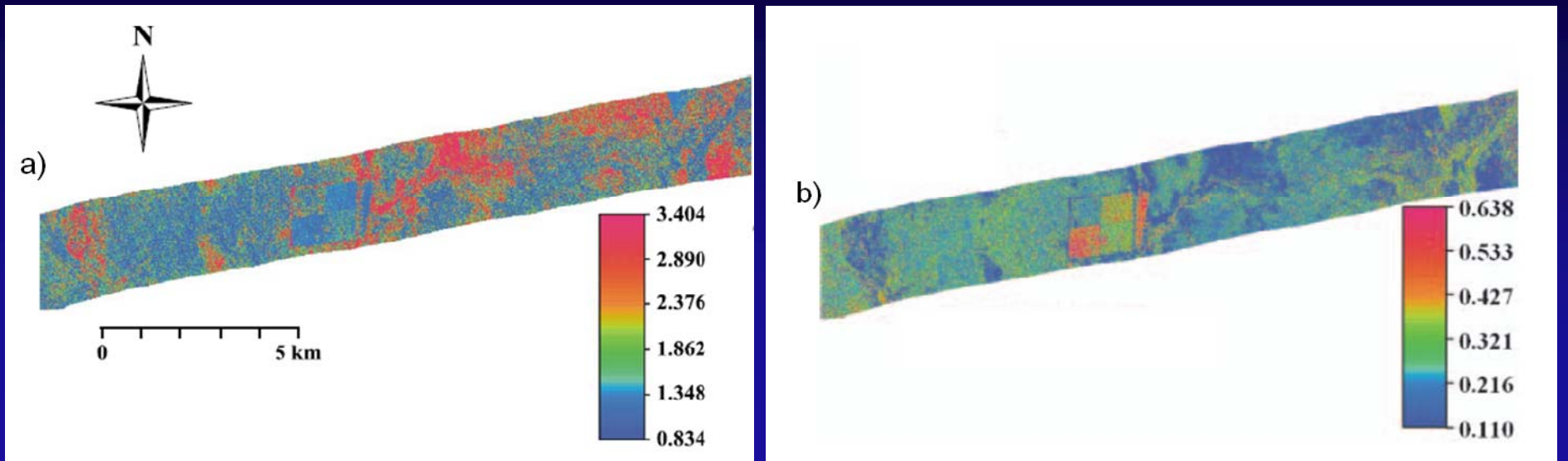
Note: see chapter 7



U.S. Geological Survey  
U.S. Department of Interior



## Maps of Showing Leaf and Canopy Chlorophyll produced using the Best spectro-biochemical models



Maps showing spatial distribution of concentration (%) of nitrogen (a) and phosphorus (b) and scatterplots obtained from the best-trained neural network used for mapping. Scatterplots of nitrogen (%) (c) and phosphorus (%) (d). From Mutanga and Skidmore [6] and Mutanga and Kumar [59]

Note: see chapter 9



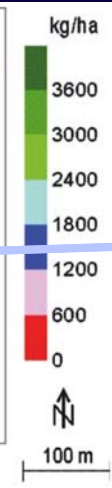
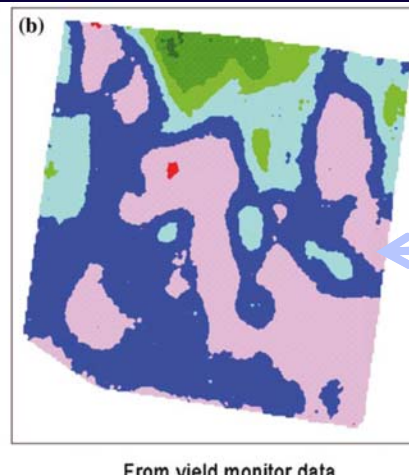
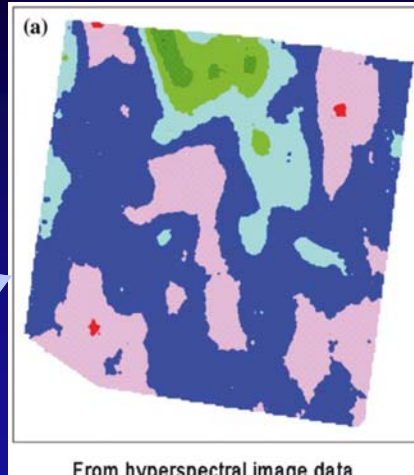
U.S. Geological Survey  
U.S. Department of Interior



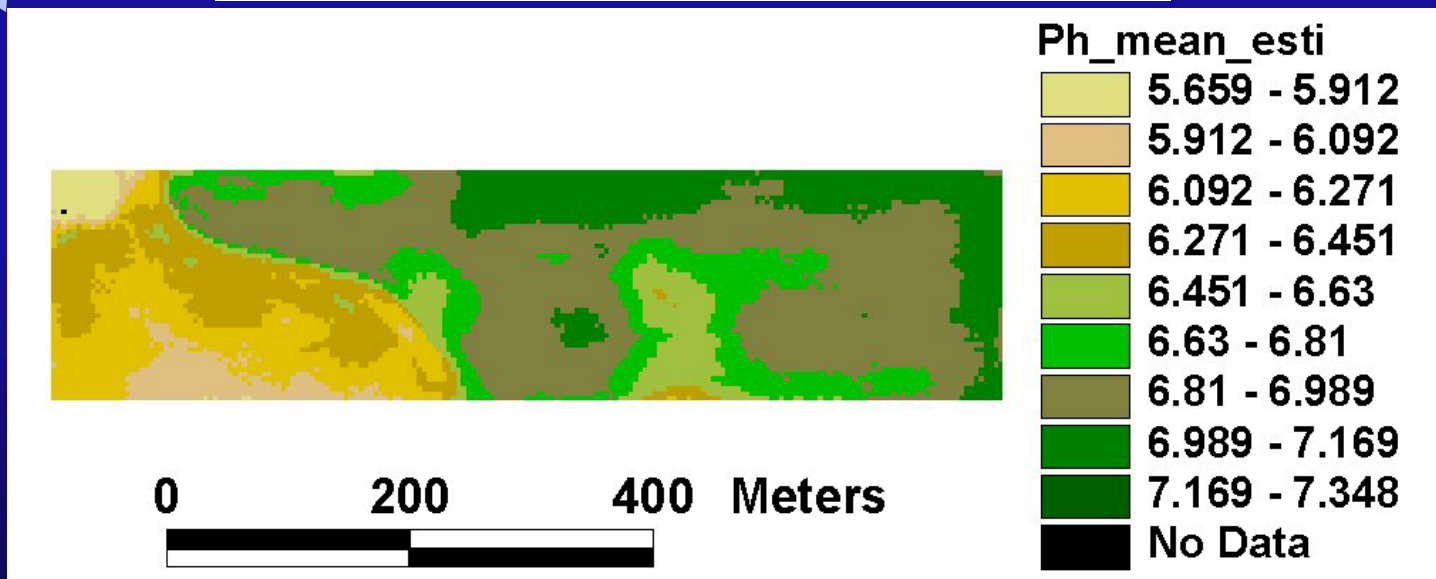
## Maps of Nitrogen and Ph produced using

Best narrowband models mapping yield (top left ) and Ph (bottom) compared with yield monitor data (top right)

Maps produced  
using the best  
Hyperspectral  
narrowband  
models



Maps produced  
using yield  
monitor



Note: see chapter 25



U.S. Geological Survey  
U.S. Department of Interior



# Methods of Classifying Vegetation Classes or categories Increased Accuracies over Broadband Data



## **Methods of Classifying Vegetation Classes or Categories Using hyperspectral narrowband data**

- 1. Multivariate and Partial Least Square Regression,**
- 2. Discriminant analysis**
- 3. unsupervised classification (e.g., Clustering),**
- 4. supervised approaches**
  - A. Spectral-angle mapping or SAM,**
  - B. Maximum likelihood classification or MLC,**
  - C. Artificial Neural Network or ANN,**
  - D. Support Vector Machines or SVM.**

.....All these methods have merit; it remains for the user to apply them to the situation of interest.

**Note: see chapter 5**



## Methods of Classifying Vegetation Classes or Categories Discriminant Model or Classification Criterion (DM) to Test

- **DISCRIM (SAS, 2011) develops a discriminant model (DM)**
- **to classify each observation into one of the groups.**
- The classification criterion is based on individual within group covariance matrices or pooled covariance matrix
- Each observation is placed in the class from which it has the smallest generalized squared distance (Rao, 1973). generalized squared distance function is defined by:

$$D_j^2 = (x - \bar{x}_j)' \text{cov}^{-1}_j (x - \bar{x}_j)$$



# Methods of Classifying Vegetation Classes or Categories

**Discriminant Model or Classification Criterion (DM) to Test  
How Well 5 different Crops are Discriminated using 9 Narrowbands?**

Generalized Squared Distance Function:

$$D_j^2(X) = (X - \bar{X}_j)^T \text{COV}^{-1}(X - \bar{X}_j)$$

Posterior Probability of Membership in each CROPTY:

$$\Pr(j|X) = \frac{\exp(-.5 D_j^2(X))}{\sum_k \exp(-.5 D_k^2(X))}$$

Number of Observations and Percent Classified into weed

From weed	ag	as	cao	cho	te	total commission	Errors of commission
ag	51 85.00	2 3.33	5 8.33	2 3.33	0 0.00	60	15
as	0 0.00	22 75.86	0 0.00	0 0.00	7 24.14	29	24
cao	2 9.09	0 0.00	20 90.91	0 0.08	0 0.00	22	9
cho	0 0.00	0 0.00	0 0.00	67 100.00	0 0.00	67	0
te	0 0.00	1 5.00	1 5.00	0 0.00	18 90.00	20	11
total	53	25	26	69	25	198	178
Errors of omission	4	12	6	3	28		(i.e., 178/198)

Overall accuracy = 89.9 %

$$K_{\hat{h}} = \left( N \sum_{i=1}^r X_{ii} - \sum_{i=1}^r X_{i+} * X_{+i} \right) / \left( N^2 - \sum_{i=1}^r X_{i+} * X_{+i} \right)$$

where, r is the number of rows in the matrix,  $X_{ii}$  is the number of observations in row i and column i,  $X_{i+}$  and  $X_{+i}$  are the marginal totals of i and column i respectively, and N is the total number of observations (Bishop et al. 1975).

Thereby,

$$K_{\hat{h}} = ((198) * (178) - (9,600)) / ((198)^2 - (9,600))$$

$$\text{Where, } (53*60) + (25*29) + (26*22) + (69*67) + (25*20) = 9,600$$

$$K_{\hat{h}} = 0.87$$

# Methods of Classifying Vegetation Classes or Categories

## Discriminant Model or Classification Criterion (DM) to Test

### How Well 6 different Crops are Discriminated using 12 Narrowbands?

Results (from spring 1998 data) using Discriminant Model or Classification Criterion (DM) Crops: barley (ba), chickpea (ch), cumin (cu), lentil (le), vetch (ve), and wheat (wh) using 12 narrow-bands (centered at- units in nm): 489, 518, 547, 575, 604, 661, 675, 704, 718, 846, 904, 975.

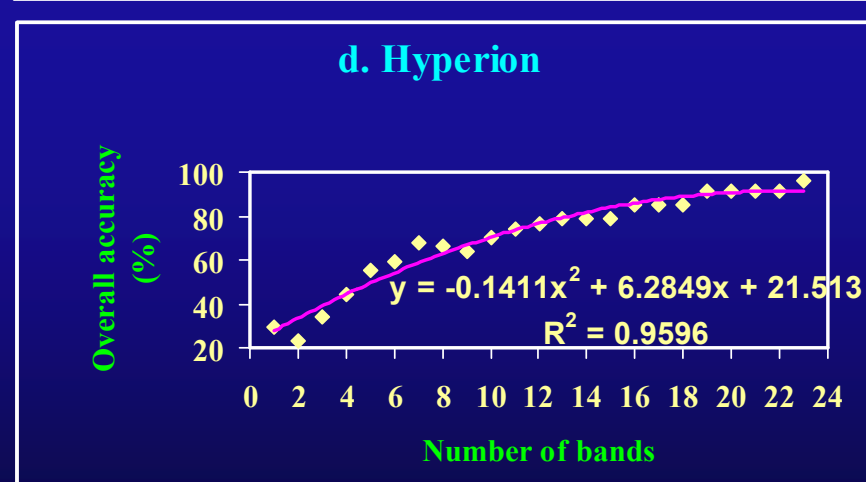
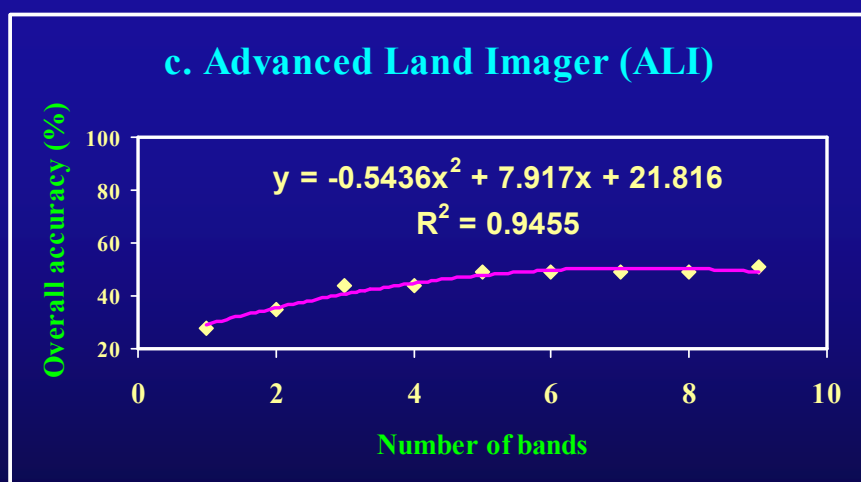
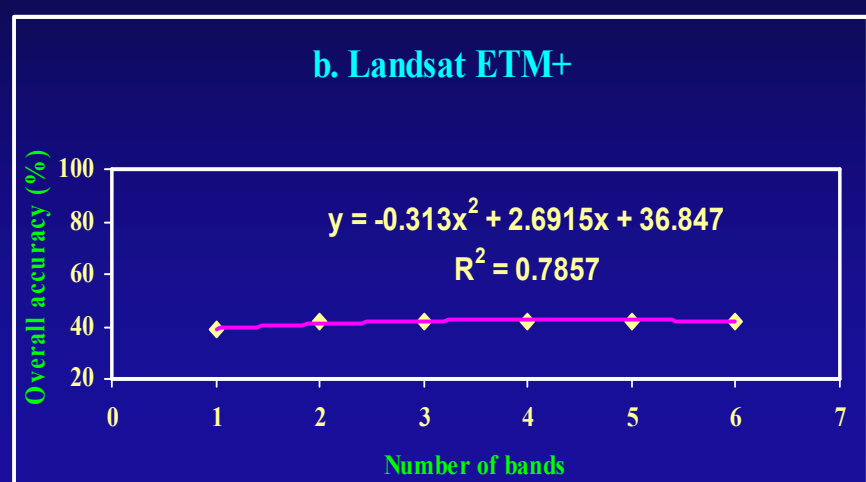
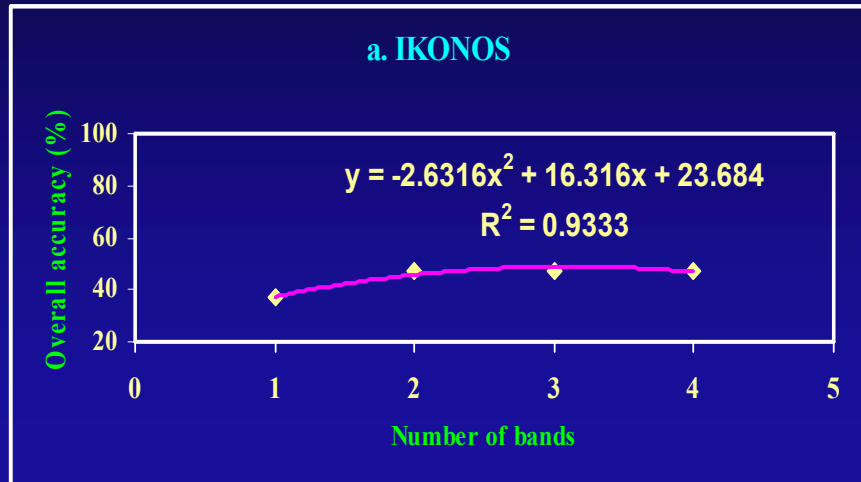
Number of Observations (sample) and Percent Classified into CROPTY (accuracy):

From CROPTY	ba	ch	cu	le	ve	wh	Total
ba	37	0	5	0	1	1	44 (sample)
	84.09	0.00	11.36	0.00	2.27	2.27	100.00 (accuracy)
ch	0	12	2	0	0	0	14
	0.00	85.71	14.29	0.00	0.00	0.00	100.00
cu	0	0	17	0	0	0	17
	0.00	0.00	100.00	0.00	0.00	0.00	100.00
le	0	3	3	15	2	0	23
	0.00	13.04	13.04	65.22	8.70	0.00	100.00
ve	3	1	1	0	9	0	14
	21.43	7.14	7.14	0.00	64.29	0.00	100.00
wh	5	1	1	0	0	57	64
	7.81	1.56	1.56	0.00	0.00	89.06	100.00
Total	45	17	29	15	12	58	176
Percent	25.57	9.66	16.48	8.52	6.82	32.95	100.00

# Methods of Classifying Vegetation Classes or Categories

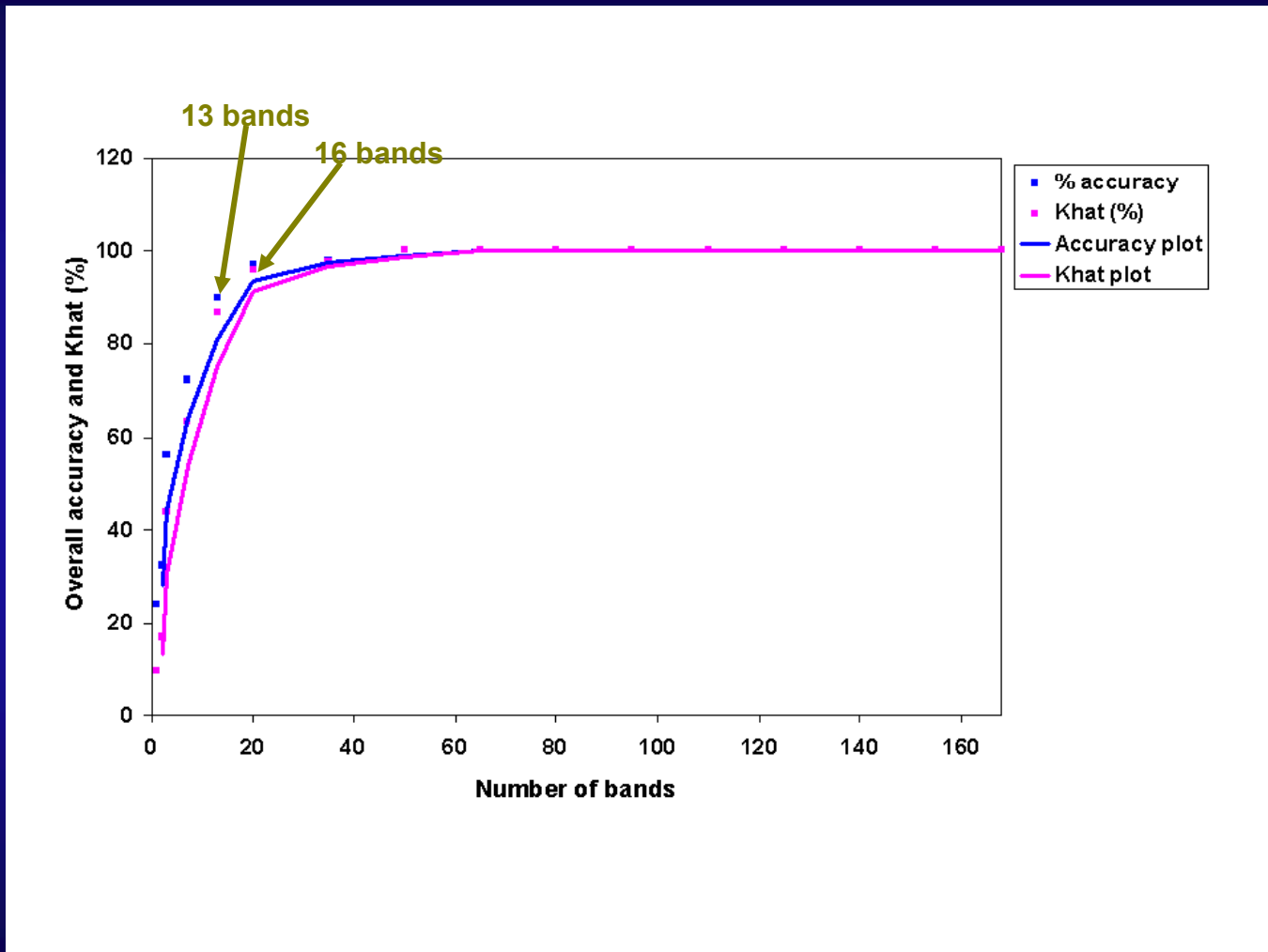
## Discriminant Model or Classification Criterion (DM) to Test

How Well 12 different Vegetation are Discriminated using different Combinations of Broadbands vs. Narrowbands?



# Methods of Classifying Vegetation Classes or Categories

## Optimal bands in classifying 12 distinct vegetation and crop types

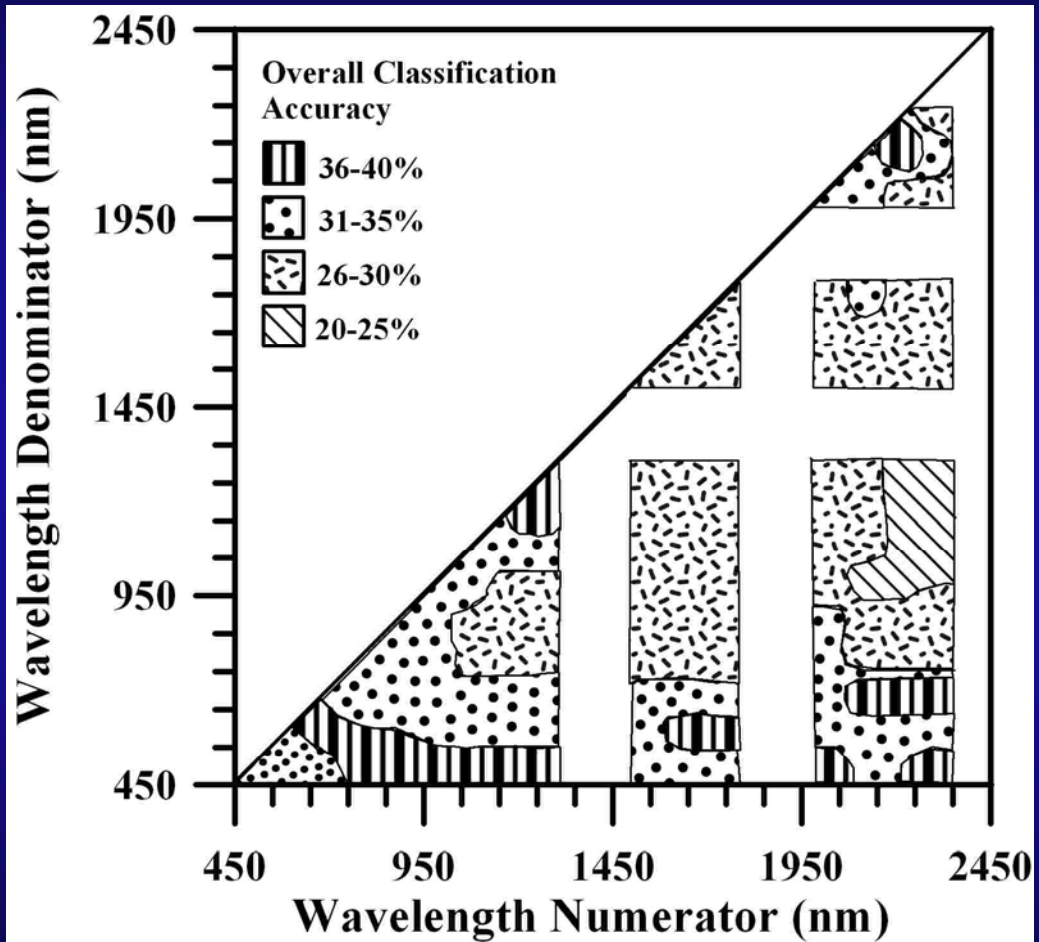


**Note:** Typically, about 20 narrow-bands provide optimal information in classifying and/or Modeling Crops and Vegetation. Adding more bands in visible, near-infrared, and short-wave infrared (400-2500 nm) does not necessarily increase information content.



# Methods of Classifying Vegetation Classes or Categories

## Hyperspectral narrowband in classifying Sugarcane Varieties



The potential of the Hyperion narrowband ratios to discriminate sugarcane varieties. Results around 1400 and 1900 nm were omitted due to atmospheric water vapor absorption. Source: Adapted from Galvão et al. [13].

Note: see chapter 17



U.S. Geological Survey  
U.S. Department of Interior



# Hyperspectral Data Analysis for Croplands and Vegetation

## Stepwise Discriminant Analysis (SDA) to Test How Well Different Crops are Discriminated from One Another

4. Stepwise discriminant analysis (SDA) [STEPDISC algorithm of SAS (SAS, 1999)]. discrimination indicators are:
  - 4a. Wilks' Lambda (lesser the value greater the discrimination between crops)
  - 4b. Pillai Trace (greater the value greater the discrimination between crops)
  - 4c. Average Squared Canonical Correlation (greater the value greater the discrimination between crops)

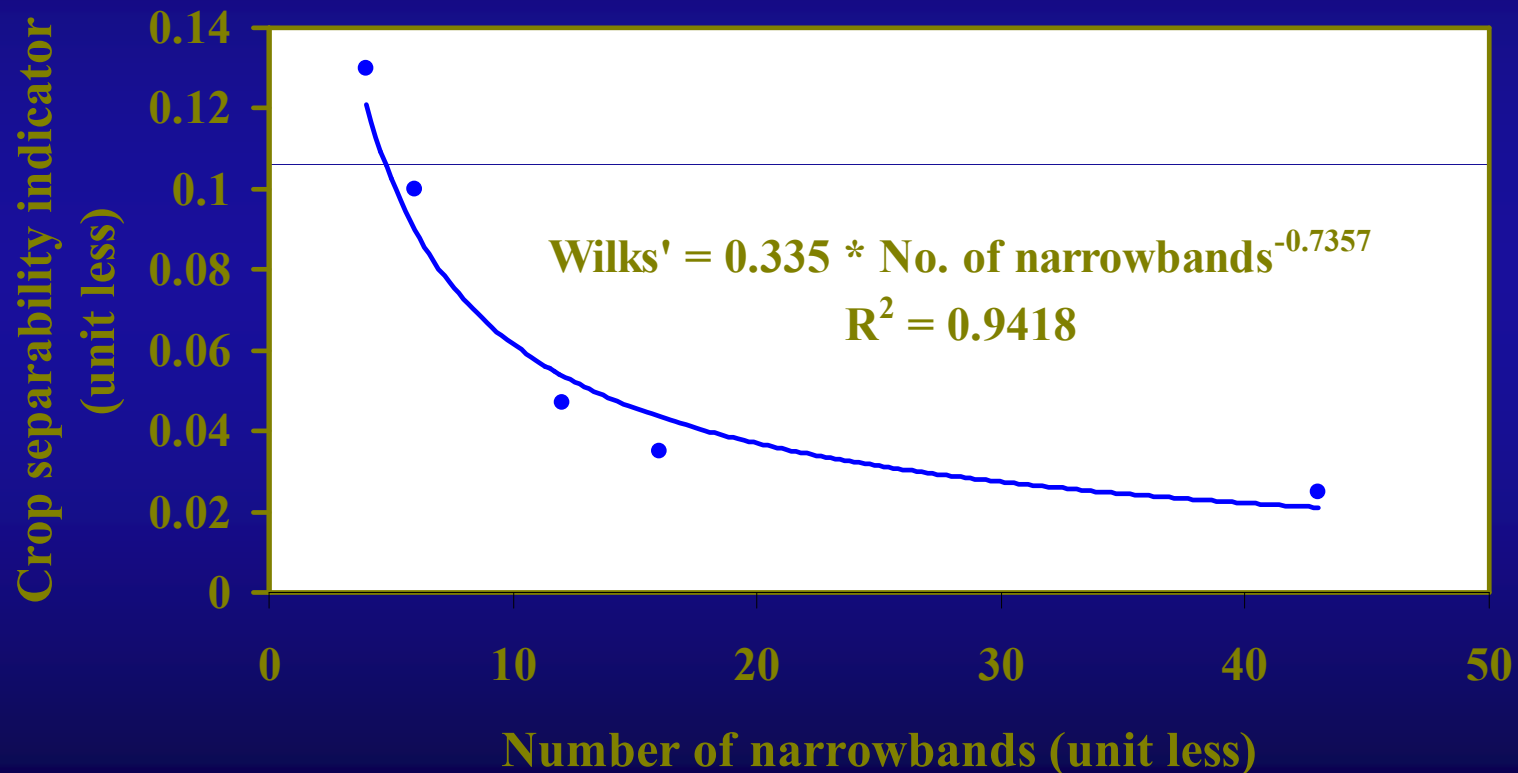


# Hyperspectral Data Analysis for Croplands and Vegetation

## Stepwise Discriminant Analysis (SDA) to Test How Well 6 Different Crops are Discriminated from One Another

### Wilks' Lambda

Lesser the value of Wilks' Lambda  
greater the Spectral Separability between 6 Crops Studied

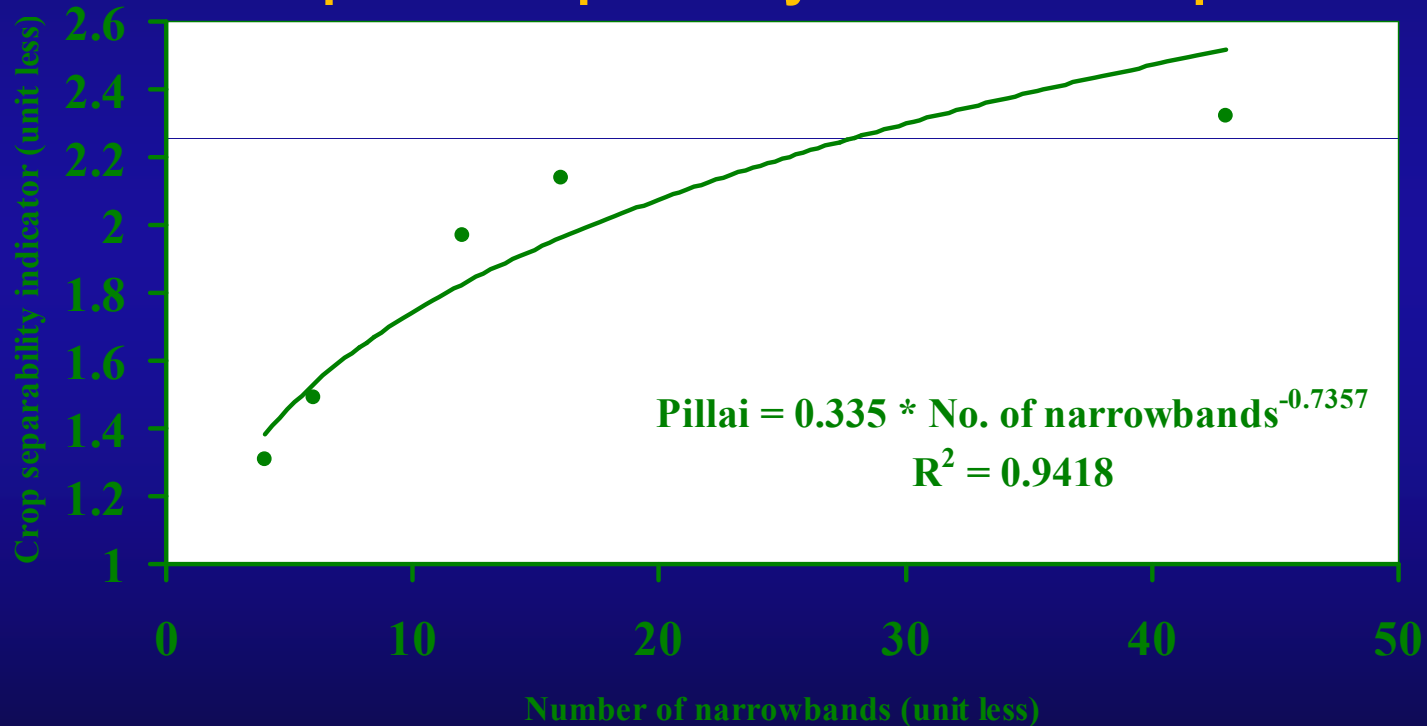


# Hyperspectral Data Analysis for Croplands and Vegetation

## Stepwise Discriminant Analysis (SDA) to Test How Well 6 Different Crops are Discriminated from One Another

### Pillai Trace

Greater the value of Pillai Trace  
greater is the Spectral Separability between 6 Crops Studied



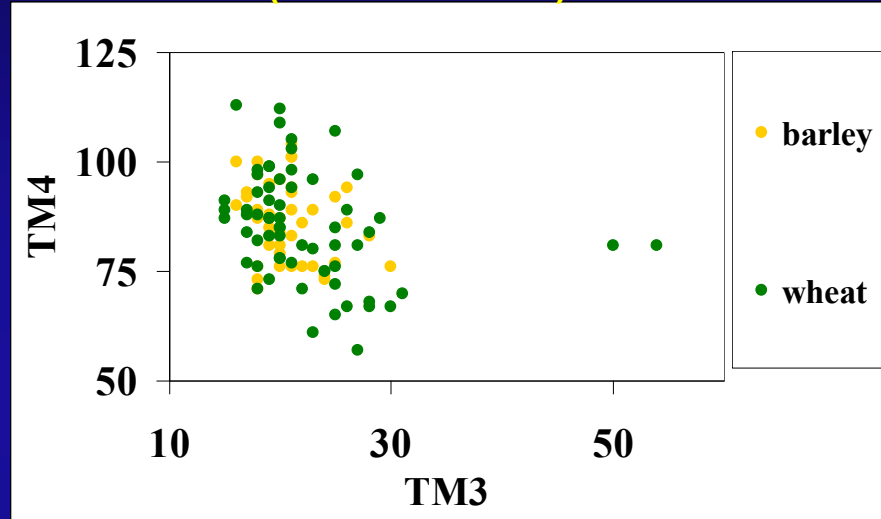
# Methods of Separating Vegetation Classes or categories Distinct Advantages over Broadband Data



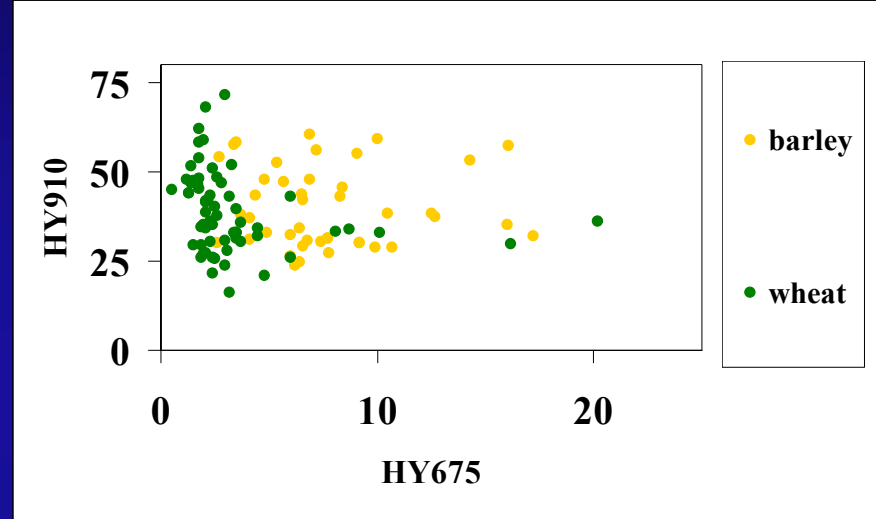
# Methods of Separating Vegetation Classes or Categories

## Broadbands vs. Narrowbands in Separating Vegetation Characteristics

**Broad-band (Landsat-5 TM) NIR vs. Red**



**Narrow-band NIR vs. Red**



Barley



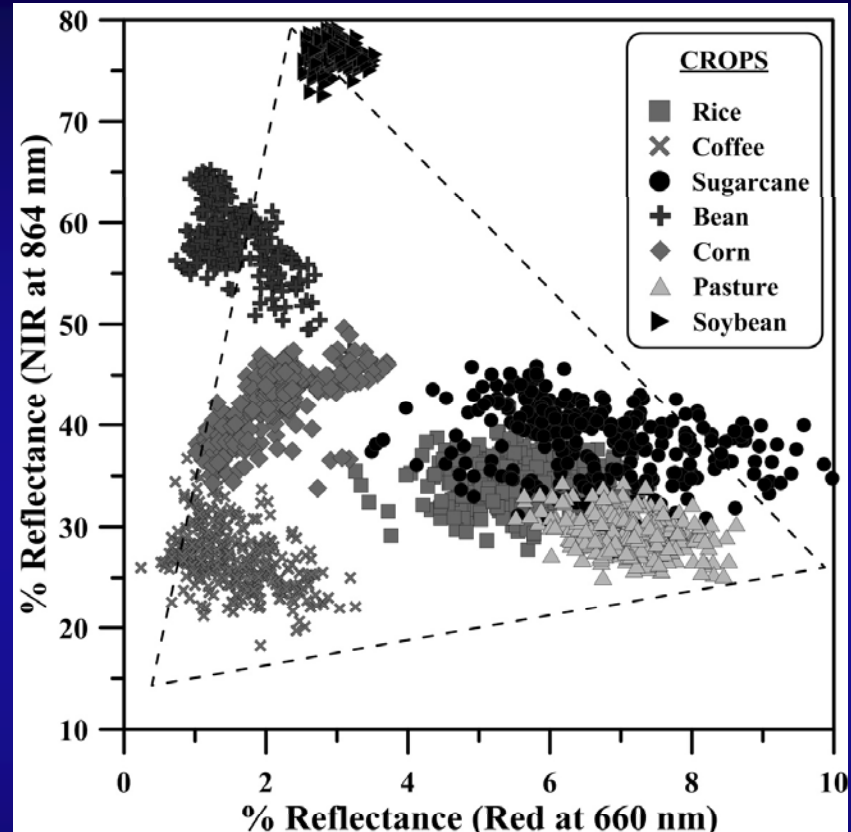
Wheat

Numerous narrow-bands provide unique opportunity to discriminate different crops and vegetation.

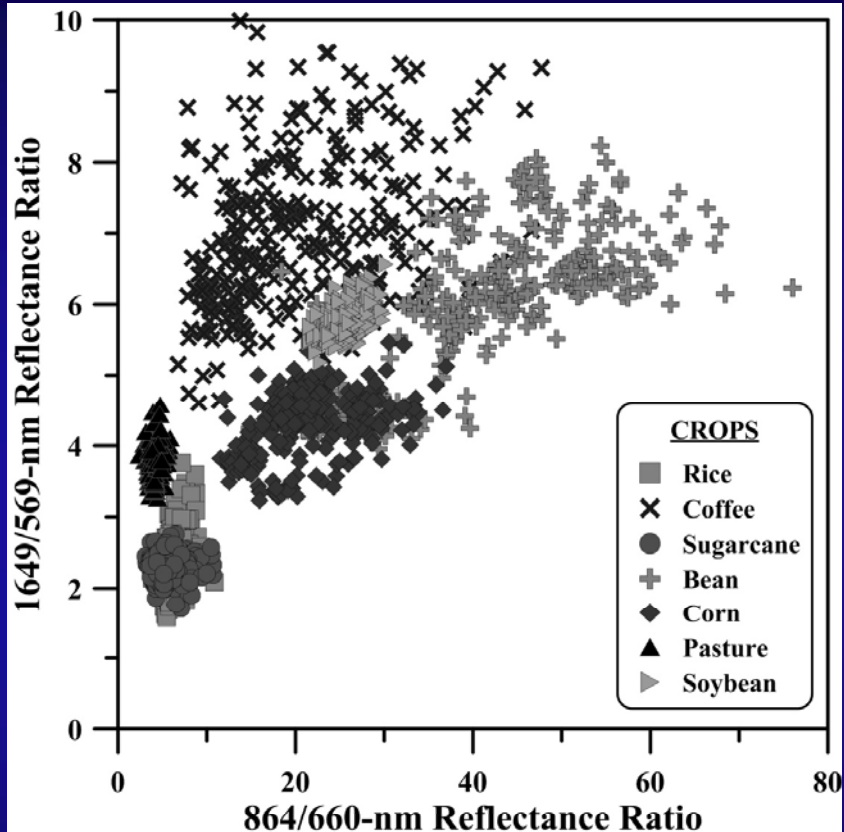


# Methods of Separating Vegetation Classes or Categories

## Hyperion Narrowbands in Separating Vegetation\Crop Types (e.g., Crops in Brazil)



Relationships between red and near infrared (NIR) Hyperion bands for the studied crop types. The triangle is discussed in the text.



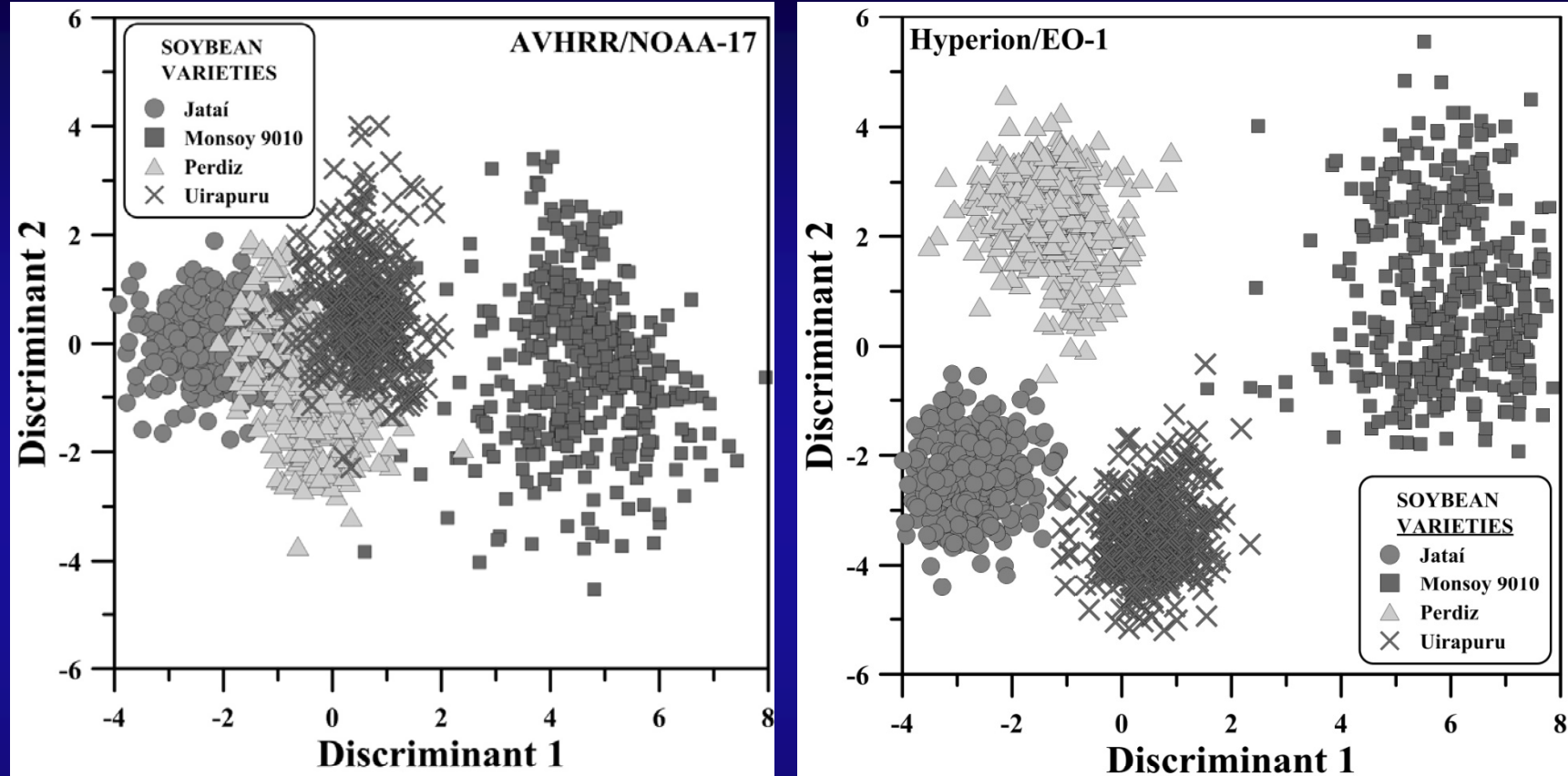
Variation in NIR-1/red and SWIR-1/green reflectance ratios for the crop types under study.

Note: see chapter 17



# Methods of Separating Vegetation Classes or Categories

## Hyperion Narrowbands in Separating Vegetation\Crop Types (e.g., Soybeans in Brazil)



Projection of the (a) AVHRR/NOAA-17 and (b) Hyperion/EO-1 discriminant scores for four of the seven studied soybean cultivars.

Note: see chapter 17



U.S. Geological Survey  
U.S. Department of Interior



## Hyperspectral Remote Sensing Vegetation Note to Workshop Participants

The materials presented in this workshop are strictly for use by the workshop participants and should not be used anywhere without the written permission from the main presenter: Prasad Thenkabail or John Lyon or Dean Riley.

Thenkabail, P.S., Lyon, G.J., and Huete, A. 2011. Book entitled: “Advanced Hyperspectral Remote Sensing of Terrestrial Environment”. 28 Chapters. CRC Press- Taylor and Francis group, Boca Raton, London, New York. Pp. 781 (80+ pages in color).

